ONE-DIMENSIONAL ELASTIC WAVE PROPAGATION IN A BAR WITH THERMALLY-INDUCED LONGITUDINAL INHOMOGENEITY

Thesis for the Degree of Ph. D.

MICHIGAN STATE UNIVERSITY

Rajinder K. Khetarpal

1966

This is to certify that the

thesis entitled

ONE-DIMENSIONAL ELASTIC WAVE PROPAGATION IN
A BAR WITH THERMALLY-INDUCED
LONGITUDINAL INHOMOGENEITY

presented by

Rajinder K. Khetarpal

has been accepted towards fulfillment
of the requirements for

Ph.D. degree in Mechanics

Department of
Metallurgy, Mechanics and Materials Science

Lawrence E. Malvern
Major professor
Lawrence E. Malvern

Date March 28, 1966

ABSTRACT

ONE-DIMENSIONAL ELASTIC WAVE PROPAGATION IN A BAR WITH THERMALLY-INDUCED LONGITUDINAL INHOMOGENEITY

by Rajinder K. Khetarpal

A temperature gradient along the length of an elastic bar gives rise to a variation in the modulus of elasticity E and the density ρ along the length of the bar. Hence the longitudinal elastic wave speed $c = \sqrt{E/\rho}$ becomes a function of the axial coordinate. When the thermal gradient and the dependence of E and ρ on temperature are known, the problem becomes one of wave propagation along an inhomogeneous elastic bar with known values of the variable wave speed $c(x)$. The change in density due to a change in temperature has a small effect on the wave speed for the cases considered, the primary effect being produced by the change in the modulus, which may be reduced as much as 20 percent in steel when the temperature is raised to 1200° F.

Numerical integration by the method of characteristics was programmed and used on the Control Data Corporation 3600 computer. The numerical solutions for two cases were compared with the experimental data obtained: (1) for a stainless steel bar with a temperature gradient at the middle, and (2) for a stainless steel bar with the loaded end hot and the other cold; both bars were loaded at one end by a flat-topped stress pulse. Experimental records of the transmitted pulses in both cases agreed very closely with the numerical solutions. For the bar heated at the middle a reflected

pulse of strain with a magnitude of 5% of the incident pulse was observed experimentally as compared with 7% predicted by the numerical solution. The transmitted strain pulse, after passing through the gradient of rising temperature, showed at the point of highest temperature a continuous slow rise in amplitude after the initial jump, while at a second room-temperature gage beyond the hot region the amplitude was nearly the same as in the incident pulse. The transmitted pulse in the bar with one end hot was slightly different and had a higher magnitude than the incident pulse recorded on the striker bar.

An analytical study was also made of the periodic longitudinal vibrations in a free-free bar with one end hot and the other end cold, excited at the hot end in the first case by a sinusoidally varying displacement and in the second case by a sinusoidally varying stress. An explicit solution is possible when the elastic modulus E is a linear, exponential, or power function of the position in the bar. For a numerical solution, programs were written to solve the periodic vibration problem by finite-difference methods for an arbitrary temperature distribution.

For a 20-inch-long Type 303 stainless steel bar, the effect on the periodic longitudinal vibration was studied for several temperature distributions varying from room temperature to $1200^{\circ}F$ for excitation frequencies of 5000; 7500; 10,000; 12,500; 15,000; 17,500; and 20,000 cps. The numerical solutions agreed with the explicit solutions up to six significant figures in the cases where explicit solutions were available.

ONE-DIMENSIONAL ELASTIC WAVE PROPAGATION IN A BAR WITH THERMALLY-INDUCED LONGITUDINAL INHOMOGENEITY

by

Rajinder K. Khetarpal

A THESIS

Submitted to
Michigan State University
in partial fulfillment of the requirements
for the degree of

DOCTOR OF PHILOSOPHY

in

Mechanics

Department of
Metallurgy, Mechanics and Materials Science

1966

ACKNOWLEDGMENTS

I wish to express my sincere appreciation to Professor Lawrence E. Malvern for his suggestion of this problem, and for his invaluable aid, guidance, and counsel throughout this research. For his aid in the planning and setting up of the apparatus and his help to me in so many other ways I shall always be grateful.

Sincere thanks are also due to Dr. Terry Triffet, Dr. George E. Mase, and Dr. Norman L. Hills for their services on my guidance committee. I wish to also thank Mr. F. T. Bromley and Mr. Donald Childs for their help in mounting the strain gages and thermocouples; and special thanks are given to Mr. Robert B. Engle for his help in planning the apparatus and in the experimental work. I am grateful to Mrs. Barbara Judge for her careful typing of the manuscript.

This project was supported by the National Science Foundation under Grant No. G-24898 through the Division of Engineering Research at Michigan State University.

For my parents in India whose personal sacrifice and trust has made my education possible I will always have the greatest love and respect. I am also thankful to my perfect wife for her help and assistance throughout this project.

TABLE OF CONTENTS

LIST OF FIGURES

NOMENCLATURE

c	Elastic wave speed, also a defined constant in Chapter 4.
c_o	Elastic wave speed at room temperature
C	Non-dimensional elastic wave speed, $= c(x)/c_o$
D	Non-dimensional elastic modulus, $= E(x)/E_o$
D_1 to D_6	Constants in Chapter 4
E	Elastic modulus
E_o	Elastic modulus at room temperature
J_p	Bessel's function of the first kind and order p
k	A constant, with units of $(\text{sec.})^{-1}$ in Chapter 3 Also other defined constants in Chapter 4
L	Length of the bar
n	A defined constant
P	Amplitude of the stress end condition
S	Non-dimensional stress, $= \sigma/E_o$
t	Time
T	Non-dimensional time, $= t/k$
u	Longitudinal displacement, considered positive when in the negative x-direction
U	Amplitude of the displacement end condition
v	Particle velocity, considered positive when in the negative x-direction
V	Non-dimensionalized particle velocity, $= v/c_o$
x	Initial coordinate of cross section
X	Non-dimensional distance, $= kx/c_o$
Y	Non-dimensional strain, $= \epsilon$

Y_p	Bessel's function of the second kind and order p
ϵ	Strain, considered positive in compression
ρ	Density
σ	Stress, considered positive when compressive
ω	Circular frequency

CHAPTER I

INTRODUCTION

1.1. Purpose and Objectives

It is well known that the mechanical properties of a material change with the temperature. Among other changes in mechanical properties due to a change in temperature, the changes in the modulus of elasticity and the density affect the propagation of a wave. The purpose of the present investigation is to study the effect of a thermally-induced inhomogeneity on the propagation of a one-dimensional elastic disturbance.

The problems investigated in this study have the following possible applications: (a) Interpretation of pressure-bar records from hot or radioactive environments (see for example Chiddister*, 1961), (b) Finding the critical frequencies and solving resonance problems of bars subjected to varying temperatures, (c) Calibration of high-temperature strain gages, and (d) Obtaining the value of the elastic modulus at elevated temperatures.

A temperature gradient along the length of an elastic bar gives rise to a variation in the elastic modulus E and the density ρ along the length of the bar. Hence the longitudinal elastic wave speed $c = \sqrt{\frac{E}{\rho}}$ in the bar becomes a function of the axial coordinate.

---

* Surnames followed by dates refer to Bibliography.

When the thermal gradient and the dependence of E and ρ on temperature are known, the problem becomes one of the wave propagation along an inhomogeneous elastic bar with known values of the variable wave speed $c(x)$. The change in the density due to a change in temperature is quite small. Based on the value of the coefficient of expansion for Type 303 steel given in the Metals Handbook (1948), the difference in the values of the density at $75^{\circ}F$ and $1200^{\circ}F$ is 3.89% and the resulting difference in the values of the elastic wave speed at $1200^{\circ}F$ is only 1.98% (the values are given in Sec. 6.1). Therefore the density can be considered constant, and the primary effect is produced by the change in the elastic modulus, which may be reduced as much as 20% in steel when the temperature is raised to $1200^{\circ}F$. The inhomogeneity in this study is therefore prescribed as a variation in magnitude of the elastic modulus only.

The present investigation had the following objectives: (a) To study the effect of the thermally-induced inhomogeneity on the propagation of a pulse in an elastic slender bar with an arbitrary temperature distribution along its length. (b) To study the effect of the thermally induced inhomogeneity on the periodic vibrations of an elastic slender bar with an arbitrary temperature distribution along its length and various boundary conditions. (c) To set up an experiment to study the effect of the thermally-induced inhomogeneity on the propagation of a pulse produced by an impact in an elastic slender bar with a temperature distribution along its length, and

compare it with the outcome of the objective (a).

Numerical integration by the method of characteristics was programmed and used on the Control Data Corporation 3600 computer. The program was used on five specific problems, calculating results:

1. to compare with the experimental pulse-propagation study on the bar heated at its center;
2. to compare with the experimental pulse-propagation study on the bar heated at one end;
3. to verify the results of Chiddister (1961), which he obtained by approximating an experimentally-obtained thermal gradient by a series of steps;
4. to verify the results of Lindholm (1963), which he obtained by a series method for the special case $E = Eo\,(\frac{x}{kL})^{n}$; and
5. to solve a modified version of Lindholm's problem with variation according to a cubic power law in one-fourth the bar, while the rest of the bar had a uniform elastic modulus.

Two experimental pulse propagation studies were made on Type 303 stainless steel test bars:

1. Bar Heated at the Middle. A 6-foot-long bar was heated at the middle to a maximum temperature of 1200°F by a 5-inch-long coaxial furnace and impacted longitudinally at one end by a 4-foot-long striker bar. The pulse produced in the test bar was recorded by three strain gages, two at room temperature and one high-temperature gage

at the middle of the bar. The first room-temperature gage recorded the incident pulse and the reflection from the thermal gradient, while the second recorded the transmitted pulse in the region beyond the heated middle portion of the bar.

2. Bar Heated at the Impact End. A 4-foot-long bar was heated at one end by the same coaxial furnace and impacted as in the first experiment. In this second experiment one of the room-temperature gages was on the striker bar.

Results in both experiments agreed very closely with the numerical solutions. In the case of the bar heated at the middle, the maximum reflected pulse was 7% of the incident pulse according to the calculations and 5% from the experiment. The initial jump and the amplitude of the transmitted strain pulse recorded at the second room-temperature gage were nearly the same as the incident pulse. The amplitude of the pulse at the point of highest temperature in the bar heated at the middle showed a continuous slow rise after the initial jump. The transmitted pulse in the bar struck at the hot end was slightly different and had a higher magnitude than the pulse recorded on the striker bar.

An analytical study was also made of the periodic longitudinal vibrations in a free-free bar with one end hot and the other end cold, excited at the hot end in the first case by a sinusoidally varying displacement and in the second case by a sinusoidally varying stress. An explicit solution is possible when the thermally-induced inhomogeneity is one such that the elastic modulus E is a function of the

position in the bar of the form

	$E = Eo + kx$	Datta (1956)
or	$E = Eo\, e^{kx}$	Sur (1961)
or	$E = Eo\, (\frac{x}{kL})^{n}$	Lindholm (1963)

These problems have been solved by converting the wave equation to a form of Bessel's equation. The solution of the displacement wave equation has been obtained by the same method as that used by the authors cited. In addition, the explicit solutions of the stress wave equation with the same type of inhomogeneities as in the case of the displacement wave equation have been obtained in the present investigation.

In the present investigation programs were written to solve the periodic vibration problem numerically by finite differences for an arbitrary temperature distribution. These programs were used to determine how certain thermal gradients affect the periodic longitudinal vibration of a 20-inch-long Type 303 stainless steel bar. For the excitation frequencies of 5000, 7500, 10,000, 12,500, 15,000, 17,500, and 20,000 cps, explicit solutions of the stress and displacement were obtained for the thermally-induced inhomogeneity in which the elastic modulus varies with the distance as $Eo + kx$, $Eo\, e^{kx}$ and $Eo\, (\frac{x}{kL})^{2}$; and numerical solutions of the stress and displacement were obtained for the same three cases as a check and in addition for variation as $Eo\, (\frac{x}{kL})^{3/2}$ and for a temperature distribution measured in the laboratory under conditions similar to those of the

pulse-propagation experiments. The value of k in each case was such that one end of the bar was at 75°F and the other end at 1200°F. With these choices of the constants the exponential and power function variations of E(x) do not depart much from the linear variation in the 20-inch bar, with the result that those solutions are also very close to the solution for linear variation. The numerical solutions agreed with the explicit solutions up to six significant figures in the cases where explicit solutions were obtained. The solutions were also obtained for the same bar with a uniform temperature of 75°F in one case and 1200°F in the other. Plotting all the above solutions, it was found that the solutions, for the cases of varying temperatures in the bar, were always between the solutions obtained for the uniform temperatures of 75°F and 1200°F. The presence and the location of the nodes, the critical frequencies, and the amplitude, were all affected by the inhomogeneity in the bar.

1.2. Background

A considerable amount of work has been done on inhomogeneity (see Olszak, 1959). Sternberg and Chakaravorty (1959) have considered the problem of the propagation of a shear shock wave from a circular hole in a semi-infinite plate, where the hole is subjected to suddenly rising uniform shearing tractions and the shear modulus of the material of the plate is proportional to an arbitrary power of the radial distance from the center of the hole. Cristescu (1959) has considered the propagation of waves in elastic-plastic non-homogeneous thin and semi-infinite rods. In the elastic region he took $\sigma = E(x)\epsilon$.

Perzyna (1959) also considered the propagation of elastic-plastic waves in a non-homogeneous bar for a general type of non-homogeneity. He analyzed the problem with $\sigma = f(\epsilon, x)$. Both Cristescu and Perzyna formulated the problem by the method of characteristics in the same manner as will be done in this investigation, but they did not include any numerical solutions. Datta (1956) has studied the propagation of sinusoidal and impulsive disturbances in a bar having linear variation of the elastic parameters; he obtained the solution for the impulsive loading by Laplace transform techniques. Ghosh (1961) has studied the problem of extensional vibration of a bar having linear variation of the elastic parameters, and excited by the impact of an elastic load; he used operational methods. Sur (1961) has studied the propagation of sinusoidal and impulsive disturbances in a bar having exponential variation of the elastic parameters, and he too obtained the solution for the impulsive loading by Laplace transform techniques. Chiddister (1961) studied the problem of pulse propagation in a bar with thermally-induced longitudinal inhomogeneity by approximating the thermal gradient by five step-discontinuities separating regions of constant temperature and superposing the waves calculated by simple reflection theory. Chiddister used his approximate solution to interpret the pressure-bar records from the hot environments where his specimen was located. As was mentioned above, this is one of the important applications of the present investigation. Lindholm (1963) solved the problem of an elastic disturbance propagating in a nonhomogeneous bar of finite length by using the

principle of virtual work. He prescribed the nonhomogeneity as a modulus of elasticity continuously varying with position in the bar, given by $E = E_o(\frac{x}{kL})^n$, and solved the pulse propagation problem by a superposition of sinusoidal solutions at different frequencies. In his investigation of the pulse propagation he found an apparent absence of reflections. An explanation of this apparent difference from the results of the present investigation is given in Sec.7.1(c.iii).

CHAPTER II

DERIVATION OF THE WAVE EQUATION

Three different forms of the governing equations of wave propagation will be derived here: a set of two first-order partial differential equations for the unknown stress and particle velocity; a second-order wave equation for the displacement; and a second-order wave equation for the stress (see Timoshenko, 1955).

These governing equations of motion for the one-dimensional theory of longitudinal wave propagation in a bar of uniform cross-section, with the elastic modulus varying along the length of the bar, are obtained by assuming that plane sections remain plane and that across these sections the stress is uniform, and that the displacements are small.

At a time t, let $u(x, t)$ be the displacement of the cross-section initially at a distance x from the left-hand end of the bar. At the section under consideration the strain ϵ and the particle velocity v are then

$$\epsilon = \frac{\partial u}{\partial x} \tag{2.1}$$

$$v = \frac{\partial u}{\partial t} \tag{2.2}$$

In this discussion the stress and strain are considered positive when they are compressive, and the displacement and the particle velocity are considered positive when they are in the negative x direction.

By differentiating Eq. (2.1) with respect to time and Eq. (2.2) with respect to x, and eliminating u, we get the equation of continuity

$$\frac{\partial \epsilon}{\partial t} = \frac{\partial v}{\partial x} \tag{2.3}$$

The equation of motion can be written as

$$\frac{\partial \sigma}{\partial x} = \rho(x) \frac{\partial v}{\partial t} \tag{2.4}$$

In addition to equations (2.3) and (2.4) we have Hooke's law

$$E(x)\, \epsilon = \sigma$$

or,

$$E(x) \frac{\partial \epsilon}{\partial t} = \frac{\partial \sigma}{\partial t} \tag{2.5}$$

Substituting Eq. (2.5) in Eq. (2.3),

$$\frac{1}{E(x)} \frac{\partial \sigma}{\partial t} = \frac{\partial v}{\partial x}$$

We therefore have a system of two linear first-order partial differential equations. The system is written as

$$\left.\begin{aligned} \frac{1}{E(x)} \frac{\partial \sigma}{\partial t} - \frac{\partial v}{\partial x} &= 0 \\ \frac{\partial \sigma}{\partial x} - \rho(x) \frac{\partial v}{\partial t} &= 0 \end{aligned}\right\} \tag{2.6}$$

Now from Eq. (2.1) and Hooke's law

$$\sigma = E(x) \frac{\partial u}{\partial x}$$

or,

$$\frac{\partial \sigma}{\partial x} = \frac{\partial}{\partial x} \left\{ E(x) \frac{\partial u}{\partial x} \right\} \tag{2.7}$$

From equations (2.4) and (2.2)

$$\frac{\partial \sigma}{\partial x} = \rho(x) \frac{\partial^2 u}{\partial t^2} \tag{2.8}$$

so that,

$$\frac{\partial}{\partial x} \{ E(x) \frac{\partial u}{\partial x} \} = \rho(x) \frac{\partial^2 u}{\partial t^2} \tag{2.9}$$

Eq. (2.9) is the one-dimensional wave equation. Perzyna (1959) gave a similar derivation for the wave equation, Eq. (14) in his paper. Lindholm (1963) begins with the same wave equation.

From equations (2.3) and (2.5)

$$\frac{\partial \sigma}{\partial t} = E(x) \frac{\partial v}{\partial x}$$

so that

$$\frac{1}{E(x)} \frac{\partial^2 \sigma}{\partial t^2} = \frac{\partial^2 v}{\partial t \partial x} \tag{2.10}$$

Differentiating Eq. (2.4) with respect to x yields

$$\frac{\partial}{\partial x} (\frac{1}{\rho(x)} \frac{\partial \sigma}{\partial x}) = \frac{\partial^2 v}{\partial x \partial t} \tag{2.11}$$

From equations (2.10) and (2.11)

$$E(x) \frac{\partial}{\partial x} (\frac{1}{\rho(x)} \frac{\partial \sigma}{\partial x}) = \frac{\partial^2 \sigma}{\partial t^2} \tag{2.12}$$

If the variation in density is negligible, we get the following stress wave equation

$$E(x) \frac{\partial^2 \sigma}{\partial x^2} = \rho \frac{\partial^2 \sigma}{\partial t^2} \tag{2.13}$$

or,

$$c^2(x) \frac{\partial^2 \sigma}{\partial x^2} = \frac{\partial^2 \sigma}{\partial t^2} \tag{2.14}$$

where,

$$c(x) = \sqrt{\frac{E(x)}{\rho}} \tag{2.15}$$

$c(x)$ is the elastic bar-wave speed.

The system of two first-order equations will be used in the third chapter to study pulse propagation by the method of characteristics, while the two second-order wave equations will be used in the fourth chapter to study the sinusoidal stress and displacement standing waves.

CHAPTER III

PULSE PROPAGATION

3.1. Solution by the Method of Characteristics

We have obtained a system of two linear first-order differential equations, Eq. (2.6), for the pulse propagation in a bar.

$$\left.\begin{aligned} \frac{1}{E(x)} \frac{\partial \sigma}{\partial t} - \frac{\partial v}{\partial x} &= 0 \\ \frac{\partial \sigma}{\partial x} - \rho(x) \frac{\partial v}{\partial t} &= 0 \end{aligned}\right\} \qquad (3.1)$$

Since the system is hyperbolic, it is suitable for numerical solution by the method of characteristics (Courant and Hilbert, 1962).

For Eq. (3.1), we have $\sum_i \left(a_{ki} \frac{\partial u^i}{\partial x} + b_{ki} \frac{\partial u^i}{\partial t}\right) = 0$

$$u^i = \begin{bmatrix} \sigma \\ u \end{bmatrix}, \quad a_{ki} = \begin{bmatrix} 0 & -1 \\ 1 & 0 \end{bmatrix}, \quad b_{ki} = \begin{bmatrix} \frac{1}{E(x)} & 0 \\ 0 & -\rho(x) \end{bmatrix}$$

And the characteristic curves are defined by

$$\begin{aligned} dx &= + c(x)\, dt \\ dx &= - c(x)\, dt \end{aligned} \qquad (3.2)$$

where $c(x) = \sqrt{\frac{E(x)}{\rho(x)}}$ is the speed of propagation of the elastic wave front.

The interior differential equations holding along the characteristics corresponding to Eq. (3.2) are

$$d\sigma - \rho(x)\, c(x)\, dv = 0$$

$$d\sigma + \rho(x)\, c(x)\, dv = 0 \qquad (3.3)$$

Both Cristescu (1959) and Perzyna (1959) give the equations defining the characteristics, and also interior differential equations relating v and ϵ for the elastic-plastic problem, but the papers cited included no actual numerical solutions.

For most of the metals, e.g. steel, the coefficient of expansion per unit volume is quite small. And because density is mass per unit volume, the change in density due to the temperature change is also small (see Sec. 6.1) and will be neglected in this investigation.

The system of Eqs. (3.2) and (3.3) can be treated by a numerical procedure. The variables are first non-dimensionalized by the following transformation.

$$S = \frac{\sigma}{E_o} \qquad X = \frac{kx}{c_o}$$

$$Y = \epsilon \qquad D = \frac{E(x)}{E_o}$$

$$V = \frac{v}{c_o} \qquad C = \frac{c(x)}{c_o}$$

$$T = kt$$

where E_o and c_o are the elastic modulus and the wave propagation speed at room temperature; ($E_o = \rho\, c_o^2$); k has the units of sec.$^{-1}$, and its value is chosen for convenience.

The transformed characteristic curves and the interior differential equations along them can be written as

$$\left.\begin{aligned} dS - C\,dV = 0 \quad &\text{along the curve} \quad dX = C\,dT \\ dS + C\,dV = 0 \quad &\text{along the curve} \quad dX = -C\,dT \end{aligned}\right\} \tag{3.4}$$

For numerical calculations these equations are treated as finite-difference equations, with dS and dV replaced by ΔS and ΔV, respectively and C replaced by an average value on the characteristic segment. The XT-plane is subdivided by a mesh of characteristic curves at finite intervals of ΔT and ΔX. The characteristics are plotted with a constant interval of ΔT, and ΔX is allowed to vary.

As shown in Fig. 3.1, for $X > 0$ there are two characteristics passing through each mesh point. Therefore at any mesh point P of the XT-plane the solution can be obtained by solving two difference equations along the appropriate characteristics, if we already have the solution for the two neighboring points A and B.

For the points along the edges of the bar, one of the unknowns is prescribed, so that one equation will be sufficient to give the solution.

Further details of the numerical solution are given in the next section.

3.2. Numerical Procedure

We write the interior differential equations, Eq. (3.4) as difference equations, with the average value of C along a segment approximated by the arithmetic mean of its two end values, and obtain

$$\left.\begin{aligned}(S_P - S_A) - \frac{(C_P + C_A)}{2}(V_P - V_A) &= 0\\ (S_P - S_B) + \frac{(C_P + C_B)}{2}(V_P - V_B) &= 0\end{aligned}\right\} \qquad (3.5)$$

These equations are solved simultaneously to give the values of the dimensionless stress S and velocity V at the point P of Figure 3.1 in terms of the values of S and V at A and B. Proceeding point-by-point in the mesh and using Eq. (3.5), we obtain the values of S and V for all the points in the field of characteristics.

The characteristic field can be constructed by solving the characteristic difference equations, based on Eq. (3.2), which can be done without solving the propagation problem. The calculations with Eq. (3.5) then give the solution at the mesh points.

There are three possible types of points to be considered for a wave propagation in a semi-infinite bar: Leading Wave Front; Impacted End; and General Interior Point. For a finite bar the points at the other end also require special treatment.

3.2(a). Leading Wave Front

Along the leading wave front the values of the stress, strain, and the velocity are zero for a continuously rising pulse. For a discontinuous jump, the values after the jump are obtained by equating impulse to the change of momentum and by continuity to give the jump conditions

$$\left.\begin{aligned} \Delta S &= - C\Delta V \\ \Delta V &= - C\Delta Y \\ \Delta S &= C^2 \Delta Y \end{aligned}\right\} \qquad (3.6)$$

3.2(b). Impacted End

Only one equation is available for the impacted end. Assuming that one boundary condition is known at this end, the solution can be obtained by considering the propagation along $dX = - CdT$. Two possible cases are

(a) The Stress Boundary Condition is Known:

Let the stress at the point $X = 0$ be $S_o(T)$. Then Eq. (3.5) can be written as

$$\begin{aligned} S_P &= S_o \\ (S_P - S_B) + \frac{(C_P + C_B)}{2} (V_P - V_B) &= 0 \end{aligned} \qquad (3.7)$$

The solution of Eq. (3.7) can be written as

$$\left.\begin{aligned} S_P &= S_o \\ Y_P &= \frac{S_o}{D_P} \\ V_P &= V_B - \frac{2}{C_P + C_B} (S_o - S_B) \end{aligned}\right\} \qquad (3.8)$$

(b) The Strain Boundary Condition is Known:

Let the strain boundary condition be $Y(0,T) = Y_o(T)$.

The equations for this boundary condition are

$$\left.\begin{aligned} Y_P &= Y_o \\ S_P &= D_P Y_P \\ (S_P - S_B) &+ \frac{(C_P + C_B)}{2} (V_P - V_B) = 0 \end{aligned}\right\} (3.9)$$

The solution of Eq. (3.9) can be written as

$$\left.\begin{aligned} S_P &= D_P Y_o \\ Y_P &= Y_o \\ V_P &= V_B - \frac{2}{C_P + C_B} (D_P Y_o - S_B) \end{aligned}\right\} (3.10)$$

(c) General Interior Point

For a general interior point the Eq. (3.5) can be written as

$$\left.\begin{aligned} (S_P - S_A) - \frac{(C_P + C_A)}{2} (V_P - V_A) &= 0 \\ (S_P - S_B) + \frac{(C_P + C_B)}{2} (V_P - V_B) &= 0 \end{aligned}\right\} (3.11)$$

The solution of Eq. (3.11) can be written as

$$S_P = \frac{C_P + C_B}{2C_P + C_A + C_B} S_A + \frac{C_P + C_A}{2C_P + C_A + C_B} S_B + \frac{(C_P + C_A)(C_P + C_B)}{2(2C_P + C_A + C_B)} (V_B - V_A) \quad (3.12)$$

$$Y_P = \frac{S_P}{D_P}$$

$$V_P = \frac{1}{2C_P + C_A + C_B} \{ (C_P + C_A) V_A + (C_P + C_B) V_B - 2S_A + 2S_B \}$$

The equations, Eq. (3.8), Eq. (3.10) and Eq. (3.12), have been programmed in Fortran for the CDC-3600 computer. The program is given in Appendix B.

Two of the possible boundary conditions at the other end of the bar (opposite from the impact end) are free end and fixed end. At a free end, stress is equal to zero, so that at all the mesh points falling at that end of the bar the non-dimensional stress S will be zero. At a fixed end, particle velocity is equal to zero, so that at all the mesh points falling at the end of the bar the non-dimensional particle velocity V will be zero. In both cases only one of the Eq. s (3.5) is used to obtain a solution.

The program has been used to solve five different problems:

1. Pulse propagation in a 6-foot stainless steel bar with the experimental temperature distribution in the middle. The maximum temperature was 1200°F. The measured temperature distribution is given in Fig. 3.2. Temperature was measured at 24 points 0.8 in. apart on one side of the temperature distribution. For the other side, the temperature distribution was taken to be a mirror image of this side.

2. Pulse propagation in a 4-foot stainless steel bar with the experimental temperature distribution such that the impacted end was at 1200°F. The measured temperature distribution is given in Fig. 3.3. Temperature was measured at 20 points one inch apart.

3. Verification of the results obtained by Chiddister (1961).

4. Verification of the results obtained by Lindholm (1963).

5. Solution of a modified version of Lindholm's problem with variation according to a cubic power law in one-fourth of the bar, while the rest of the bar had a uniform elastic modulus.

Each mesh point was designated as (i, j) where i is the number of the characteristic with positive slope through the mesh point; for example, i=1 identifies the leading wave front X = CT; and j is the number of mesh point on the characteristic (see Fig. 3.1). In the first problem the final mesh had 900 horizontal intervals, spaced so that the time Δt taken by the wave to travel across each interval was the same, namely Δt equal to 0.4104 microseconds. In the second problem the final mesh had 960 horizontal intervals each covered by the wave in time Δt equal to 0.2564 microseconds. For the third and fourth problems 100 horizontal intervals were used and for the fifth problem 160 intervals.

3.3. Computation of c and the First Characteristic

The elastic wave speed c(x) is equal to $\sqrt{\frac{E(x)}{\rho}}$. Garafalo (1960) found that the elastic modulus of 18-8 stainless steel could be represented as a linear function of temperature. The slope of his curve of modulus versus temperature was used to construct the linear plot given in Fig. 3.4 for the Type 303, 18-8 stainless steel specimen bar used in the present study. The room temperature value was determined experimentally and used with the slope from Garafalo's paper to construct the plot. At 75°F the experimentally determined value was

$$E_o = 29.0 \times 10^6 \quad \text{psi.},$$

while from Garafalo's paper

$$\text{Slope} = -6.47 \times 10^3 \quad \text{psi}/^{\circ}\text{F}.$$

From the values of the temperature measured at various points as mentioned in Section 3.2, the values of the elastic modulus were obtained from the linear relation illustrated in Fig. 3.4 at those points. These in turn were used to get the elastic wave speed versus distance curves shown in Fig. 3.5 and Fig. 3.6.

The procedure of Sections 3.1 and 3.2 leads to the values of S, Y, and V at mesh points of the characteristic net. To make this into a solution in terms of X and T, it is necessary to determine the characteristic net, i.e. to find values of X and T at each mesh point. For this we find a curve between X and T, which will be the leading-wave front characteristic curve. Other characteristic curves of the same family are parallel to it at intervals of $2\Delta T$ above it.

To obtain the leading wave front we start from the equation of the characteristic

$$dX = C\,dT$$

$$\text{or} \quad T = \int_o^X \frac{1}{C}\, dX \tag{3.13}$$

Eq. (3.13) is integrated by Simpson's rule, using the numerical data cited above in Figures 3.5 and 3.6 (non-dimensionalized). The interval from 0 to X is divided into 2m equal intervals by points

X_0, X_1, X_2, ..., X_{2m}, and the integral is evaluated by the following numerical Simpson's rule. (See for example Milne (1949), page 121.)

$$\int_{X_o}^{X_{2m}} y\, dX = \frac{h}{3} \{ y_o + y_{2m} + 4 (y_1 + y_3 + \ldots + y_{2m-1}) + 2 (y_2 + y_4 + \ldots + y_{2m-2}) \}$$

In Fig. 3.7 and Fig. 3.8 curves between dimensional values of x and t are shown for the leading wave front. These were obtained by integrating the dimensionalized form of Eq. (3.13). The reason for the equal x intervals here is that the experimental data on temperature was taken at points spaced at equal distances. The mesh-point values for equal time intervals were subsequently obtained by interpolation. At first glance these curves may appear straight, but a closer look will disclose definite deviations from linearity in the heated region, around 30 inches from the end in Fig. 3.7, and near the hot end in Fig. 3.8.

3.4. Calculation Procedure

Three types of temperature distribution conditions are of interest for pulse propagation in a bar subjected to a longitudinal impact.

1. One end hot and the other cold. Impact at the hot end.
2. One end hot and the other cold. Impact at the cold end.
3. Both ends cold. Hot region in the middle of the bar.

The numerical and experimental procedures for the first two cases are similar, so only the first and the third cases are considered here.

3.4(a). Impact at the Hot End of the Bar Fig. 3.9(a)

Assuming that the shape and the magnitude of the incident pulse are known, the field of characteristics is calculated first, choosing a suitable time interval. The time interval was considered sufficiently small if a solution obtained by choosing the grid still smaller only changes the sixth digit of the solution. Along the leading wave front the values of the stress, strain, and the velocity are zero for a continuously rising pulse. The procedure is illustrated by the schematic drawing of Fig. 3.10. The slope of the characteristics varies in the region where the temperature varies, and is constant where the temperature is uniform.

For a finite bar, for which we have to consider the reflections from the ends, the total time taken for the wave front to travel from one end to the other end of the bar is calculated from the leading wave-front XT-curve. Then a time interval of the grid is calculated by dividing the total time by the number of divisions estimated to be large enough for sufficient accuracy. The grid spacing can also be manipulated so that the grid point falls on the bar at a point where a strain gage is mounted in the experimental measurements, in order to obtain directly the calculated values without plotting extra curves.

Following the procedure mentioned in Sec. 3.2 and solving Eq. (3.8), Eq. (3.10), and Eq. (3.12), the value for non-dimensional stress and velocity can be calculated at all the points of the grid.

3.4(b). Hot Region in the Middle of the Bar

This is the case in which a traveling pulse passes through a temperature gradient like that of Fig. 3.9(b). Again assuming the incident pulse is known, the field of characteristics is calculated first with a suitable time interval. The field of characteristics is shown schematically in Fig. (3.11). Again characteristics have varying slope in the region of varying temperature and become straight where temperature is uniform. Grid spacing is again calculated for convenience, accuracy, and position of the gage station in experimental measurements.

Again solving Eq. (3.8), Eq. (3.10), and Eq. (3.12), and introducing the boundary conditions, the non-dimensional value of the stress and velocity can be calculated at all the points of the grid.

Plotting the value of stress or strain on all the grid points on a line X equal to a constant X_1, the stress versus time or strain versus time curve can be obtained for the point on the bar at distance X_1 from the impacted end.

3.5. Description of the Problem

Two types of pulse propagation problems were solved by the numerical methods. The solutions, obtained by the method of characteristics, are given in Sec. 7. The two problems solved to compare with the experiments are

1. Bar Heated at the Middle. A 6-foot-long bar was heated at the middle to a maximum temperature of 1200°F and impacted longitudinally at one end by a 4-foot-long striker bar. The

temperature distribution in the bar is given in Fig. 3.2. The solutions of the pulse propagation were obtained and compared at the location of the strain gages in the experimental set-up described in Sec. 5.2, i.e. two room-temperature gages located one foot from each end of the bar and one high-temperature gage located at the middle of the bar.

2. Bar Heated at Impacted End. A 4-foot-long bar was heated at one end to a maximum temperature of 1200°F and impacted as in the first case. The temperature distribution in the bar is given in Fig. 3.3. Again the solutions were obtained and compared at the location of the strain gages in the experimental set-up described in Sec. 5.2.

In the first problem the temperature was measured at 22 points spaced 0.8 inches apart, starting from the center of the bar, and in the second problem the temperature was measured at 16 points spaced one inch apart starting from the hot end. The description of the experimental measurements is given in Sec. 5.4. With these measured values of temperature the values of the elastic modulus were obtained from the linear relation of Fig. 3.4 and the wave speed $c(x) = \sqrt{E(x)/\rho}$ calculated as plotted in Fig. 3.5.

For the first problem, the incident pulse was obtained from the output (Fig. 7.1) of the first room-temperature strain gage, located one foot from the impacted end (Fig. 5.3) before the reflections from the thermal gradient reached it. The pulse being flat-topped when reflections are absent (Fig. 7.1a), the incident pulse was assumed to be 486 microseconds long and flat-topped with an amplitude given by

the first room-temperature gage. The incident pulse obtained from the oscilloscope record of Fig. 7.1b is shown in Fig. 3.12; it was used in the solution of the problem as input data for the computer program described in Appendix B. This strain pulse at the room-temperature gage station was converted to stress by multiplication with the room-temperature elastic modulus. Because the recording station is so far from the impact end, three-dimensional effects are believed insignificant in this problem.

For the second problem, the incident pulse was obtained from the output (Fig. 7.2) of the room-temperature gage located on the striker bar (Fig. 5.3) 25 inches from the impact end. The incident pulse was assumed to be 486 microseconds long and flat-topped with an amplitude obtained from the gage on the striker bar. The incident pulse obtained from the oscilloscope record of Fig. 7.2b is shown in Fig. 3.13. It was used in the numerical solution of the problem as input data for the computer program described in Appendix B. This strain pulse in the room-temperature striker bar is assumed convertible to stress at the impact end of the specimen by multiplication with the room-temperature elastic modulus. The assumption neglects three-dimensional effects in the vicinity of the impact ends of the two bars. Since three-dimensional effects are known to be present at the impact end (see Bell, 1960), some error may be introduced by the simplifying assumption used.

The incident pulses shown in Fig. 3.12 and Fig. 3.13 are obtained by drawing a smooth curve through the experimentally measured points. As can be seen in Figs. 7.1 and 7.2 there was

noise on the signal. Experimental points were measured only at points clearly on the pulse.

The Fortran programs for numerical solution of both of the above mentioned problems have been described in Appendix B and programs are given at the end of the Appendix. The results obtained from the numerical solution of these problems have been given and discussed in Sec. 7.3.

The programs were also used for three other problems:

3. Verification of Chiddister's (1961) Results. This was the first calculation made with the program written for Problem 1 above in order to check the program. The results of this calculation showed good agreement with Chiddister's results, obtained by approximating the thermal gradient with five step discontinuities. These results are not reproduced in this dissertation.

4. Verification of Lindholm's (1963) Results. Lindholm calculated the propagation of a half-sine-wave pulse along a bar with $E = E_o(\frac{x}{kL})^n$. The results are discussed in Sec. 7.1 (c.iii).

5. Modified Lindholm Problem. To demonstrate that reflections would be obtained from a steeper gradient varying as a power law, the following problem was solved. With the same values of maximum and minimum E, the length of the part of the bar where the inhomogeneity existed was reduced to one-fourth the length of the bar in Lindholm's third problem, with the variation following the same cubic law as in his problem, and E was taken uniform along the other three-fourths of the bar. The length of the pulse was again taken approximately one-fourth of the length of the bar. This gave a

c(x) of the form

$$c(x) = c_o\left[1 + .296\,(x - \tfrac{3}{4}L)^{3/2}\right]$$

in the region where E was varying. The results are given in Sec. 7.1 (c.iii).

CHAPTER IV

PERIODIC VIBRATIONS

4.1. Introduction

The solution of the wave equation for the periodic vibrations of a bar with a thermally-induced longitudinal inhomogeneity can be obtained numerically for a general kind of inhomogeneity, and analytically for some specific kinds of inhomogeneity. Analytic solutions of the wave equation in a bar with a thermal gradient have apparently been obtained only for cases where the inhomogeneity in the modulus of elasticity caused by the thermal gradient is of the following types:

1. $E(x) = E_o + kx$ (Datta, 1956)

2. $E(x) = E_o e^{kx}$ (Sur, 1961)

3. $E(x) = E_o (\frac{x}{kL})^n$ (Lindholm, 1963)

and the variation in density is assumed negligible. The analytic solution method is discussed in Sec. 4.2. For a general case of inhomogeneity we have to use numerical methods for the solution of the wave equation because of the absence of analytic solutions. The numerical method is described in Sec. 4.3.

Both the analytic solutions and numerical solutions are obtained for two types of boundary conditions: first a free-free bar with a source of disturbance producing periodic displacement at the hot end;

and second a free-free bar with a source of disturbance producing periodic stress at the hot end. The solutions in each case are obtained both for the displacement amplitude and the stress amplitude of the periodic vibrations. The analytic and numerical results obtained for a 20-inch-long Type 303 stainless steel bar with various types of inhomogeneity are discussed in Section 7.4.

4.2. Analytic Solutions

4.2(a). $E(x) = E_o + kx$

4.2(a.i). Displacement Wave Equation

From Eq. (2.9), neglecting variations in ρ, the differential equation is

$$\frac{\partial}{\partial x} \left(E(x) \frac{\partial u}{\partial x}\right) = \rho \frac{\partial^2 u}{\partial t^2}$$

Substituting the value of $E(x)$ we get

$$\frac{\partial}{\partial x} \left\{ (E_o + kx) \frac{\partial u}{\partial x} \right\} = \rho \frac{\partial^2 u}{\partial t^2} \tag{4.1}$$

To obtain a periodic solution of Eq. (4.1) let

$$u(x, t) = u(x)\, e^{i\omega t}$$

The resulting ordinary differential equation for $u(x)$ is

$$(E_o + kx) \frac{d^2 u}{dx^2} + k \frac{du}{dx} + \rho\omega^2 = 0 \tag{4.2}$$

We transform this equation to a Bessel's equation, Eq. (4.4) below, by the following substitutions. First let

$$z = E_o + kx$$

to obtain

$$z \frac{d^2u}{dz^2} + \frac{du}{dz} + \rho \frac{\omega^2}{k^2} u = 0 \qquad (4.3)$$

Then substitute

$$z = \frac{s^2k^2}{4\rho\omega^2} \qquad \text{or} \qquad s = \frac{2\omega\sqrt{\rho z}}{2k}$$

$$\frac{ds}{dz} = \frac{\omega\sqrt{\rho}}{k} z^{-1/2} \qquad \text{and} \qquad \frac{d^2s}{dz^2} = -\frac{\omega\sqrt{\rho}}{2k} z^{-3/2}$$

to transform Eq. (4.3), after division by $\frac{\omega^2\rho}{k^2}$, to

$$\frac{d^2u}{ds^2} + \frac{1}{s}\frac{du}{ds} + u = 0 \qquad (4.4)$$

which is a Bessel's equation with general solution

$$u = AJ_o(s) + BY_o(s) \qquad (4.5)$$

Hence the complete solution as given by Datta (1956) is

$$u(x, t) = \{ AJ_o(\frac{2\omega\sqrt{\rho z}}{k}) + BY_o(\frac{2\omega\sqrt{\rho z}}{k}) \} \; e^{i\omega t} \qquad (4.6)$$

where

$$z = E_o + kx$$

A and B are determined from the Boundary Conditions.

Case 1 Let there be a source of disturbance producing periodic displacement $Ue^{i\omega t}$ at $x = L$, and let the end $x = 0$ be

free. The boundary conditions are

$$u]_{x=L} = Ue^{i\omega t}$$

$$\frac{\partial u}{\partial x}]_{x=0} = 0$$

From Eq. (4.6),

$$\frac{\partial u}{\partial x} = -\frac{k}{2\sqrt{x}}\left[A\left\{\frac{2\omega\sqrt{\rho}}{k} J_1\left(\frac{2\omega\sqrt{\rho z}}{k}\right)\right\} + B\left\{\frac{2\omega\sqrt{\rho}}{k} Y_1\left(\frac{2\omega\sqrt{\rho z}}{k}\right)\right\}\right] e^{i\omega t} \tag{4.7}$$

Now, if we denote z at $x = 0$ by z_o, and z at $x = L$ by z_L, the second boundary condition yields

$$A = -B \frac{Y_1\left(\frac{2\omega\sqrt{\rho z_o}}{k}\right)}{J_1\left(\frac{2\omega\sqrt{\rho z_o}}{k}\right)} \tag{4.8}$$

so that

$$u = B \frac{1}{J_1\left(\frac{2\omega\sqrt{\rho z_o}}{k}\right)} \left\{ -J_o\left(\frac{2\omega\sqrt{\rho z}}{k}\right) Y_1\left(\frac{2\omega\sqrt{\rho z_o}}{k}\right) + Y_o\left(\frac{2\omega\sqrt{\rho z}}{k}\right) J_1\left(\frac{2\omega\sqrt{\rho z_o}}{k}\right)\right\} e^{i\omega t} \tag{4.8}$$

With

$$D_1 = Y_o\left(\frac{2\omega\sqrt{\rho z_L}}{k}\right) J_1\left(\frac{2\omega\sqrt{\rho z_o}}{k}\right) - J_o\left(\frac{2\omega\sqrt{\rho z_L}}{k}\right) Y_1\left(\frac{2\omega\sqrt{\rho z_o}}{k}\right)$$

the first boundary condition yields

$$A = -\frac{U}{D_1} \; Y_1 \left(\frac{2\omega\sqrt{\rho z_o}}{k}\right)$$

and

$$B = \frac{U}{D_1} \; J_1 \left(\frac{2\omega\sqrt{\rho z_o}}{k}\right) \qquad (4.9)$$

Eq. (4.9) is the same as given by Datta (1956).

Substituting these values of A and B in Eq. (4.6), we obtain the value of u(x, t). The stress σ (x, t) is given by

$$\sigma(x, t) = E(x)\epsilon = (E_o + kx)\frac{\partial u}{\partial x} = kz\frac{\partial u}{\partial z}$$

so that

$$\sigma(x, t) = -\omega\sqrt{\rho z}\left\{ A J_1 \left(\frac{2\omega\sqrt{\rho z}}{k}\right) + B Y_1 \left(\frac{2\omega\sqrt{\rho z}}{k}\right)\right\} e^{i\omega t} \qquad (4.10)$$

where A and B are given by Eq. (4.9).

Case 2 Let there be a source of disturbance producing a periodic stress $Pe^{i\omega t}$ at x = L, and let the end x = 0 be free. The boundary conditions are

$$(E_o + kx)\frac{\partial u}{\partial x}\Big]_{x=L} = Pe^{i\omega t}$$

$$\frac{\partial u}{\partial x}\Big]_{x=0} = 0$$

Again the second boundary condition yields Eq. (4.8). Using the first boundary condition and writing

$$D_2 = Y_1 \left(\frac{2\omega\sqrt{\rho z_L}}{k}\right) J_1 \left(\frac{2\omega\sqrt{\rho z_o}}{k}\right) - J_1 \left(\frac{2\omega\sqrt{\rho z_L}}{k}\right) Y_1 \left(\frac{2\omega\sqrt{\rho z_o}}{k}\right)$$

we get

$$P = B \frac{\sqrt{\rho z_L}\,\omega(-D_2)}{J_1\left(\frac{2\omega\sqrt{\rho z_o}}{k}\right)}$$

whence

$$\left.\begin{aligned} A &= P \frac{Y_1\left(\frac{2\omega\sqrt{\rho z_o}}{k}\right)}{\omega\sqrt{\rho z_L}\, D_2} \\ \text{and} \\ B &= -P \frac{J_1\left(\frac{2\omega\sqrt{\rho z_o}}{k}\right)}{\omega\sqrt{\rho z_L}\, D_2} \end{aligned}\right\} \qquad (4.11)$$

Eq. (4.11) is the same as that given by Datta (1956). Substituting these values of A and B in Eq. (4.6) we obtain the value of u(x, t), and in Eq. (4.10) we obtain the value of σ (x, t).

4.2(a.ii) Stress Wave Equation

The differential equation is Eq. (2.13) when variations in ρ are neglected.

$$E(x) \frac{\partial^2 \sigma}{\partial x^2} = \rho \frac{\partial^2 \sigma}{\partial t^2}$$

Substituting the value of E(x) we get

$$(E_o + kx) \frac{\partial^2 \sigma}{\partial x^2} = \rho \frac{\partial^2 \sigma}{\partial t^2} \qquad (4.12)$$

To obtain a periodic solution of Eq. (4.12) let

$$\sigma(x, t) = \sigma(x)\, e^{i\omega t}$$

The resulting ordinary differential equation for $\sigma(x)$ is

$$(E_o + kx)\ \frac{d^2\sigma}{dx^2} + \rho\omega^2\sigma = 0 \qquad (4.13)$$

We transform this equation to a Bessel's equation, Eq. (4.16) below, by the following substitutions. First let

$$z = E_o + kx$$

to obtain

$$z\,k^2\ \frac{d^2\sigma}{dz^2} + \rho\omega^2\sigma = 0 \qquad (4.14)$$

Then substitute

$$z = \frac{s^2k^2}{4\rho\omega^2} \qquad \text{or} \qquad s = \frac{2\omega\sqrt{\rho z}}{k}$$

to transform equation (4.14), after division by $\omega^2\rho$, to

$$\frac{d^2\sigma}{ds^2} - \frac{1}{s}\ \frac{d\sigma}{ds} + \sigma = 0 \qquad (4.15)$$

Finally the change of dependent variable

$$\sigma = s\theta$$

brings Eq. (4.15) into a convenient form of the Bessel's equation

$$\frac{d^2\theta}{ds^2} + \frac{1}{s}\ \frac{d\theta}{ds} + \left(1 - \frac{1}{s^2}\right)\theta = 0 \qquad (4.16)$$

whose general solution is

$$\theta = A\,J_1(s) + B\,Y_1(s)$$

so that

$$\sigma = s\{A J_1(s) + B Y_1(s)\} \tag{4.17}$$

Hence the complete solution of the wave equation Eq. (4.12) is

$$\sigma(x,t) = \frac{2\omega\sqrt{\rho z}}{k} \{ A J_1 (\frac{2\omega\sqrt{\rho z}}{k}) + B Y_1 (\frac{2\omega\sqrt{\rho z}}{k})\} e^{i\omega t} \tag{4.18}$$

A and B are determined from the boundary conditions.

Example Let there be a source of disturbance producing a periodic stress $Pe^{i\omega t}$ at $x = L$, and let the end $x = 0$ be free. The boundary conditions are

$$\sigma]_{x=L} = Pe^{i\omega t}$$

$$\sigma]_{x=0} = 0$$

The secondary boundary condition yields

$$A = - B \frac{Y_1 (\frac{2\omega\sqrt{\rho z_o}}{k})}{J_1 (\frac{2\omega\sqrt{\rho z_o}}{k})}$$

so that

$$\sigma(x,t) = \frac{2\omega\sqrt{\rho z}}{k} \frac{B}{J_1 (\frac{2\omega\sqrt{\rho z_o}}{k})} \{ Y_1 (\frac{2\omega\sqrt{\rho z}}{k}) J_1 (\frac{2\omega\sqrt{\rho z_o}}{k}) - Y_1 (\frac{2\omega\sqrt{\rho z_o}}{k}) J_1 (\frac{2\omega\sqrt{\rho z}}{k}) \} e^{i\omega t} \tag{4.19}$$

With

$$D_2 = Y_1 (\frac{2\omega\sqrt{\rho z_L}}{k}) J_1 (\frac{2\omega\sqrt{\rho z_o}}{k}) - Y_1 (\frac{2\omega\sqrt{\rho z_o}}{k}) J_1 (\frac{2\omega\sqrt{\rho z_L}}{k})$$

the first boundary condition yields

$$P = \frac{2\omega\sqrt{\rho z_L}}{k} \frac{D_2}{J_1\left(\frac{2\omega\sqrt{\rho z_o}}{k}\right)} B$$

whence

$$\left.\begin{aligned} A &= -P \frac{k}{2\omega\sqrt{\rho z_L}} \frac{Y_1\left(\frac{2\omega\sqrt{\rho z_o}}{k}\right)}{D_2} \\ \text{and} \\ B &= P \frac{k}{2\omega\sqrt{\rho z_L}} \frac{J_1\left(\frac{2\omega\sqrt{\rho z_o}}{k}\right)}{D_2} \end{aligned}\right\} \quad (4.20)$$

Substituting the values of A and B in Eq. (4.18) we obtain the value of $\sigma(x, t)$.

4.2(b). $E(x) = E_o e^{kx}$

4.2(b.i). Displacement Wave Equation

From Eq. (2.9), neglecting variations in ρ, the differential equation is

$$\frac{\partial}{\partial x}\left(E(x) \frac{\partial u}{\partial x}\right) = \rho \frac{\partial^2 u}{\partial t^2}$$

Substituting the value of $E(x)$ we get

$$\frac{\partial}{\partial x}\left(E_o e^{kx} \frac{\partial u}{\partial x}\right) = \rho \frac{\partial^2 u}{\partial t^2} \quad (4.21)$$

Let

$$z = e^{-kx}$$

Then Eq. (4.21) becomes

$$E_o k^2 z \frac{\partial^2 u}{\partial z^2} = \rho \frac{\partial^2 u}{\partial t^2} \quad (4.22)$$

To obtain a periodic solution of Eq. (4.22) let

$$u(z,t) = u(z)\,e^{i\omega t}$$

Then Eq. (4.22) yields an ordinary differential equation for $u(z)$

$$z\,\frac{d^2u}{dz^2} + \frac{\rho\omega^2}{E_o k^2}\,u = 0 \qquad (4.23)$$

To transform this into Bessel's equation, Eq. (4.25) below, let

$$z = \frac{s^2k^2E_o}{4\rho\omega^2} \qquad \text{or} \qquad s = \frac{2\omega}{k}\sqrt{\frac{\rho z}{E_o}}$$

$$\frac{ds}{dz} = \frac{\omega}{k}\sqrt{\frac{\rho}{E_o z}}$$

After division by $\frac{\omega^2\rho}{k^2E_o}$, Eq. (4.23) becomes

$$\frac{d^2u}{ds^2} - \frac{1}{s}\,\frac{du}{ds} + u = 0 \qquad (4.24)$$

The change of dependent variable $u = s\theta$ then transforms Eq. (4.24) into

$$\frac{d^2\theta}{ds^2} + \frac{1}{s}\,\frac{d\theta}{ds} + \left(1 - \frac{1}{s^2}\right)\theta = 0 \qquad (4.25)$$

This Bessel's equation has the general solution

$$\theta = A\,J_1(s) + B\,Y_1(s)$$

so that

$$u = s\{A\,J_1(s) + B\,Y_1(s)\} \qquad (4.26)$$

Hence the complete solution of Eq. (4.21), as given by Sur (1961), is with $z = e^{-kx}$

$$u(x, t) = \frac{2\omega}{k}\sqrt{\frac{\rho z}{E_o}}\left\{A\, J_1\left(\frac{2\omega}{k}\sqrt{\frac{\rho z}{E_o}}\right) + B\, Y_1\left(\frac{2\omega}{k}\sqrt{\frac{\rho z}{E_o}}\right)\right\} e^{i\omega t} \qquad (4.27)$$

A and B are determined from the boundary conditions.

Case 1 Let there be a source of disturbance producing periodic displacement $Ue^{i\omega t}$ at $x = L$, and let the end $x = 0$ be free. The boundary conditions are

$$u\big]_{x=L} = Ue^{i\omega t}$$

$$\frac{\partial u}{\partial x}\Big]_{x=0} = 0$$

Now, from Eq. (4.27)

$$\frac{\partial u}{\partial x} = -\frac{2\omega^2}{k}\frac{\rho z}{E_o}\left\{A\, J_o\left(\frac{2\omega}{k}\sqrt{\frac{\rho z}{E_o}}\right) + B\, Y_o\left(\frac{2\omega}{k}\sqrt{\frac{\rho z}{E_o}}\right)\right\} e^{i\omega t} \qquad (4.28)$$

Hence from the second boundary condition

$$A = -B\,\frac{Y_o\left(\frac{2\omega}{k}\sqrt{\frac{\rho z_o}{E_o}}\right)}{J_o\left(\frac{2\omega}{k}\sqrt{\frac{\rho z_o}{E_o}}\right)} \qquad (4.29)$$

Writing (note $z_o = 1$)

$$s_o = \frac{2\omega}{k}\sqrt{\frac{\rho z_o}{E_o}} \qquad z\big]_{x=0} = z_o = 1 \quad \text{and} \quad z\big]_{x=L} = z_L$$

and

$$D_3 = Y_1\left(\frac{2\omega}{k}\sqrt{\frac{\rho z_L}{E_o}}\right) J_o\left(\frac{2\omega}{k}\sqrt{\frac{\rho z_o}{E_o}}\right) - J_1\left(\frac{2\omega}{k}\sqrt{\frac{\rho z_L}{E_o}}\right) \cdot Y_o\left(\frac{2\omega}{k}\sqrt{\frac{\rho z_o}{E_o}}\right)$$

we get

$$u(x,t) = B \frac{s}{J_o(s_o)} \{ Y_1(s) J_o(s_d) - J_1(s) Y_o(s_d) \} e^{i\omega t}$$

The first boundary condition then yields

$$\left.\begin{aligned} A &= -U \frac{k}{2\omega}\sqrt{\frac{E_o}{\rho z_L}} \quad \frac{Y_o\left(\frac{2\omega}{k}\sqrt{\frac{\rho z_o}{E_o}}\right)}{D_3} \\ B &= U \frac{k}{2\omega}\sqrt{\frac{E_o}{\rho z_L}} \quad \frac{J_o\left(\frac{2\omega}{k}\sqrt{\frac{\rho z_o}{E_o}}\right)}{D_3} \end{aligned}\right\} \quad (4.30)$$

Eq. (4.30) is the same as obtained by Sur (1961).

Substituting these values of A and B in equation (4.27), we obtain the value of $u(x,t)$. The stress $\sigma(x,t)$, is given by

$$\sigma(x,t) = E_o e^{kx} \left(\frac{\partial u}{\partial x}\right)$$

or, using Eq. (4.28)

$$\sigma(x,t) = -\frac{2\omega^2 \rho}{k} \{ A J_o(s) + B Y_o(s) \} e^{i\omega t} \quad (4.31)$$

where A and B are given by the Eq. (4.30).

Case 2 Let there be a source of disturbance producing periodic stress $P e^{i\omega t}$ at $x = L$, and let the end $x = 0$ be free. The boundary conditions are

$$E_o e^{kx} \left.\frac{\partial u}{\partial x}\right]_{x=L} = P e^{i\omega t}$$

$$\left.\frac{\partial u}{\partial x}\right]_{x=0} = 0$$

Again the second boundary condition yields Eq. (4.29) and with

$$D_4 = Y_o\left(\frac{2\omega}{k}\sqrt{\frac{\rho z_L}{E_o}}\right) J_o\left(\frac{2\omega}{k}\sqrt{\frac{\rho z_o}{E_o}}\right) - J_o\left(\frac{2\omega}{k}\sqrt{\frac{\rho z_L}{E_o}}\right) Y_o\left(\frac{2\omega}{k}\sqrt{\frac{\rho z_o}{E_o}}\right)$$

the other boundary condition yields

$$\left.\begin{aligned} A &= P\ \frac{k}{2\omega^2\rho}\ \left\{\ \frac{Y_o\left(\frac{2\omega}{k}\sqrt{\frac{\rho z_o}{E_o}}\right)}{D_4}\ \right\} \\ B &= -\ P\ \frac{k}{2\omega^2\rho}\ \ \frac{J_o\left(\frac{2\omega}{k}\sqrt{\frac{\rho z_o}{E_o}}\right)}{D_4} \end{aligned}\right\} \qquad (4.32)$$

Eq. (4.32) is the same as obtained by Sur (1961). Substituting the values of A and B in Eq. (4.27) we obtain the value of $u(x, t)$, and in Eq. (4.31) we obtain the value of $\sigma(x, t)$.

4.2(b.ii). Stress Wave Equation

The differential equation, neglecting variation in ρ, is again from Eq. (2.13)

$$E(x)\ \frac{\partial^2\sigma}{\partial x^2} = \rho\ \frac{\partial^2\sigma}{\partial t^2}$$

Substituting the value of $E(x)$ we get

$$E_o\ e^{kx}\ \ \frac{\partial^2\sigma}{\partial x^2} = \rho\ \frac{\partial^2\sigma}{\partial t^2} \qquad (4.33)$$

To obtain a periodic solution of Eq. (4.33) let

$$\sigma(x, t) = \sigma(x)\ e^{i\omega t}$$

Eq. (4.33) yields an ordinary differential equation for $\sigma(x)$.

$$E_o e^{kx} \frac{d^2\sigma}{dx^2} + \rho\omega^2\sigma = 0 \qquad (4.34)$$

This can also be brought into a standard form of Bessel's equation, Eq. (4.36) below, by the following substitutions. First let

$$z = e^{-kx}$$

to obtain

$$z \frac{d^2\sigma}{dz^2} + \frac{d\sigma}{dz} + \frac{\rho\omega^2}{E_o k^2}\sigma = 0 \qquad (4.35)$$

Then substitute

$$z = \frac{E_o s^2 k^2}{4\rho\omega^2}$$

or

$$s = \frac{2\omega}{k}\sqrt{\frac{\rho z}{E_o}} \quad , \quad \frac{ds}{dz} = \frac{\omega}{k}\sqrt{\frac{\rho}{E_o z}}$$

to transform Eq. (4.35), after dividing by $\frac{\omega^2\rho}{k^2 E_o}$, to

$$\frac{d^2\sigma}{ds^2} + \frac{1}{s}\frac{d\sigma}{ds} + \sigma = 0 \qquad (4.36)$$

whose general solution is

$$\sigma = A J_o(s) + B Y_o(s) \qquad (4.37)$$

Hence the complete solution of Eq. (4.33) is

$$\sigma(x,t) = \{ A J_o(\frac{2\omega}{k}\sqrt{\frac{\rho z}{E_o}}) + B Y_o(\frac{2\omega}{k}\sqrt{\frac{\rho z}{E_o}}) \} e^{i\omega t} \qquad (4.38)$$

Again A and B are determined from the boundary conditions.

Example Let there be a source of disturbance producing a periodic stress $Pe^{i\omega t}$ at $x = L$, and let the end $x = 0$ be free. The boundary conditions are

$$\sigma \Big]_{x=L} = Pe^{i\omega t}$$

$$\sigma \Big]_{x=0} = 0$$

From the second boundary condition

$$A = - B \frac{Y_o(\frac{2\omega}{k}\sqrt{\frac{\rho z_o}{E_o}})}{J_o(\frac{2\omega}{k}\sqrt{\frac{\rho z_o}{E_o}})}$$

so that

$$\sigma(x, t) = \frac{B}{J_o(s_o)} \{ -J_o(s) Y_o(s_o) + Y_o(s) J_o(s_o) \} e^{i\omega t} \quad (4.39)$$

Again with

$$D_4 = - J_o(\frac{2\omega}{k}\sqrt{\frac{\rho z_L}{E_o}}) Y_o(\frac{2\omega}{k}\sqrt{\frac{\rho z_o}{E_o}}) + Y_o(\frac{2\omega}{k}\sqrt{\frac{\rho z_L}{E_o}}) J_o(\frac{2\omega}{k}\sqrt{\frac{\rho z_o}{E_o}})$$

the first boundary condition yields

$$\left.\begin{aligned} A &= - P \frac{Y_o(\frac{2\omega}{k}\sqrt{\frac{\rho z_o}{E_o}})}{D_4} \\ B &= + P \frac{J_o(\frac{2\omega}{k}\sqrt{\frac{\rho z_o}{E_o}})}{D_4} \end{aligned}\right\} \quad (4.40)$$

Using the values of A and B in Eq. (4.38) we obtain the value of σ (x, t).

4.2(c). $E(x) = E_o \left(\frac{x}{kL}\right)^n$

Here E_o is the elastic modulus at $x = kL$, n may assume any real value, and k is a constant whose value determines the total amount of variation of the modulus in a bar of given length. In the examples treated the bar will lie between $x = kL$ and $x = (k+1)L$ (see Lindholm, 1963).

4.2(c.i). Displacement Wave Equation

From Eq. (2.9), neglecting variation in ρ, the differential equation is

$$\frac{\partial}{\partial x}\left(E(x)\,\frac{\partial u}{\partial x}\right) = \rho\,\frac{\partial^2 u}{\partial t^2}$$

Substituting the value of E(x) we obtain

$$\frac{\partial}{\partial x}\left\{E_o\left(\frac{x}{kL}\right)^n \frac{\partial u}{\partial x}\right\} = \rho\,\frac{\partial^2 u}{\partial t^2} \tag{4.41}$$

$$E_o\left(\frac{x}{kL}\right)^n \frac{\partial^2 u}{\partial x^2} + E_o\,\frac{n}{kL}\left(\frac{x}{kL}\right)^{n-1}\frac{\partial u}{\partial x} = \rho\,\frac{\partial^2 u}{\partial t^2}$$

For a periodic solution let

$$u(x, t) = u(x)\, e^{i\omega t}$$

to obtain an ordinary differential equation for u(x)

$$E_o\left(\frac{x}{kL}\right)^n \frac{d^2 u}{dx^2} + E_o\,\frac{n}{kL}\left(\frac{x}{kL}\right)^{n-1}\frac{du}{dx} + \rho\omega^2 u = 0 \tag{4.42}$$

For $n \neq 2$ we transform this to a Bessel's equation, Eq. (4.44), by the following subsitutions. The case $n = 2$ is treated separately, beginning with Eq. (4.52). First let

$$z = x/kL$$

to obtain

$$\frac{d^2u}{dz^2} + \frac{n}{z}\frac{du}{dz} + \frac{\rho\omega^2k^2L^2}{E_o}\frac{1}{z^n}u = 0 \qquad (4.43)$$

Then let $u = z^{(\frac{1-n}{2})}\theta$

whence

$$\frac{du}{dz} = \frac{1-n}{2}z^{(\frac{-1-n}{2})}\theta + z^{(\frac{1-n}{2})}\frac{d\theta}{dz}$$

and

$$\frac{d^2u}{dz^2} = (\frac{1-n}{2})(\frac{-1-n}{2})z^{(\frac{-3-n}{2})}\theta + (1-n)z^{(\frac{-1-n}{2})}\frac{d\theta}{dz} + z^{(\frac{1-n}{2})}\frac{d^2\theta}{dz^2}$$

Substituting these in equation (4.43) and dividing by $z^{(\frac{1-n}{2})}$ we obtain

$$\frac{d^2\theta}{dz^2} + \frac{1}{z}\frac{d\theta}{dz} - \{(\frac{1-n}{2})^2\frac{1}{z^2} - \frac{1}{z^n}\frac{\rho\omega^2k^2L^2}{E_o}\}\theta = 0$$

Now let

$$y = (\frac{2}{2-n})\omega kL\sqrt{\frac{\rho}{E_o}}z^{(\frac{2-n}{2})}$$

$$\frac{dy}{dz} = \omega kL\sqrt{\frac{\rho}{E_o}}z^{-n/2}$$

$$\frac{d^2y}{dz^2} = \frac{-n}{2}\omega kL\sqrt{\frac{\rho}{E_o}}z^{(\frac{-2-n}{2})}$$

to obtain, after collecting terms and dividing by $\frac{\omega^2 k^2 L^2 \rho\, z^{-n}}{E_o}$,

$$\frac{d^2\theta}{dy^2} + \frac{1}{y}\frac{d\theta}{dy} + \left\{ 1 - \frac{(1-n)^2}{2} \quad z^{(n-2)} \frac{E_o}{\omega^2 k^2 L^2 \rho} \right\} \theta = 0$$

which reduces to

$$\frac{d^2\theta}{dy^2} + \frac{1}{y}\frac{d\theta}{dy} + \left\{ 1 - \left(\frac{1-n}{2-n}\right)^2 \quad \frac{1}{y^2} \right\} \theta = 0 \qquad (4.44)$$

since

$$y^2 = \frac{4}{(2-n)^2} \quad \omega^2 k^2 L^2 \quad \frac{\rho}{E_o} \quad z^{(2-n)}$$

Eq. (4.44) is a Bessel's equation of order $p = \left| \frac{1-n}{2-n} \right|$ with the general solution

$$\theta = A\, J_p(y) + B\, Y_p(y)$$

whence

$$u = z^{\left(\frac{1-n}{2}\right)} \{ A\, J_p(y) + B\, Y_p(y) \qquad (4.45)$$

Hence the complete solution of the wave equation Eq. (4.41), for all values of n except 2, as given by Lindholm (1963), is

$$u(x, t) = z^{\left(\frac{1-n}{2}\right)} \{ A\, J_p(y) + B\, Y_p(y) \} \quad e^{i\omega t} \qquad (4.46)$$

where

$$z = \frac{x}{kL}$$

$$p = \left| \frac{1-n}{2-n} \right|$$

and

$$y = \left(\frac{2}{2-n}\right) \omega\, kL \sqrt{\frac{\rho}{E_o}} \quad \left(\frac{x}{kL}\right)^{\frac{2-n}{2}}$$

A and B are determined from the boundary conditions.

Case 1 Let there be a source of disturbance producing periodic displacement $Ue^{i\omega t}$ at $x = (k+1)L$, and let the end $x = kL$ be free. The boundary conditions are

$$u]_{x=(k+1)L} = Ue^{i\omega t}$$

$$\frac{\partial u}{\partial x}]_{x=kL} = 0$$

Now, from Eq. (4.46)

for $n < 1$ or $n > 2$

$$\frac{\partial u}{\partial x} = z^{\left(\frac{1-2n}{2}\right)} \omega \sqrt{\frac{\rho}{E_o}} \left\{ A J_{-\frac{1}{2-n}}(y) + B Y_{-\frac{1}{2-n}}(y) \right\} e^{i\omega t} \qquad (4.47)$$

and for $1 \leq n < 2$

$$\frac{\partial u}{\partial x} = - z^{\left(\frac{1-2n}{2}\right)} \omega \sqrt{\frac{\rho}{E_o}} \left\{ A J_{\frac{1}{2-n}}(y) + B Y_{\frac{1}{2-n}}(y) \right\} e^{i\omega t}$$

From the second boundary condition:

for $1 \leq n < 2$

$$A = - B \frac{Y_{\frac{1}{2-n}}(y_{kL})}{J_{\frac{1}{2-n}}(y_{kL})}$$

while for $n < 1$ and $n > 2$

$$A = - B \frac{Y_{-\frac{1}{2-n}}(y_{kL})}{J_{-\frac{1}{2-n}}(y_{kL})} \qquad (4.48)$$

With

$$D_5 = \{ Y_p(y_{(k+1)L}) J_r(y_{kL}) - J_p(y_{(k+1)L}) Y_r(y_{kL}) \}$$

the other boundary condition yields

$$Ue^{i\omega t} = \left(\frac{k+1}{k}\right)^{\frac{1-n}{2}} B\left\{ \frac{D_5}{J_r(y_{kL})} \right\} e^{i\omega t}$$

so that

$$\left.\begin{aligned} A &= -U\left(\frac{k}{k+1}\right)^{\frac{1-n}{2}} \left\{ \frac{Y_r(y_{kL})}{D_5} \right\} \\ \text{and} \\ B &= U\left(\frac{k}{k+1}\right)^{\frac{1-n}{2}} \left\{ \frac{J_r(y_{kL})}{D_5} \right\} \end{aligned}\right\} \qquad (4.49)$$

where

$$r = \frac{1}{2-n} \qquad \text{for } 1 \leq n < 2$$

$$r = -\frac{1}{2-n} \qquad \text{for } n < 1 \text{ and } n > 2$$

By substituting these values of A and B in Eq. (4.46), we can obtain the value of $u(x, t)$. The stress $\sigma(x, t)$ is given by

$$\sigma(x, t) = E(x)\epsilon = E_o \left(\frac{x}{kL}\right)^n \frac{\partial u}{\partial x}$$

Therefore from Eq. (4.47)

$$\sigma(x, t) = (n-2) E_o z^{1/2} \omega \sqrt{\frac{\rho}{E_o}} \{ A J_r(y) + B Y_r(y) \} e^{i\omega t} \qquad (4.50)$$

where

$$r = \frac{1}{2-n} \qquad \text{for } 1 \leq n < 2$$

$$r = -\frac{1}{2-n} \qquad \text{for } n < 1 \text{ and } n > 2$$

A and B are given by Eq. (4.49).

Case 2 Let there be a source of disturbance producing periodic stress $P e^{i\omega t}$ at $x = (k+1)L$, and let the end $x = kL$ be free. The boundary conditions are

$$E(x) \frac{\partial u}{\partial x}\Big]_{x=(k+1)L} = P e^{i\omega t}$$

$$\frac{\partial u}{\partial x}\Big]_{x=kL} = 0$$

Again, from the second boundary condition, with

$$D_6 = Y_r(y_{(k+1)L})\, J_r(y_{kL}) - J_r(y_{(k+1)L})\, Y_r(y_{kL})$$

we obtain

$$\left.\begin{aligned} A &= r(2-n)\, U \left(\frac{k}{k+1}\right)^{1/2} \frac{1}{\omega\sqrt{E_o \rho}} \left\{ \frac{Y_r(y_{kL})}{D_6} \right\} \\ B &= r(n-2) \quad U \left(\frac{k}{k+1}\right)^{1/2} \frac{1}{\omega\sqrt{E_o \rho}} \left\{ \frac{J_r(y_{kL})}{D_6} \right\} \end{aligned}\right\} \qquad (4.51)$$

where

$$r = \frac{1}{2-n} \qquad \text{for } 1 \leq n < 2$$

$$r = -\frac{1}{2-n} \qquad \text{for } n < 1 \text{ and } n > 2$$

Substituting these values of A and B into Eq. (4.46) we obtain the value of $u(x, t)$ and into Eq. (4.50) we obtain the value of $\sigma(x, t)$.

4.2(c.ii). Special Case for n = 2

For $n = 2$, the differential equation, Eq. (4.41), is

$$\frac{E_o}{k^2 L^2} \left(x^2 \frac{\partial^2 u}{\partial x^2} + 2x \frac{\partial u}{\partial x}\right) = \rho \frac{\partial^2 u}{\partial t^2} \tag{4.52}$$

For a periodic solution let $u = u(x)\, e^{i\omega t}$. Then $u(x)$ satisfies

$$x^2 \frac{d^2 u}{dx^2} + 2x \frac{du}{dx} + cu = 0 \tag{4.53}$$

where

$$c = \frac{\rho \omega^2 k^2 L^2}{E_o}$$

Let $z = \log_e x$ to obtain

$$\frac{d^2 u}{dz^2} + \frac{du}{dz} + cu = 0 \tag{4.54}$$

with general solution

$$u = x^{-z/2} \{ A \cos(gz) + B \sin(gz) \}$$

where

$$g = \sqrt{c - 1/4}$$

The complete solution of Eq. (4.52), as given by Lindholm (1963), is (with $z = \log_e x$)

$$u(x, t) = x^{-1/2} \{ A \cos(gz) + B \sin(gz) \}\ e^{i\omega t} \tag{4.55}$$

A and B are determined from the boundary conditions.

Case 1 Let there be a source of disturbance producing periodic displacement $U e^{i\omega t}$ at $x = (k+1)L$, and let the end $x = kL$ be free. The boundary conditions are

$$u]_{x=(k+1)L} = U e^{i\omega t}$$

$$\frac{\partial u}{\partial x}]_{x=kL} = 0$$

From Eq. (4.55)

$$\frac{\partial u}{\partial x} = \{ x^{-3/2} g[-A \sin(gz) + B \cos(gz)] - \frac{1}{2} x^{-3/2} [A \cos(gz) + B \sin(gz)]\} e^{i\omega t} \qquad (4.56)$$

From the second boundary condition

$$A = B \frac{g \cos(gz_o) - \frac{1}{2} \sin(gz_o)}{g \sin(gz_o) + \frac{1}{2} \cos(gz_o)} \qquad (4.57)$$

where

$$z_o = \log_e kL$$

Using the other boundary condition, and writing

$$z_L = \log_e (k+1)L$$

$$Y1_0 = g \sin(gz_o) + \frac{1}{2} \cos(gz_o)$$

$$Y1_L = g \sin(gz_L) + \frac{1}{2} \cos(gz_L)$$

$$Y2_0 = g \cos(gz_o) - \frac{1}{2} \sin(gz_o)$$

$$Y2_L = g \cos(gz_L) - \frac{1}{2} \sin(gz_L)$$

we obtain

$$\left.\begin{aligned} A &= U\{(k+1)L\}^{1/2} \frac{Y2_0}{Y2_0 \cos(gz_L) + Y1_0 \sin(gz_L)} \\ B &= U\{(k+1)L\}^{1/2} \frac{Y1_0}{Y2_0 \cos(gz_L) + Y1_0 \sin(gz_L)} \end{aligned}\right\} \quad (4.58)$$

Substituting these values of A and B into the Eq. (4.55) we obtain the value of u(x, t). The stress $\sigma(x, t)$ is given by

$$\sigma(x, t) = E(x)\,\epsilon = E_o \left(\frac{x}{kL}\right)^2 \frac{\partial u}{\partial x}$$

or from Eq. (4.56)

$$\sigma(x, t) = \frac{E_o x^{1/2}}{k^2 L^2} \left[-A\left\{ g \sin(gz) + \frac{1}{2} \cos(gz) \right\} + B\left\{ g \cos(gz) - \frac{1}{2} \sin(gz) \right\} \right] e^{i\omega t} \quad (4.59)$$

where A and B are given by Eq. (4.58).

Case 2 Let there be a source of disturbance producing periodic stress $Pe^{i\omega t}$ at $x = (k+1)L$, and let the end $x = kL$ be free. The boundary conditions are

$$E(x) \frac{\partial u}{\partial x}\Big]_{x=(k+1)L} = Pe^{i\omega t}$$

$$\frac{\partial u}{\partial x}\Big]_{x=kL} = 0$$

Again from the second boundary condition we obtain equation (4.57). Using the other boundary condition, and writing

$$Y1_0 = g \sin(gz_o) + \frac{1}{2} \cos(gz_o)$$

$$Y1_L = g \sin(gz_L) + \frac{1}{2} \cos(gz_L)$$

$$Y2_0 = g \cos(gz_o) - \frac{1}{2} \sin(gz_o)$$

$$Y2_L = g \cos(gz_L) - \frac{1}{2} \sin(gz_L)$$

we obtain

$$\left.\begin{aligned} A &= \frac{k^2 L^2}{E_o \{(k+1)L\}^{1/2}} \left\{ \frac{Y2_0}{Y1_0 Y2_L - Y2_0 Y1_L} \right\} P \\ B &= \frac{k^2 L^2}{E_o \{(k+1)L\}^{1/2}} \left\{ \frac{Y1_0}{Y1_0 Y2_L - Y2_0 Y1_L} \right\} P \end{aligned}\right\} \quad (4.60)$$

Substituting these values of A and B in Eq. (4.55) we obtain the value of $u(x, t)$ and in Eq. (4.59) we obtain the value of $\sigma(x, t)$.

4.2(d). E(x) = E a Constant

The differential equation is

$$E \frac{\partial^2 u}{\partial x^2} = \rho \frac{\partial^2 u}{\partial t^2} \quad (4.61)$$

$u(x,t) = u(x) e^{i\omega t}$

For a periodic solution let $u = ue^{i\omega t}$ so that $u(x)$ satisfies

$$\frac{d^2 u}{dx^2} + \frac{\rho}{E} \omega^2 u = 0 \quad (4.62)$$

with general solution

$$u = A \sin\left(\omega x \sqrt{\frac{\rho}{E}}\right) + B \cos\left(\omega x \sqrt{\frac{\rho}{E}}\right)$$

The complete solution of Eq. (4.61) is

$$u(x, t) = \left\{ A \sin\left(\omega x \sqrt{\frac{\rho}{E}}\right) + B \cos\left(\omega x \sqrt{\frac{\rho}{E}}\right) \right\} e^{i\omega t} \quad (4.63)$$

A and B are determined from the boundary conditions.

Case 1 Let there be a source of disturbance producing periodic displacement $Ue^{i\omega t}$ at $x = L$, and let the end $x = 0$ be free. The boundary conditions are

$$u]_{x=L} = Ue^{i\omega t}$$

$$\frac{\partial u}{\partial x}]_{x=0} = 0$$

From the second boundary condition $A = 0$, and

$$u(x, t) = B \cos (\omega x \sqrt{\frac{\rho}{E}}) \, e^{i\omega t}$$

From the other boundary condition

$$B = U \frac{1}{\cos (\omega L \sqrt{\frac{\rho}{E}})} \tag{4.64}$$

The complete solution is

$$u(x, t) = U \frac{\cos (\omega x \sqrt{\frac{\rho}{E}})}{\cos (\omega L \sqrt{\frac{\rho}{E}})} \, e^{i\omega t} \tag{4.65}$$

The stress $\sigma (x, t)$ is given by

$$\sigma (x, t) = E \frac{\partial u}{\partial x}$$

whence

$$\sigma (x, t) = - U \omega \sqrt{\rho E} \frac{\sin (\omega x \sqrt{\frac{\rho}{E}})}{\cos (\omega L \sqrt{\frac{\rho}{E}})} \, e^{i\omega t} \tag{4.66}$$

Case 2 Let there be a source of disturbance producing periodic stress $P e^{i\omega t}$ at $x = L$, and let the end $x = 0$ be free. The boundary conditions are

$$E \frac{\partial u}{\partial x}\Big]_{x=L} = P e^{i\omega t}$$

$$\frac{\partial u}{\partial x}\Big]_{x=0} = 0$$

From the second boundary condition we get $A = 0$, while the first boundary condition yields

$$B = - P \frac{1}{\omega\sqrt{\rho E}\ \sin\left(\omega L\sqrt{\frac{\rho}{E}}\right)}$$

$$u(x, t) = - P \frac{1}{\omega\sqrt{\rho\ E}} \frac{\cos\left(\omega x\sqrt{\frac{\rho}{E}}\right)}{\sin\left(\omega L\sqrt{\frac{\rho}{E}}\right)} e^{i\omega t} \qquad (4.67)$$

and

$$\sigma(x, t) = P \frac{\sin\left(\omega x\sqrt{\frac{\rho}{E}}\right)}{\sin\left(\omega L\sqrt{\frac{\rho}{E}}\right)} \qquad (4.68)$$

In both the cases of constant E

1. $u(x, t) = 0$ when $\cos\left(\omega x\sqrt{\frac{\rho}{E}}\right) = 0$, or displacement nodes are located at

$$x = \left(n + \frac{1}{2}\right) \pi \frac{1}{\omega}\sqrt{\frac{E}{\rho}} \quad n=0, 1, 2, 3, \ldots \qquad (4.69)$$

when these positions fall inside the bar.

2. $\sigma(x, t) = 0$ when $\sin(\omega x\sqrt{\frac{\rho}{E}}) = 0$, or stress nodes are located at

$$x = n\pi \frac{1}{\omega}\sqrt{\frac{E}{\rho}} \qquad n=0, 1, 2, 3, \ldots \tag{4.70}$$

when these positions fall inside the bar.

3. For the displacement boundary condition, Case 1, resonance occurs when $\cos(\omega L\sqrt{\frac{\rho}{E}}) = 0$; and for the stress boundary condition, Case 2, resonance occurs when $\sin(\omega L\sqrt{\frac{\rho}{E}}) = 0$; or when

Case 1

$$\omega = (n + \frac{1}{2}) \frac{\pi}{L}\sqrt{\frac{E}{\rho}} \qquad n=0, 1, 2, \ldots \tag{4.71}$$

Case 2

$$\omega = \frac{n\pi}{L}\sqrt{\frac{E}{\rho}} \qquad n = 1, 2, 3, \ldots$$

For a 20-inch bar of Type 303 stainless steel some of the resonance frequencies are:

<u>For Case 1.</u> (Displacement B.C.)

i. Bar at room temperature ($75^{\circ}F$)

2,470; 7,410; 12,350; 17,290; 22,230; .... cps.

ii. Bar at $1200^{\circ}F$

2,138; 6,416; 10,690; 14,966; 19,242; .... cps.

<u>For Case 2.</u> (Stress B.C.)

i. Bar at room temperature ($75^{\circ}F$)

4,940; 9,880; 14,820; 19,760; 24,700; .... cps.

ii. Bar at $1200^{\circ}F$

4,275; 8,551; 12,826; 17,101; 21,376; .... cps.

4.3. Numerical Solution (Case of General Variation of Temperature)

4.3(a). Formulation of Algebraic Equations

From Eq. (2.9), neglecting variation in ρ, the displacement wave equation is

$$\frac{\partial}{\partial x}\left(E(x)\frac{\partial u}{\partial x}\right) = \rho\frac{\partial^2 u}{\partial t^2} \tag{4.72}$$

For a periodic solution let $u(x,t) = u(x)\,e^{i\omega t}$ so that $u(x)$ satisfies the ordinary differential equation

$$\frac{d}{dx}\left(E(x)\frac{du}{dx}\right) + \rho\omega^2 u = 0$$

$$\frac{d^2u}{dx^2} + \frac{1}{E(x)}\frac{dE(x)}{dx}\frac{du}{dx} + \frac{\rho\omega^2}{E(x)}u = 0 \tag{4.73}$$

Divide the length of the bar into a mesh of n equal intervals of length $h = L/n$. The central-difference quotients approximating the derivatives are

$$\frac{du}{dx} \approx \frac{u_{i+1} - u_{i-1}}{2h}$$

$$\frac{d^2u}{dx^2} \approx \frac{u_{i+1} + u_{i-1} - 2u_i}{h^2}$$

Also $x_j = (j-1)\,h = (j-1)\,\frac{L}{n}$ $\quad 1 \le j \le n+1$ *

Eq. (4.73) is thus approximated at each mesh point by

$$\frac{u_{i+1} - 2u_i + u_{i-1}}{h^2} + \frac{1}{E(x_i)}\left\{\frac{E(x_{i+1}) - E(x_{i-1})}{2h}\right\}\left(\frac{u_{i+1} - u_{i-1}}{2h}\right) + \frac{\rho\omega^2}{E(x_i)}u_i = 0$$

*In order to agree with the computer program language the numbering of the points varies from 1 to n+1 instead of from 0 to n.

or

$$\left[1 - \frac{\{E(x_{i+1}) - E(x_{i-1})\}}{4\,E(x_i)}\right] u_{i-1}$$

$$+ \left(\frac{\rho\,\omega^2 h^2}{E(x_i)} - 2\right) u_i$$

$$+ \left[1 + \frac{\{E(x_{i+1}) - E(x_{i-1})\}}{4\,E(x_i)}\right] u_{i+1} = 0 \qquad (4.74)$$

We write Eq. (4.74) at each interior mesh point and also at an end point where a stress boundary condition is imposed. The stress boundary furnishes a condition on $\frac{\partial u}{\partial x}$, which permits expressing the value of u at one fictitious mesh point outside the bar in terms of the value at an adjacent interior mesh point. Solution of the simultaneous system of linear equations then gives the value of u at each mesh point. We consider two different cases of boundary conditions.

Case 1 Let there be a source of disturbance producing a periodic displacement $U e^{i\omega t}$ at the end $x = L$, and let the end $x = 0$ be free. The boundary conditions are

$$u\Big]_{x=L} = U e^{i\omega t}$$

$$\frac{\partial u}{\partial x}\Big]_{x=0} = 0 = \frac{u_2 - u_o}{2h}$$

From the second boundary condition

$$u_2 = u_o$$

Now, writing equations for points 1 to n in Eq. (4.74) and using the

boundary conditions, we obtain for

i=1,

$$\left(\frac{\rho\omega^2 h^2}{E(x_1)} - 2\right) u_1 + 2 u_2 = 0$$

i=2,

$$\left[1 - \frac{\{E(x_3) - E(x_1)\}}{4 E(x_2)}\right] u_1 + \left(\frac{\rho\omega^2 h^2}{E(x_2)} - 2\right) u_2 + \left[1 + \frac{\{E(x_3) - E(x_1)\}}{4 E(x_2)}\right] u_3 = 0$$

i=3,

$$\left[1 - \frac{\{E(x_4) - E(x_2)\}}{4 E(x_3)}\right] u_2 + \left(\frac{\rho\omega^2 h^2}{E(x_3)} - 2\right) u_3 + \left[1 + \frac{\{E(x_4) - E(x_2)\}}{4 E(x_3)}\right] u_4 = 0$$

$$\begin{array}{cc} \cdot & \cdot \\ \cdot & \cdot \\ \cdot & \cdot \\ \cdot & \cdot \end{array}$$

i=n,

$$\left[1 - \frac{\{E(x_{n+1}) - E(x_{n-1})\}}{4 E(x_n)}\right] u_{n-1} + \left(\frac{\rho\omega^2 h^2}{E(x_n)} - 2\right) u_n + \left[1 + \frac{\{E(x_{n+1}) - E(x_{n-1})\}}{4 E(x_n)}\right] U = 0$$

We have n equations and n unknowns. These equations can be written in the matrix form

$$A\, U' = K$$

where A is the tri-diagonal matrix

$$A = \begin{bmatrix} a_{11} & a_{12} & 0 & 0 & - & - & - & - & - & - & 0 \\ a_{21} & a_{22} & a_{23} & - & & - & - & - & - & - & 0 \\ 0 & a_{32} & a_{33} & & & & & & & & \\ 0 & 0 & a_{43} & & & & & & & & \\ & & & & & & & & & & \\ & & & & & & & & & & \\ & & & & & & & & a_{n-1,n-2} & a_{n-1,n-1} & a_{n-1,n} \\ 0 & 0 & - & - & - & - & 0 & & a_{n,n-1} & a_{nn} & \end{bmatrix} \tag{4.75}$$

with

$$a_{ii} = \frac{\rho\omega^2 h^2}{E(x_i)} - 2 \qquad \text{for } i=1,\ 2,\ \ldots,\ n$$

$$a_{i,i-1} = \left[1 - \frac{\{ E(x_{i+1}) - E(x_{i-1}) \}}{4\, E(x_i)} \right]$$

$$\text{for } i=2,\ 3,\ \ldots,\ n$$

$$a_{12} = 2$$

$$a_{i,i+1} = \left[1 + \frac{\{ E(x_{i+1}) - E(x_{i-1}) \}}{4\, E(x_i)} \right]$$

$$\text{for } i=2,\ 3,\ \ldots,\ n-1$$

The rest of the a_{ij} are zero.

$$U' = \begin{bmatrix} u_1 \\ u_2 \\ u_3 \\ \cdot \\ \cdot \\ \cdot \\ u_n \end{bmatrix} \qquad K = \begin{bmatrix} 0 \\ 0 \\ 0 \\ \cdot \\ \cdot \\ \cdot \\ k_n \end{bmatrix}$$

where

$$k_n = -\left[1 + \frac{\{ E(x_{n+1}) - E(x_{n-1}) \}}{4\, E(x_n)} \right] U$$

Now to obtain the value of stress from these values of displacement we use the relation

$$\sigma(x) = E(x) \frac{\partial u}{\partial x}$$

so that

$$\sigma(x_i) = E(x_i) \left(\frac{u_{i+1} - u_{i-1}}{2h}\right) \tag{4.76}$$

Equation (4.76) gives us the value of stress at any interior mesh point. For the stress at the end $x = L$, we can use a backward difference formula

$$\sigma(x_{n+1}) = \frac{1}{2}\{E(x_n) + E(x_{n+1})\} \left(\frac{u_{n+1} - u_n}{h}\right) \tag{4.77}$$

Case 2 Let there be a source of disturbance producing a periodic stress $Pe^{i\omega t}$ at the end $x = L$, and let the end $x = 0$ be free. The boundary conditions are

$$E(x) \frac{\partial u}{\partial x}\Big]_{x=L} = E(x_{n+1}) \left(\frac{u_{n+2} - u_n}{2h}\right) e^{i\omega t} = Pe^{i\omega t}$$

$$\frac{\partial u}{\partial x}\Big]_{x=0} = \frac{u_2 - u_o}{2h} = 0$$

From the boundary conditions

$$u_{n+2} = 2h \frac{P}{E(x_{n+1})} + u_n$$

$$u_2 = u_o$$

Again writing the equations for points 1 to n+1 and using the boundary conditions we obtain the same equations as in the first case for i=1 to n-1, and in addition we get for

i=n

$$\left[1 - \frac{\{E(x_{n+1}) - E(x_{n-1})\}}{4\,E(x_n)}\right] u_{n-1} + \left(\frac{\rho\omega^2 h^2}{E(x_n)} - 2\right) u_n + \left[1 + \frac{\{E(x_{n+1}) - E(x_{n-1})\}}{4\,E(x_n)}\right] u_{n+1} = 0$$

i=n+1

$$2\,u_n + \left(\frac{\rho\omega^2 h^2}{E(x_{n+1})} - 2\right) u_{n+1} + \frac{2h\,P}{E(x_{n+1})}\left[1 + \frac{\{E(x_{n+1}) - E(x_n)\}}{2\,E(x_{n+1})}\right] = 0$$

This again can be written in the matrix form

$$A\,U = K$$

where the tri-diagonal n+1 by n+1 matrix A

$$A = \begin{bmatrix} a_{11} & a_{12} & 0 & 0 & \cdots & 0 \\ a_{21} & a_{22} & a_{23} & & \cdots & 0 \\ 0 & a_{32} & a_{33} & & & \\ 0 & 0 & a_{43} & & & \\ \vdots & \vdots & & \ddots & & \vdots \\ & & & a_{n,n-1} & a_{n,n} & a_{n,n+1} \\ 0 & 0 & \cdots & 0 & a_{n+1,n} & a_{n+1,n+1} \end{bmatrix} \qquad (4.78)$$

has elements

$$a_{ii} = \left(\frac{\rho\omega^2 h^2}{E(x_i)} - 2\right) \qquad i=1,\ 2,\ \ldots,\ n+1$$

$$a_{i,i-1} = \left[1 - \frac{\{E(x_{i+1}) - E(x_{i-1})\}}{4\,E(x_i)}\right] \qquad i=2,\ 3,\ \ldots,\ n$$

$$a_{n+1,\,n} = 2$$

$$a_{12} = 2$$

$$a_{i,\,i+1} = \left[\, 1 + \frac{\{\, E(x_{i+1}) - E(x_{i-1})\}}{4\, E(x_i)}\right] \qquad i=2,\ 3,\ \ldots,\ n$$

The rest of the a_{ij} are zero.

$$U = \begin{bmatrix} u_1 \\ u_2 \\ u_3 \\ \cdot \\ \cdot \\ \cdot \\ u_n \\ u_{n+1} \end{bmatrix} \qquad K = \begin{bmatrix} 0 \\ 0 \\ 0 \\ \cdot \\ \cdot \\ \cdot \\ 0 \\ k_{n+1} \end{bmatrix}$$

where

$$k_{n+1} = -\frac{2hP}{E(x_{n+1})}\left[\, 1 + \frac{\{\, E(x_{n+1}) - E(x_n)\}}{2\, E(x_{n+1})}\right]$$

Again stress at any point of the mesh can be obtained by using Eq. (4.76) or Eq. (4.77), depending upon the point.

4.3(b). Solution of the Algebraic Equations

We have to solve the equation

$$A\, U = K$$

where

$$a_{n+1,\,n} = 2$$

$$a_{12} = 2$$

$$a_{i,\,i+1} = \left[\, 1 + \frac{\{\, E(x_{i+1}) - E(x_{i-1})\,\}}{4\, E(x_i)}\right] \qquad i=2,\ 3,\ \ldots,\ n$$

The rest of the a_{ij} are zero.

$$U = \begin{bmatrix} u_1 \\ u_2 \\ u_3 \\ \cdot \\ \cdot \\ \cdot \\ u_n \\ u_{n+1} \end{bmatrix} \qquad K = \begin{bmatrix} 0 \\ 0 \\ 0 \\ \cdot \\ \cdot \\ \cdot \\ 0 \\ k_{n+1} \end{bmatrix}$$

where

$$k_{n+1} = -\frac{2hP}{E(x_{n+1})}\left[\, 1 + \frac{\{\, E(x_{n+1}) - E(x_n)\,\}}{2\, E(x_{n+1})}\right]$$

Again stress at any point of the mesh can be obtained by using Eq. (4.76) or Eq. (4.77), depending upon the point.

4.3(b). Solution of the Algebraic Equations

We have to solve the equation

$$A\, U = K$$

where

$$A = \begin{bmatrix} a_{11} & a_{12} & 0 & 0 & \cdots & 0 \\ a_{21} & a_{22} & a_{23} & \cdots & & 0 \\ 0 & a_{32} & a_{33} & & & \\ 0 & 0 & a_{43} & & & \\ \vdots & \vdots & & \ddots & & \\ & & & a_{m-1,m-2} & a_{m-1,m-1} & a_{m-1,m} \\ 0 & 0 & \cdots & 0 & a_{m,m-1} & a_{m,m} \end{bmatrix}$$

$$\mathbf{U} = \begin{bmatrix} u_1 \\ u_2 \\ u_3 \\ \vdots \\ u_m \end{bmatrix} \qquad \mathbf{K} = \begin{bmatrix} 0 \\ 0 \\ 0 \\ \vdots \\ k_m \end{bmatrix}$$

4.3(b.i). Direct Solution

The matrix equation can conveniently be solved by the direct method (see Hammings, 1962).

We can write the tridiagonal matrix A as the product of a lower triangular matrix L and an upper triangular matrix Z. Then the original matrix equation

$$L Z U = K ,$$

by use of

$$Z\,U = V\,,$$

becomes

$$L\,V = K$$

The resolution into two triangular matrix factors is made as follows. For the tridiagonal matrix A it is possible to choose the triangular matrices so that all elements are zero except those on the diagonal and one adjacent parallel row.

$$\begin{bmatrix} \ell_{11} & & & & \\ \ell_{21} & \ell_{22} & & & \\ & \ell_{32} & \ell_{33} & & \\ & & \ddots & \ddots & \\ & & & \ell_{m,m-1} & \ell_{m,m} \end{bmatrix} \begin{bmatrix} z_{11} & z_{12} & & & \\ & z_{22} & z_{23} & & \\ & & z_{33} & z_{34} & \\ & & & \ddots & z_{m-1,m} \\ & & & & z_{m,m} \end{bmatrix}$$

$$= \begin{bmatrix} a_{11} & a_{12} & & & \\ a_{21} & a_{22} & a_{23} & & \\ & a_{32} & a_{33} & a_{34} & \\ & & \ddots & \ddots & a_{m-1,m} \\ & & & a_{m,m-1} & a_{m,m} \end{bmatrix}$$

By matrix multiplication

$$\ell_{11}\ z_{11} = a_{11}$$

$$\ell_{11}\ z_{12} = a_{12}$$

and the rest of $z_{ij} = 0$ for $j > 2$.

If we arbitrarily choose all diagonal elements of L to be unity

$$\ell_{11} = \ell_{22} = \ell_{33} = \cdots = \ell_{m,m} = 1 ,$$

then

$$z_{11} = a_{11}$$

$$z_{12} = a_{12}$$

Now

$$\ell_{21} \; z_{11} = a_{21}$$

or

$$\ell_{21} = \frac{a_{21}}{z_{11}} = \frac{a_{21}}{a_{11}}$$

Similarly

$$\ell_{21} \, z_{12} + \ell_{22} \, z_{22} = a_{22}$$

yielding

$$z_{22} = a_{22} - \ell_{21} \, z_{12}$$

$$\ell_{22} \, z_{23} = a_{23}$$

or

$$\ell_{32} \, z_{22} = a_{32}$$

$$\ell_{32} = \frac{a_{32}}{z_{22}}$$

$$\ell_{32} \, z_{23} + \ell_{33} \, z_{33} = a_{33}$$

or

$$z_{33} = a_{33} - \ell_{32}\, z_{23}$$

In general

$$\left.\begin{aligned} \ell_{rr} &= 1 & z_{r,\,r+1} &= a_{r,\,r+1} \\ & & z_{11} &= a_{11} \\ \ell_{r+1,\,r} &= \frac{a_{r+1,\,r}}{z_{rr}} & z_{rr} &= a_{rr} - \ell_{r,\,r-1}\; z_{r-1,\,r} \\ & & &= a_{rr} - \frac{a_{r,\,r-1}}{z_{r-1,\,r-1}}\; a_{r-1,\,r} \end{aligned}\right\} \quad (4.79)$$

All other elements of the two triangular matrices are zero.

Now to find V components of the equation

$$L\,V = K$$

$$\begin{bmatrix} \ell_{11} & & & & \\ \ell_{21} & \ell_{22} & & & \\ & \ell_{32} & \ell_{33} & & \\ & & \ddots & \ddots & \\ & & & \ell_{m,\,m-1} & \ell_{mm} \end{bmatrix} \begin{bmatrix} v_1 \\ v_2 \\ v_3 \\ \cdot \\ \cdot \\ \cdot \\ v_m \end{bmatrix} = \begin{bmatrix} k_1 \\ k_2 \\ k_3 \\ \cdot \\ \cdot \\ \cdot \\ k_m \end{bmatrix} \quad (4.80)$$

we proceed as follows:

From Eq. (4.80) we obtain

$$\ell_{11}\, v_1 = k_1$$

$$\ell_{21}\, v_1 + \ell_{22}\, v_2 = k_2$$

$$\ell_{32}\, v_2 + \ell_{33}\, v_3 = k_3$$

so that

$$v_1 = k_1$$

$$v_2 = k_2 - \ell_{21}\, v_1$$

$$v_3 = k_3 - \ell_{32}\, v_2$$

or

$$v_r = k_r - \ell_{r,\,r-1}\, v_{r-1} \tag{4.81}$$

Further we have

$$Z\,U = V$$

$$\begin{bmatrix} z_{11} & z_{12} & & & \\ & z_{22} & z_{23} & & \\ & & \ddots & \ddots & \\ & & & z_{m-1,\,m} & \\ & & & & z_{mm} \end{bmatrix} \begin{bmatrix} u_1 \\ u_2 \\ u_3 \\ \vdots \\ u_m \end{bmatrix} = \begin{bmatrix} v_1 \\ v_2 \\ v_3 \\ \vdots \\ v_m \end{bmatrix} \tag{4.82}$$

from which

$$z_{mm}\, u_m = v_m$$

$$z_{m-1,\,m-1}\, u_{m-1} + z_{m-1,\,m}\, u_m = v_{m-1}$$

So in general

$$\left.\begin{aligned} z_{rr}\, u_r + z_{r,\,r+1}\, u_{r+1} &= v_r \qquad \text{for } 1 \le r \le m-1 \\ z_{rr}\, u_r &= v_r \qquad \text{for } r = m \end{aligned}\right\} \tag{4.83}$$

From Eq. (4.83)

$$u_m = \frac{v_m}{z_{mm}}$$

and

$$u_r = (v_r - z_{r,r+1}\, u_{r+1})\ \frac{1}{z_{rr}} \qquad (4.84)$$

The above is the direct method of solution as given by Hammings (1962).

For application of this method, we had for Eq. (4.81)

$$k_r = 0 \qquad \text{for } r \neq m$$

and

$$k_m \neq 0$$

Therefore

$$v_r = 0 \qquad \text{for } r \neq m$$

$$v_r = k_r \qquad \text{for } r = m$$

Hence Eq. (4.83) and Eq. (4.84) reduce to

$$z_{rr}\, u_r + z_{r,r+1}\, u_{r+1} = 0 \qquad \text{for } 1 \leq r \leq m-1$$

$$z_{rr}\, u_r = k_r \qquad \text{for } r = m$$

and therefore

$$u_m = \frac{k_m}{z_{mm}}$$

$$u_r = -\frac{z_{r,r+1}}{z_{rr}}\, u_{r+1} \qquad \text{for } 1 \leq r \leq m-1 \qquad (4.85)$$

Eq. (4.79) and Eq. (4.85) give us the direct solution of the equations.

4.3(b.ii). Iteration

The solution obtained by the above method might have an accumulated round-off error which could become large as the number of equations increases. To get more accurate results we could use the Gauss-Seidel iterative method (see for example, Varga, 1962, page 57-58), using the results of the direct method as the starting set of values.

Let $u_r^{(n)}$ be the set of values obtained after nth iteration and let $u_r^{(n+1)}$ be the set of values obtained after (n+1)th iteration. Then the Gauss-Seidel method of iteration can be written as

$$a_{i,i-1}\, u_{i-1}^{(n+1)} + a_{ii}\, u_i^{(n+1)} + a_{i,i+1}\, u_{i+1}^{(n)} = k_i \qquad (4.86)$$

These equations can be solved one at a time for the new value $u_i^{(n+1)}$, since $u_{i+1}^{(n)}$ is known from the previous iteration and $u_{i-1}^{(n+1)}$ has already been calculated during the current iteration. The start of each iteration uses the modified equation obtained by using the boundary condition at the free end $x = 0$. This yields the iterative form

$$a_{11}\, u_1^{(n+1)} + 2\, u_2^{(n)} = 0 \qquad (4.87)$$

for $u_1^{(n+1)}$.

The iteration is continued until the maximum difference between successive values is less than or equal to a preassigned value, which

was chosen to be 0.00001 in the problem solved. It turned out that the iteration procedure did not in fact change the results of the direct solution in the problems considered.

4.4. Description of the Problem

For a 20-inch-long Type 303 stainless steel bar with one end at $75^{\circ}F$ and the other at $1200^{\circ}F$, the analytic solutions of the periodic vibrations were obtained for three types of inhomogeneity, and the numerical solutions of the periodic vibrations were obtained for five types of inhomogeneity. In each case the inhomogeneity was expressed either in terms of the elastic modulus or the temperature varying with the distance along the length of the bar. For comparison, analytic solutions of the periodic vibrations were also obtained for a uniform temperature distribution along the length of the bar.

The cases of inhomogeneity for which analytic solutions were obtained are:

1. $E(x) = E_o + kx$
2. $E(x) = E_o e^{kx}$
3. $E(x) = E_o \left(\frac{x}{20k}\right)^2$

The cases of inhomogeneity for which numerical solutions were obtained are

1. $E(x) = E_o + kx$
2. $E(x) = E_o e^{kx}$
3. $E(x) = E_o \left(\frac{x}{20k}\right)^2$
4. $E(x) = E_o \left(\frac{x}{20k}\right)^{3/2}$

5. Experimental temperature distribution given in Fig. 3.3.

In each case the value of k is such that the one end of the bar is at 75^{o}F and the other at 1200^{o}F, and E_o is the value of the elastic modulus at 75^{o}F and is equal to 29.0×10^{6} lbs./sq. in.

Analytic solutions of the above mentioned first three cases were obtained by the methods described in Sec. 4.2. Calculations were done on the computer using the values of Bessel functions J_0, J_1, Y_0, Y_1 obtained from the table of Bessel's functions by Chistova (1959).

The numerical solutions of the above mentioned five cases were obtained by solving the finite difference equations by the method described in Sec. 4.3. The calculations for these cases were also done on the computer. The program for the numerical solutions is described in Appendix B-2. The cases which were solved by the analytic method were used to check the accuracy of the numerical method. The number of intervals of the finite difference mesh and the results of the iterative procedure are also discussed in Appendix B-2.

The results of the analytic solutions and numerical solutions for the above mentioned problem are shown and discussed in Sec. 7.4.

CHAPTER V

EXPERIMENTAL APPARATUS

5.1. General Description

The objective of the experimental work was to confirm the calculated solutions obtained for pulse propagation in a bar with thermally-induced inhomogeneity. As discussed in Section 3.4, two types of temperature distribution conditions are of interest for the study of the pulse propagation. For both, the method of calculations has already been discussed. To carry out these experiments the following experimental set-up was used.

A flat-topped loading pulse was obtained by a longitudinal impact. The specimen bar was struck by a four-foot stainless steel striker bar, projected by an adaptation of a commercial Hyge shock-testing machine. Two different experiments were conducted. In the first, the effect of a thermal gradient in the middle of the bar was studied. In the second experiment the effect of a thermal gradient at the impact end was studied with the pulse propagating from a hot to a cold region. A schematic drawing of the apparatus is given in Fig. 5.1 and a general view of the test set-up is shown in Fig. 5.2.

5.2. Specimen and Striker Bar

In Fig. 5.3(a) and Fig. 5.3(b) the dimensions, the arrangements, and the location of the strain gages for the specimen and the

striker bars for both the experiments are shown. The specimen and the striker bar were made of 9/16-inch-diameter centerless ground Type 303, 18-8 stainless steel drill rods. This material was selected because of its low oxidation at the higher temperatures and its good impact properties. The specimen used for the first experiment was 6 feet long, and the temperature gradient was produced by a 5-inch-long coaxial furnace at the middle of the bar. A high-temperature gage station was located at the middle of the bar and two room-temperature gage stations were located at a distance of one foot from each end. At each station two gages were mounted on opposite sides of the bar and connected to cancel the effect of bending as described in Sec. 5.5. Both the specimen and the striker bar were supported on several rubber O-rings, which in turn were supported on aluminum bearings. The O-rings allowed a sufficiently free lateral expansion of the bars that no detectable reflections were produced at these supports. In the second experiment the specimen was 4 feet long, with one end placed in the furnace so that the end was the hottest part of the bar. Two high-temperature gages were mounted at 1.125 inches, and two room-temperature gages at 25 inches, from the hot end on the specimen bar. Also two room-temperature gages were mounted at 25 inches from the impact end of the striker bar. At each station the two gages were mounted on opposite sides of the bar and connected to cancel the effects of bending as described in section 5.5. In order to minimize the three-dimensional effects, the strain gages were mounted at least one diameter away from the end of the specimen (see Bell, 1960).

The striker bar was chosen to be four feet long for two reasons: first so that the striker-bar gage could be at the same distance from the impact end as the cold-region gage on the specimen and still be far enough from the free end of the striker bar that the reflected unloading waves would not interfere with the recording there; and second so that the strain gage mounted on the striker bar used for the measurements of the incident pulse in the second experiment might not get damaged by the O-rings as the bar moved 18 inches through them to strike the specimen.

One end of each bar was rounded in order to produce an axial impact and to reduce the high frequency components of the rising portion of the pulse by giving a longer rise time (see Chiddister, 1961, page 28). The round end of the striker bar was towards the thrust column of the Hyge in order to get an axial force from it. The flat end of the striker bar was towards the round end of the specimen bar, so that the flat vertical surface of the end of the striker bar could only hit the outer-most point of the specimen, even if the bars were not exactly aligned. To absorb the energy of the impact a lead block was placed at the far end of the specimen bar. To avoid the production of a concentrated force on the lead block, the end of the specimen bar towards the lead block was kept flat.

The four-foot-long striker bar produced a 486-microsecond-long flat-topped pulse. This is twice the time required for the elastic compression pulse to travel the length of the striker bar,

since the striker bar and the specimen remained in contact until the compression pulse in the striker bar was reflected back from the free end of the striker as a tension pulse to break the contact at the interface.

5.3. Hyge Shock Tester

The pulse was produced by an impact of the striker bar, which was propelled by an adaptation of a commerical Hyge Shock Tester, Type HY-3422, manufactured by Consolidated Electrodynamics Corporation. A sketch of the Hyge is given in Fig. 5.4, and the Hyge appears in the photograph of Fig. 5.2.

The operation of the tester is in short as follows: a set pressure is introduced in chamber A. The set pressure works on the full area of the piston pushing it against a seal ring. A load pressure is then introduced in chamber B. The load pressure in chamber B applies the same force on the piston from one side as the set pressure in chamber A does from the other side when the load pressure in chamber B is about four times that of the set pressure in chamber A. Any extra load pressure in chamber B then breaks the seal, applying the full load pressure of chamber B to the whole piston area. This produces a large acceleration in the piston, which in turn accelerates the striker bar. The deceleration of the Hyge piston is accomplished by a hydraulic fluid. The full stroke of the Hyge piston is 16.75 inches. The operation is controlled from a control panel containing pressure gages and control valves.

5.4. Furnace and Temperature Measurement

The temperature gradient in the specimen was produced by a Type 123-1 Electric Multiple Unit Furnace manufactured by the Hevi-Duty Electric Company. The furnace had a 5-inch-long heating element and an internal diameter of 1.25 inches. Temperatures up to 1950°F for intermittent operations and up to 1850°F for safe continuous operations could be produced by this furnace. It has a hinged lid so that the specimen could be reached without any difficulty. To produce a certain maximum temperature a Variac type variable transformer was used to control the furnace voltage. The furnace produced a steady-state temperature distribution in the specimen in about two and a half hours. It was found that if the furnace was left on for any length of time after two and a half hours the values of temperature at each point did not vary more than $\pm$ 0.8%. This was taken to be an evidence of the steady-state temperature distribution. The portion of each bar outside the furnace was exposed to the room-temperature environment with the result that the temperature in the bar fell to room temperature at a distance of about 18 inches from the hottest point.

By experimentation a definite position of the dial on the Variac was found for both experiments, so that the maximum temperature in the steady-state temperature distribution was 1200°F in each case. To check the reproducibility of the furnace at this fixed position of the dial, several check tests were performed. For each check test the furnace was turned on two and a half hours before the test and temperatures were measured at several points of the

temperature distribution in the specimen. The reproducibility of the furnace was found to be within 0.8%. Chromel-Alumel thermocouples with Foxbord Portable Indicator Model No. 8106 were used to measure the temperatures. The scale of the indicator was calibrated by measuring the boiling point of distilled water. Two-hole elliptical ceramic tubing was used to insulate the thermocouple wire. An electric butt-welder was used to weld the thermocouples on the bar in order that the welding would not make holes in the specimen.

In the first experiment the temperature distribution was measured at 22 points spaced 0.8 inches apart, starting from the middle. Measurements were taken on only one half of the distribution; the other half was assumed to be the mirror image of the measured distribution. In the second experiment the temperature was measured at 16 points spaced 1 inch apart starting from the hot end of the specimen. The measured values were plotted and the curves smoothed very slightly. The curves of temperature versus distance are given in Fig. 3.2 and Fig. 3.3. Since the joint of the thermocouples on the bar was very sensitive to any kind of shock, and the temperature distribution had been found reproducible with a maximum variation of 0.8%, the position of the specimen in the furnace and the dial on the Variac were marked and all the thermocouples taken off the specimen before the impact tests were performed.

5.5. Strain Measuring and Recording Equipment

Etched-foil resistance strain gages manufactured by Micro-Measurement Inc. were used for the dynamic surface strain measurements at room temperatures. Type MA-09-125AD-120 gages having a gage length of 0.125 inches and a width of 0.125 inches were mounted on the bars with Eastman 910 adhesive cement. These gages were selected for several reasons: first they were suitable for the dynamic measurements; second, their gage length was small enough to indicate the sharp rise in the pulse with sufficient accuracy; and third, they were suitable for measuring strains at the surface of the stainless steel. Eastman 910 adhesive cement was used for mounting these strain gages because of the ease in mounting gages on the curved surfaces with this cement. As given by the manufacturer the resistance of these gages was 120 ± 0.2 ohms and the gage factor was 2.09 (± 0.5%).

High-temperature free-filament strain gages of Type HT-1235-4A, manufactured by Baldwin Lima Hamilton, were used for the dynamic surface strain measurements at elevated temperatures. These were selected for their safe application up to 1200°F for static measurements and up to 1500°F for dynamic measurements (according to the manufacturer). As given by the manufacturer the resistance of these gages was 350 ± 2 ohms, and the room-temperature gage factor was quoted as 4.01 (± 1%) for the strain gages used for the first experiment and 3.84 (± 2%) for the strain gages used for the second experiment. A curve relating temperature

and gage factor was also supplied by the manufacturer. At 1200°F the gage factor of these gages was found to be 79% of the value at room temperature, according to this curve.

As recommended by the manufacturer, Allen PBX ceramic cement was used for mounting the high-temperature strain gages on the specimen. Special instructions for using this cement were also supplied by the manufacturer.

To eliminate the effect of bending strains, at each gage station two strain gages were mounted diametrically opposite and aligned longitudinally on the bar. This effectively eliminated the measurement of the bending strains when the two gages were connected in series and placed in the same arm of a Wheatstone bridge as shown in Fig. 5.6(a) or in a potentiometer as shown in Fig. 5.6(b). The room-temperature gages were connected in a Wheatstone bridge circuit and the high temperature gages were connected in a potentiometer circuit. The locations of these gages are shown in Fig. 5.3.

A 240-ohm gage was used as a passive arm for the Wheatstone bridge circuit. Two 352-ohm gages, mounted on each side of a cantilever whose deflection could be varied, were used as the balancing half of the bridge. This produced a very sensitive device for balancing the bridge.

For the potentiometer circuit, two 352-ohm gages were used as the ballast resistor. Output was taken from the ballast resistor instead of from the active gages,for convenience.

Two 12-volt wet cell batteries connected in series were used to supply the voltage to all the bridges. The voltage of these batteries was measured by means of a voltmeter just before and after each experiment, with the batteries in the circuit.

The output signals from the Wheatstone bridge and the potentiometer circuit were fed to Tektronix D-Unit plug-in differential pre-amplifiers in rack-mounted Tektronix Type 127 pre-amplifier power supplies. The differential feature permits attenuation of any undesired signal by means of outphasing and is especially useful for eliminating 60-cycle pickup.

The output signal from the pre-amplifier for the potentiometer circuit was input to a Tektronix C-unit, and the signals from the pre-amplifier for the Wheatstone bridges were input to a Tektronix M-unit. The C-unit and M-unit were mounted in a Tektronix Type 555 dual-beam Cathode-Ray Oscilloscope. The C-unit is an electronic switching unit which enables two chopped signals to be displayed simultaneously on one beam of the oscilloscope, and the M-unit is also a switching unit which enables four signals to be displayed simultaneously on one beam of the oscilloscope. Only two of the four channels of the M-unit were used at a time in the experiments. The switching rate of the C-unit was 100 kc. When only two channels were in use the switching rate of each channel of the M-unit was approximately 500 kc. Sweep speeds of 50 microseconds per cm. and 100 microseconds per cm. were used for recording. The scope was triggered externally by means of a signal from two 120-ohm

strain gages mounted at 0.5 inches from the end of the striker bar and connected in opposite arms of a Wheatstone bridge for a doubled signal.

The strain pulses were permanently recorded with a Tektronix Type C-12 oscilloscope record camera, using Type 47 Polaroid Land picture roll.

CHAPTER VI

EXPERIMENTAL PROCEDURE

6.1. Determination of E, ρ and c

The elastic wave velocity at room temperature (75°F) was determined by measuring the time required for a pulse to travel four times, six times, and eight times the length of the 6-foot bar and then taking the average of the values obtained. The values of the elastic wave velocity obtained in different tests agreed up to the third digit. For this test an air gap was left between the bar and the lead block so that the successive reflections could occur at the free ends without interference. The pulse was displayed on the screen and recorded on a photograph for measurements. The average of the elastic wave velocities obtained for two, three, and four complete cycles on the photographs for four tests showed the elastic wave velocity at room temperature to be 197,600 ± 900 inches per second.

The density ρ was obtained by determining the weight and the volume of a 10 inch section of the specimen bar and was found to be 7.928 gms./c.c. compared to the value 7.93 gms./c.c. or 0.286 lbs./cu. in. given by the Metals Handbook (1948) for Type 303 stainless steel. Therefore 7.93 gms./c.c. or $(7.43 \pm .01) \times 10^{-4}$ slugs per cubic inch was taken to be the correct value for density. The weight of the bar was determined by weighing the section of the specimen bar on a Torsion balance. The volume of this section was

determined by measuring the length and the diameter of the bar at various points on the section. The value of the modulus of elasticity E_o was calculated using the relation $E_o = c_o^2 \rho$, and was found to be $(29.0 \pm 0.3) \times 10^6$ pounds per square inch compared to the value 29×10^6 pounds per square inch given by the Metals Handbook (1948) for Type 303 stainless steel. The value 29.0×10^6 pounds per square inch was then taken as the correct value of the modulus of elasticity for the specimen bar.

The density of Type 303 stainless steel at 1200°F was found to be 7.141×10^{-4} slugs/in.^{3} compared to the value of 7.43×10^{-4} slugs/in.^{3} at 75°F, indicating a difference of 3.89%. This calculation was based on a coefficient of thermal expansion of 11.1×10^{-6} ins. per in./$^\circ$F, as given in the Metals Handbook (1948). The value of the elastic wave speed at 1200°F was found to be 174404 in./sec. based on the calculated value of the density at 1200°F, compared to the value 171011 in./sec. based on the value of the density at 75°F. Therefore, for the problems considered in this investigation, the maximum error introduced into the value of the elastic wave speed is 1.98% when the variation in density due to a variation in temperature is neglected.

6.2. Electronic Calibration of the Strain Gages

The strain gages were calibrated by shunting one arm of the Wheatstone bridge, or the ballast resistor of the potentiometer circuit, by a resistor of considerably higher value brought in and out of the circuit with a switch. The shunt resistor produced a

definite signal on the screen. To produce a signal equivalent to a strain ϵ, the size of the calibration resistor R_c was calculated using the formulas (Perry Lissner, 1964, pages 90 to 96):

1. For the Wheatstone Bridge

$$R_c = \frac{R_g(1 - F\epsilon)}{F\epsilon}$$

where R_c is the resistance to simulate a strain ϵ, R_g is the resistance of the gage and F is the gage factor of the gage.

2. For the Potentiometer Circuit

$$R_c = R_b \frac{(R_b - F\epsilon R_g)}{F\epsilon R_g}$$

where again R_c is the resistance to simulate a strain ϵ, R_g is the resistance of the gage, R_b is the magnitude of the ballast resistor and F is the gage factor of the gage.

In each case the resistor produced a signal equal to that of a strain of the order of magnitude of 700 microinches per inch, since that was the order of magnitude of strain which was to be recorded. To achieve this, resistors were prepared by combining various values. For room temperature gages, a calibration resistor of 176K was used which produced a signal equal to a strain of 652 microinches per inch. For high temperature gages a calibration resistor equal to 300K was used for calibration, and it produced a signal equal to a strain of 731 microinches per inch.

Calibration signals were displayed on the oscilloscope screen and recorded on a photograph. All the strain gages were

calibrated before and after each test.

6.3. Test Procedure

The amplifiers and oscilloscope were turned on at least one-half hour before, and the strain-gage bridge voltage fifteen minutes before, a test in order to obtain nearly steady-state operating conditions. Each test was performed following the procedure below in sequence:

1. The Wheatstone bridges were balanced.
2. The battery voltage was measured.
3. All the strain gages were calibrated.
4. The oscilloscope sweep speed was set at 50 microseconds or 100 microseconds per centimeter. The triggering source switch was set at "External," and the trigger placed on "Single Sweep."
5. The vertical gain adjustments of the amplifiers were set so that the signal would remain on the screen during the test.
6. A set pressure of 15 psi. was applied to the Hyge Shock Tester.
7. The load pressure was increased to 30 psi.
8. The reset button of the single-sweep control was pressed.
9. The camera shutter was opened and left open.
10. The load pressure was increased until the Hyge fired.
11. The camera shutter was closed.
12. The load pressure was released and the piston of the Hyge was retracted.

13. The calibration shots were repeated.

14. The battery voltage was measured.

15. The specimen bar was brought back to its original marked position.

In each experiment tests were performed both at room temperature and with the temperature gradient produced on the specimen. For the high temperature tests the furnace was turned on two and a half hours before the test.

6.4. Reduction of Data

The data recorded on the photographs taken for each test was measured with a Pye two-dimensional traveling microscope, accurate to 0.01 millimeter. The calibration measurements were taken at various points along the time axis for each test, and calibration values measured at these points were the ones used to reduce the data obtained on a test shot at points in the vicinity of these on the time scale. On the test shots all the traces were measured at a series of points along the time axis. The spacing of these points was increased or decreased with the slope of the trace being measured.

CHAPTER VII

RESULTS

7.1. Pulse Propagation

7.1(a). Oscilloscope Records

The photographic records obtained from a few typical tests are shown in Fig. 7.1 and Fig. 7.2. The uppermost trace on each record is the output from the high-temperature gage. The next lower trace is the output from the transmitter gage at room temperature. The lowest is the output from the incident gage in the case of the 6 foot bar heated in the middle, Fig. 7.1, and from the gage mounted on the striker bar in the case of the 4 foot bar struck at the hot end, Fig. 7.2. Experimental points taken from these records are shown together with the calculated curves of Figs. 7.3 and 7.5.

7.1(b). Discussion of the Test Results

7.1(b.i). Results from the 6-Foot-Long Bar Heated in the Middle, Fig. 7.1

A reflection from the temperature gradient is obtained and can be spotted on the output of the incident gage in Fig. 7.1c. The reflection has a maximum value of 5.0% of the magnitude of incident pulse. This reflected pulse is followed immediately by a reflected pulse of the opposite sign with a maximum of 1.5%. Chiddister (1961) also obtained reflections in his experimental output as well as in his theoretical calculations.

The transmission through the central inhomogeneity does not affect the amplitude of the pulse transmitted and recorded at the second room-temperature gage, which shows the same amplitude as the incident pulse. It is interesting to see that the output from the transmitter gage, after the main pulse has passed, also shows a reflection from the temperature gradient (a reflection of the unloading pulse coming from the free end of the bar) clearly visible in Fig. 7.1(c).

The output from the high temperature gage, Figs. 7.1(b) and 7.1(c), shows that the magnitude of strain, after the initial jump in magnitude, continues to rise slowly to the point where the tensile unloading pulse reflected from the free end meets it. This could be considered due to several reflections back and forth within the region bounded by the thermal gradients. A similar slow rise is obtained in the numerical solutions of Sec. 7.3.

7.1(b.ii). Results from the 4-Foot-Long Bar Impacted at the Hot End, Fig. 7.2.

The outputs obtained from the high-temperature gage and the transmitter gage both show that the magnitude of the strain, after the initial jump in magnitude, continues to rise slowly to a maximum value, after which it maintains this value before being intercepted by the tensile unloading pulse reflected from the free end.

When these strain records are converted to stress by multiplying by the elastic modulus at the recording point, the stress

records at the transmitted pulse gage show slightly higher values than the stress records at the high temperature gage. Except at the steep initial rise, the maximum difference between the two is only about 1.6% at time equal to 210 microseconds. A difference is also observed in the stress pulses obtained from the numerical solution; the difference is therefore attributed to propagation through the thermal gradient rather than to experimental error, although in general the accuracy of reading the oscilloscope records is estimated as ± 2%.

7.1(c). Numerical Results

7.1(c.i). Numerical Solution Results from the 6-Foot-Long Bar Heated in the Middle, Fig. 7.3

The calculated values obtained by the method of characteristics for the 6-foot-long bar in which the pulse produced by the impact propagates through the experimentally produced thermal gradient, as discussed in Sec. 3.2, are plotted in Figs. 7.3 and 7.4 for the points on the bar where the strain gages were located. Fig. 7.3 shows the values of strains and Fig. 7.4 the values of stresses. The pulses are translated on the time axis to start at the same point. The difference between the experimental and the theoretical values obtained for the incident, the high-temperature, and the transmitter gages is less than 3% at every point except at the point when the incident gage records the reflected pulse, where the maximum difference is 5.5%. The same general shapes of the pulses are obtained by calculations as were obtained experimentally.

The estimated accuracy of reading the oscilloscope record was ± 2%.

The differences between the calculated and measured reflected pulse amplitudes are greater. The calculated values of the stress and strain obtained at the location of the incident gage show a reflected pulse with a maximum magnitude of about 7% of the incident pulse. This reflected pulse is followed immediately by a reflected pulse of the opposite sign again with a maximum of 7%. The maximum value of the reflected pulse displayed by the strain gage output in the experimental measurement was only 5% of one sign and 1.5% of the opposite sign. This is believed to be a result of the fact that the reflected pulse amplitudes in these experiments were obtained as small differences between the approximately equal incident pulse and the incident pulse with the superposed reflection.

The stress at the high-temperature gage was equal to the stress at the first and second room-temperature gages (within 2.5%), except during the initial rise or up to the first 50 microseconds after the start of the pulse and during the period when room temperature gages received the reflections.

7.1(c.ii). Results from the 4-Foot-Long Bar Struck at the Hot End, Fig. 7.5

The calculated values obtained by the method of characteristics for the 4-foot-long bar with one end hot and the other end cold, in which the pulse produced by the impact propagates through the

experimentally produced thermal gradient shown in Fig. 3.3, are plotted in Figs. 7.5 and 7.6 for the points of the bar where the high temperature gage and the transmitter gage were located. Fig. 7.5 shows the values of strains and Fig. 7.6 shows the value of stresses.

The difference between the experimental and calculated values obtained for the high-temperature gage and the transmitter gage was always less than 4% except for the first 60 microseconds in the case of the high temperature gage. The reason for the large difference in the experimental and the calculated values of the initial steep rise for the high temperature gage seems to be the absence of a clear starting point on the recorded pulse (Fig. 7.2). If the experimentally recorded pulse at the high temperature gage is translated about 8 microseconds towards the right, the maximum difference in the experimental and the calculated values for the first 50 microseconds is found to be 9% and after 50 microseconds it is found to be less than 4%.

The calculated values show that the magnitude of the stress at the high-temperature gage station after the first 80 microseconds is the same as the incident pulse (within 0.4%), while during the first 80 microseconds the difference is as high as 16%. The magnitude of the stress at the transmitter gage before the arrival of the unloading pulse from the free end is always higher than the magnitude of the stress at the high temperature gage; the maximum difference is 6% at 20 microseconds after the beginning of the pulse, becoming less than 0.5% after 80 microseconds. The experimental

values of the stress indicated the same thing but the difference was smaller than the difference between the calculated values.

7.1(c.iii). Results of Lindholm's Problem and the Modified Lindholm Problem

Lindholm (1963) did not obtain any apparent reflection in his numerical study of the problems he considered, where the inhomogeneity was expressed in terms of a varying elastic modulus E as $E_o(\frac{x}{kL})^n$ and the problem was solved by using the method of virtual work. He considered four different problems (see Lindholm, 1963) in which the bar ran from $x = kL$ to $x = (k+1)L$ and the values of E were

$$E = E_o(\frac{x}{kL})^n$$

1. $k = 2$, $n = 1$
2. $k = 5$, $n = 1$
3. $k = 2$, $n = 3$
4. $k = 6.91$, $n = 3$

As a part of the present study, these problems have been solved again by the method of characteristics described in section 3. In the present calculations, the half-sine-wave pulses were taken approximately one fourth of the total length of the bar (the same as used by Lindholm, 1963). The present calculations showed reflections with maximum values from 0.3% to 0.9% of the incident pulse, an essentially neglible reflection. The explanation for the smallness of the reflections seems to be the smallness of the gradient of the inhomogeneity present in the bar through which

the pulse propagates. To show this, Lindholm's third problem was modified as follows. With the same values of maximum and minimum E, namely E_o and 3.375 E_o, the length of the part of the bar where the inhomogeneity existed was reduced to one-fourth the length of the bar in Lindholm's third problem, with the variation following the same cubic law in his problem, and E was taken uniform along the other three-fourths of the bar. This resulted in a c(x) variation given by

$$c = c_o \qquad \text{for } 0 \leq x \leq \tfrac{3}{4} L$$

$$c = c_o\{1 + .296\,(x - \tfrac{3}{4} L)^{3/2}\} \qquad \text{for } \tfrac{3}{4} L \leq x \leq L$$

The length of the pulse was again taken approximately one-fourth of the total length of the bar. The solution then showed reflections with a maximum of 12.5% of the amplitude of the incident pulse as shown in Fig. 7.7. This value of the reflected pulse is about 40 percent of the value of 29.5%, which is the amplitude of the reflected pulse in the case where the pulse propagates through a discontinuous jump in modulus, with one side having the minimum value and the other side the maximum value. Clearly the reason for such a high value of reflection is the steep rise in the elastic modulus, as compared to the size of the pulse.

The amplitude value, 29.5%, of the reflected pulse in the case where the pulse propagates through a discontinuous jump in modulus is obtained from the formula given by Chiddister (1961, pages 100 to

103). The formula is

$$\frac{\epsilon_R}{\epsilon_I} = \frac{\sqrt{E_2} - \sqrt{E_1}}{\sqrt{E_2} + \sqrt{E_1}}$$

where E_2 is the elastic modulus on one side of the discontinuity and E_1 on the other. The values of the elastic modulus used in these calculations were $E_1 = E_o$ and $E_2 = 3.375\ E_o$ as in Lindholm's third problem.

7.2. Periodic Vibrations

7.2(a). The Results of Periodic Vibration Solutions

An analytic and numerical study of the periodic vibrations in a free-free bar with one end hot and the other cold, excited at the hot end in the first case by a sinusoidally varying displacement and in the second case by a sinusoidally varying stress, has been done by the methods described in Chapter 4 for the cases described in Sec. 4.4 for the excitation frequencies of 5000; 7500; 10,000; 12,500; 15,000; 17,500; and 20,000 cps. For the numerical solutions a mesh of 2000 intervals was used. Explicit solutions were also obtained for the same bar with a uniform temperature of $75^{\circ}F$ in one case and $1200^{\circ}F$ in the other case.

The results of all the above mentioned studies are given in Fig. 7.8 to Fig. 7.23 for the frequencies 5000; 10,000; 15,000; and 20,000 cps. For each frequency the results of displacements and stresses are given in separate figures.

The numerical solutions agreed with the explicit solutions up to the sixth significant digit for the cases where E varies as; $E_o + kx$, $E_o e^{kx}$, and $E_o(\frac{x}{kL})^2$. Therefore the same curves are obtained for the explicit and numerical solutions.

The curves for the cases where E varies as $E_o + kx$, $E_o e^{kx}$, $E_o(\frac{x}{kL})^2$, and $E_o(\frac{x}{kL})^{3/2}$ are very close. So in most cases the curves for only two cases, one with the highest values and the other with the lowest values, have been plotted here, i.e. for $E_o + kx$ and $E_o e^{kx}$. The two not plotted would plot very close to these two and mostly in between them.

7.2(b). Discussion of the Results

The numerical solutions obtained for the periodic vibration of the 20-inch-long Type 303 stainless steel bar agreed up to sixth significant figure with the explicit solution in the cases of inhomogeneity where the elastic modulus varied as $E_o + kx$, $E_o e^{kx}$ and $E_o(\frac{x}{kL})^2$. The numerical solutions obtained for the experimental temperature distribution with 2000 mesh intervals agreed with the solutions obtained with 2500 mesh intervals up to 4 significant digits. There was apparently little accumulation of round-off error in the direct numerical solution results, because iteration did not change them.

The results obtained for the cases with thermally-induced inhomogeneity were always between the results obtained for the uniform temperatures of 75^oF and 1200^oF. The presence and location of the nodes, the critical frequencies, and the amplitude

all were affected by the induced inhomogeneity as is clear from Fig. 7.8 to Fig. 7.23. The most pronounced changes are observed in curves for frequencies near one of the resonance frequencies given in Sec. 4.2(d). For example, Figs. 7.16 and 7.17 for 5000 cps show high amplitudes for the stress and displacement with the uniform room-temperature $E = 29.0 \times 10^6$ psi since this frequency is near the room-temperature resonant frequency of 4940 cps. The presence of the thermal gradient lowers the critical frequency; hence the high-temperature response at 5000 cps. is smaller. Similar effects may be noted in most of the other figures given. Only the two figures for displacement excitation at 5000 cps. are far enough from resonance to give only moderate changes. At frequencies below 1000 cps. almost no change is observed due to temperature; none of the low-frequency results have been plotted.

It was found that the results obtained for the inhomogeneities $E_o + kx$, $E_o e^{kx}$, $E_o(\frac{x}{kL})^{3/2}$ and $E_o(\frac{x}{kL})^2$ were very close to each other, the reason being that the temperature distributions which produce these inhomogeneities do not depart from each other much as is clear from Fig. 7.24.

CHAPTER VIII

SUMMARY AND CONCLUSIONS

The mechanical properties of a material change with the temperature. Among other changes, a change in the elastic modulus and the density affect the propagation of a wave. The change in density being small, the primary effect is produced by the change in the elastic modulus, and the density was considered constant in this work. The longitudinal elastic wave speed $c = \sqrt{E/\rho}$ therefore is a function of the axial coordinate. When the thermal gradient and the dependence of E on temperature are known, the problem becomes one of wave propagation along an inhomogeneous elastic bar with known values of the variable wave speed $c(x)$.

Two forms of wave propagation have been considered here; pulse propagation and periodic vibration.

Numerical integration by the method of characteristics has been programmed and used on the CDC 3600 computer. The program was used for five specific problems calculating results:

1. to compare with the experimental pulse propagation study on the bar heated at its center;

2. to compare with the experimental pulse-propagation study on the bar heated at one end;

3. to verify the results of Chiddister (1961), which he obtained by approximating an experimentally-obtained thermal gradient by a series of steps;

4. to verify the results of Lindholm (1963), which he obtained by a series method for the special case $E = E_o(\frac{x}{kL})^n$, and

5. to solve a modified version of Lindholm's problem with variation according to a cubic power law in one-fourth of the bar, while the rest of the bar had a uniform elastic modulus.

Two experiments were performed to verify the results obtained for the first two problems. Results from both experiments agreed well with the numerical solutions. In the case of the 6-foot-long bar with the thermal gradient at the middle, reflections with a maximum of 7% from the calculations and 5% from the experiments were obtained from the gradient, while the transmitted strain pulse after passing through the gradient was nearly the same as the incident pulse. The amplitude of the pulse at the point of highest temperature in the 6-foot-long bar heated at the middle showed a continuous slow rise after the initial jump, and the value of the stress here was equal to the stress at the first and second room temperature gages (within 2.5%), except during the initial rise of the pulse. The difference between the experimental and the theoretical values obtained for the incident, the high-temperature, and the transmitter gages, in the case of the bar heated in the middle, was less than 3% except at the time when the incident gage recorded the reflected pulse, where the maximum difference was 5.5%. In the case of the bar impacted at the hot end, the calculated and the experimental values showed that the magnitude of the stress at the high-temper-

ature gage station, after the initial steep rise, was the same as the incident pulse, while the magnitude of stress at the transmitter gage was always higher. The difference between the experimental and the calculated values obtained for the high-temperature gage and the transmitter gage for the bar impacted at the hot end was less than 4% except for the initial steep rise.

The numerical solution of Lindholm's problem gave the same results as his analytical solution, namely negligible reflection from the thermal gradient. However, in the modified problem, Problem 5, a reflected wave was found with maximum height equal to 12.5% of the incident wave maximum. This indicates that the reason for the lack of reflections before was that the thermal gradient was not steep enough as compared to the size of the pulse.

An analytical study has also been made of the periodic vibrations in a free-free bar with one end hot and the other end cold, excited at the hot end in the first case by a sinusoidally varying displacement and in the second case by a sinusoidally varying stress. An explicit solution is possible when the thermally-induced inhomogeneity is one where the elastic modulus E is a function of position in the bar such that

$$E = E_o + kx$$

or

$$E = E_o e^{kx}$$

or

$$E = E_o \left(\frac{x}{kL}\right)^n$$

For a numerical solution, programs have been written to solve the periodic vibration problem by the finite-difference method for any arbitrary temperature distribution.

For a 20-inch-long Type 303 stainless steel bar, the effect of the temperature distribution, varying from room temperature to 1200°F in the manners described below, on the periodic vibrations has been studied in this investigation. For the excitation frequencies of 5,000; 7,500; 10,000; 12,500; 15,000; 17,500; and 20,000 cps., the explicit solutions of the stress and displacement have been evaluated for the thermally-induced inhomogeneity in which the elastic modulus varies with the distance as $E_o + kx$, $E_o e^{kx}$, and $E(\frac{x}{kL})^2$; and numerical solutions of the stress and displacement have been obtained for the same experimental temperature distribution used in the pulse propagation tests and for the cases where the elastic modulus varies with the distance as $E_o + kx$, $E_o e^{kx}$, $E_o (\frac{x}{kL})^2$, and $E_o (\frac{x}{kL})^{3/2}$. The value of k in each case was such that one end of the bar was at 75°F and the other end at 1200°F. The numerical solutions agreed with the explicit solutions up to six significant figures in the cases where explicit solutions were available. Solutions were also obtained for the same bar with a uniform temperature of 75°F in one case and 1200°F in the other. From the plots of all the above solutions it was found that the solutions, for the cases of varying temperatures in the bar, were always between the solutions obtained for the uniform temperatures of 75°F and 1200°F. The presence and the

location of the nodes, the critical frequencies, and the amplitude, were all affected by the inhomogeneity in the bar.

Some possible applications of the present investigation are:

1. Interpretation of pressure-bar records from hot or radioactive environments.

2. Finding the critical frequencies and solving resonance problems of a bar subjected to varying temperature.

3. Determination of gage factors for high-temperature gages. This could be done by taking the experimental output of a sample gage in a known temperature distribution with the gage mounted on a material of known elastic modulus at elevated temperatures. The predicted values of the output of the gage are calculated numerically from the room-temperature gage record and then compared with the experimental output record to determine the gage factor of the gage. The results of the present study show that the manufacturer's gage factor, modified according to the temperature curve furnished, was very accurate.

4. Obtaining the value of the elastic modulus at elevated temperatures. This can be done by mounting high-temperature gages of known gage factor at a distance of about one diameter from the end of a bar of a material whose elastic modulus is to be determined and introducing a known temperature distribution with a small gradient near the end. Then a known pulse of short duration is introduced at the hot end and the output of the gage is recorded. As found in the 4-foot-long bar, the stress at the

high-temperature gage remains the same as in the incident pulse. So with the stress values of the incident pulse and the measured strains at the high-temperature gage station, the value of the elastic modulus can be obtained.

Further study in this area is recommended to include

1. A set-up of the experiment with more accurate measuring devices for the study of pulse propagation.

2. The reflected pulse measured as a difference between the pulse without reflection and the pulse with reflection and amplified.

3. Actual calibration of the high-temperature gage and determination of the elastic modulus for elevated temperatures.

4. The experimental verification of the solutions obtained for the periodic vibrations of a slender bar with thermally-induced inhomogeneity.

5. Inclusion of the density variation in the pulse-propagation calculations. This is easy to do. While it will make only a small change in the results, it should be an observable change.

BIBLIOGRAPHY

1. Chiddister, J. L., "An Experimental Study of Aluminum at High Strain Rates and Elevated Temperatures," Thesis, Michigan State University, 1961.

2. Chistova, E. A., Tables of Bessel Functions of the True Argument and of Integrals Derived from Them, Pergamon Press, New York, 1959.

3. Courant, R., and Hilbert, D., Methods of Mathematical Physics, Vol. II, Interscience, New York, 1962, p. 524 ff.

4. Cristescu, N., "On the Propagation of Elastic-Plastic Waves in Non-Homogeneous Rods," pages 429-430 in Olszak (1959).

5. Datta, A. N., "Longitudinal Propagation of Elastic Disturbance for Linear Variations of Elastic Parameters," Indian Journal of Theoretical Physics, 4, No. 2, 1956, pages 43-50.

6. Garofalo, F., "Survey of Various Special Tests Used to Determine Elastic, Plastic, and Rupture Properties of Metals at Elevated Temperatures," J. Basic Engineering published by Am. Soc. Mech. Engrs., Vol. 82, Series D, No. 4, Dec. 1960, pages 867-881.

7. Ghosh, S. K., "Dynamics of the Longitudinal Propagation of Elastic Disturbance Through a Medium Exhibiting Gradient of Elasticity," Indian Journal of Physics, 35, No. 1, Jan., 1961, pages 22-27.

8. Hammings, R. W., Numerical Methods for Scientists and Engineers, McGraw-Hill, New York, 1962.

9. Lindholm, U. S., and Doshi, K. D., "Elastic Wave Propagation in a Finite Nonhomogeneous Bar," Technical Report, Southwest Research Institute (1963); also published in the Journal of Appl. Mech., Vol. 32, No. 1, March, 1965.

10. Metals Handbook, published by the American Society of Metals, Cleveland, 1948.

11. Milne, W. E., Numerical Calculus, Princeton University Press, Princeton, 1949.

12. Nielsen, K. L., Methods in Numerical Analysis, the Macmillan Company, New York, 1964.

13. Olszak, W. (edited by), Non-Homogeneity in Elasticity and Plasticity, Symposium Warsaw, Sept. 2-9, 1958, Pergamon Press, New York, 1959.

14. Perry, C. C., and Lissner, H. R., The Strain Gage Primer, McGraw-Hill Book Co., New York, 1962.

15. Perzyna, P., "The Problem of Propagation of Elastic Plastic Waves in a Non-Homogeneous Bar," pages 431-438 in Olszak, (1959).

16. Sternberg, E., and Chakravorty, J. G., "On the Propagation of Shock Waves in a Nonhomogeneous Medium," Trans. ASME, Journal of Appl. Mech., 26, No. 4, 1959, pages 528-536. See also pages 369-371 in Olszak, (1959).

17. Sur, S. P., "A Note on the Longitudinal Propagation of Elastic Disturbance in a Thin Inhomogeneous Elastic Rod," Indian Journal of Theoretical Physics, Vol. 9, No. 4, Dec. 1961, pages 61-67.

18. Timoshenko, S., Vibrational Problems in Engineering, D. Van Nostrand Co., Inc., Princeton, 1955.

19. Varga, R. S., Matrix Iterative Analysis, Prentice-Hall, Inc., Englewood Cliffs, 1962.

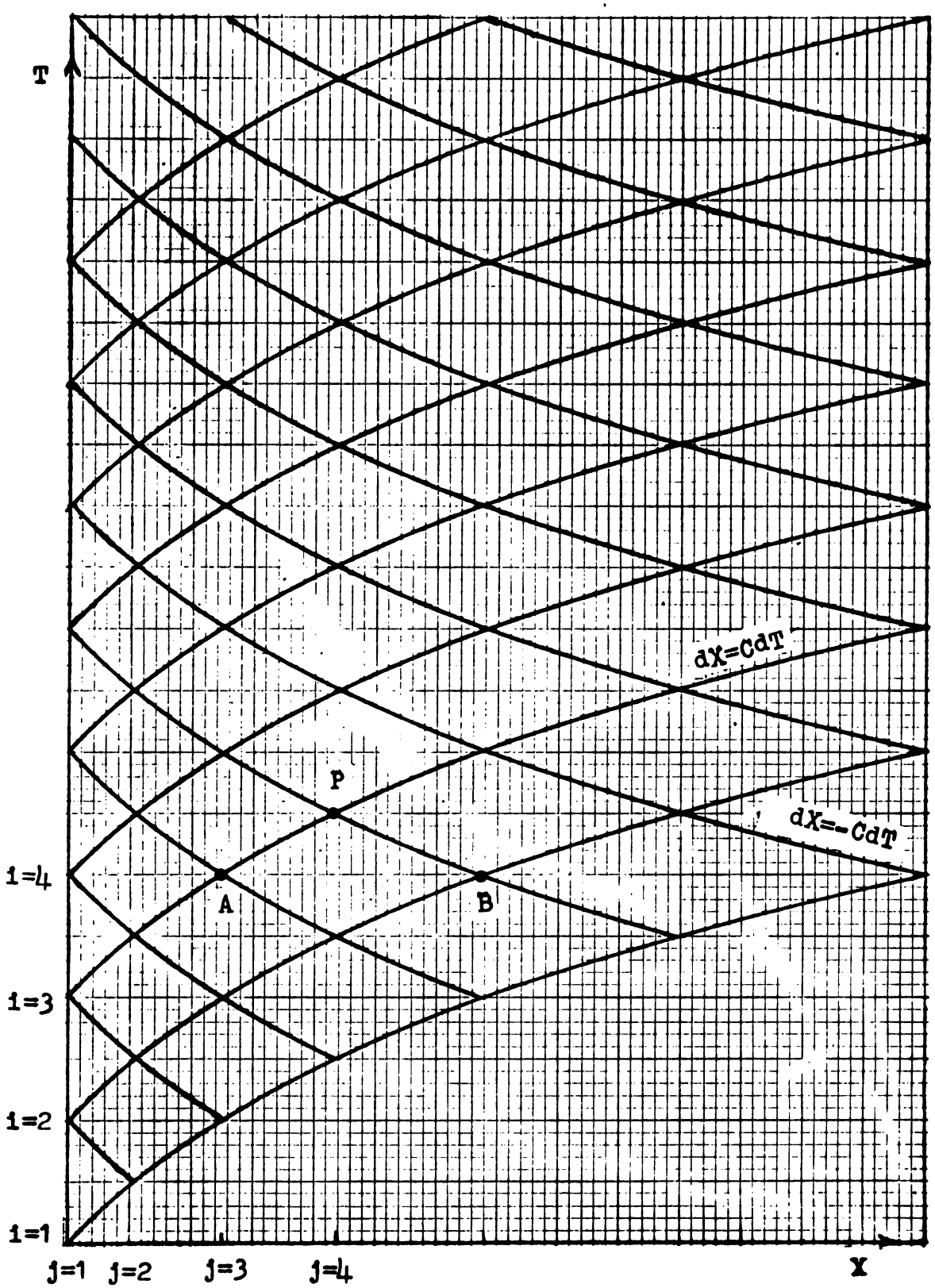

Fig. 3.1 The Characteristics in the XT-Plane

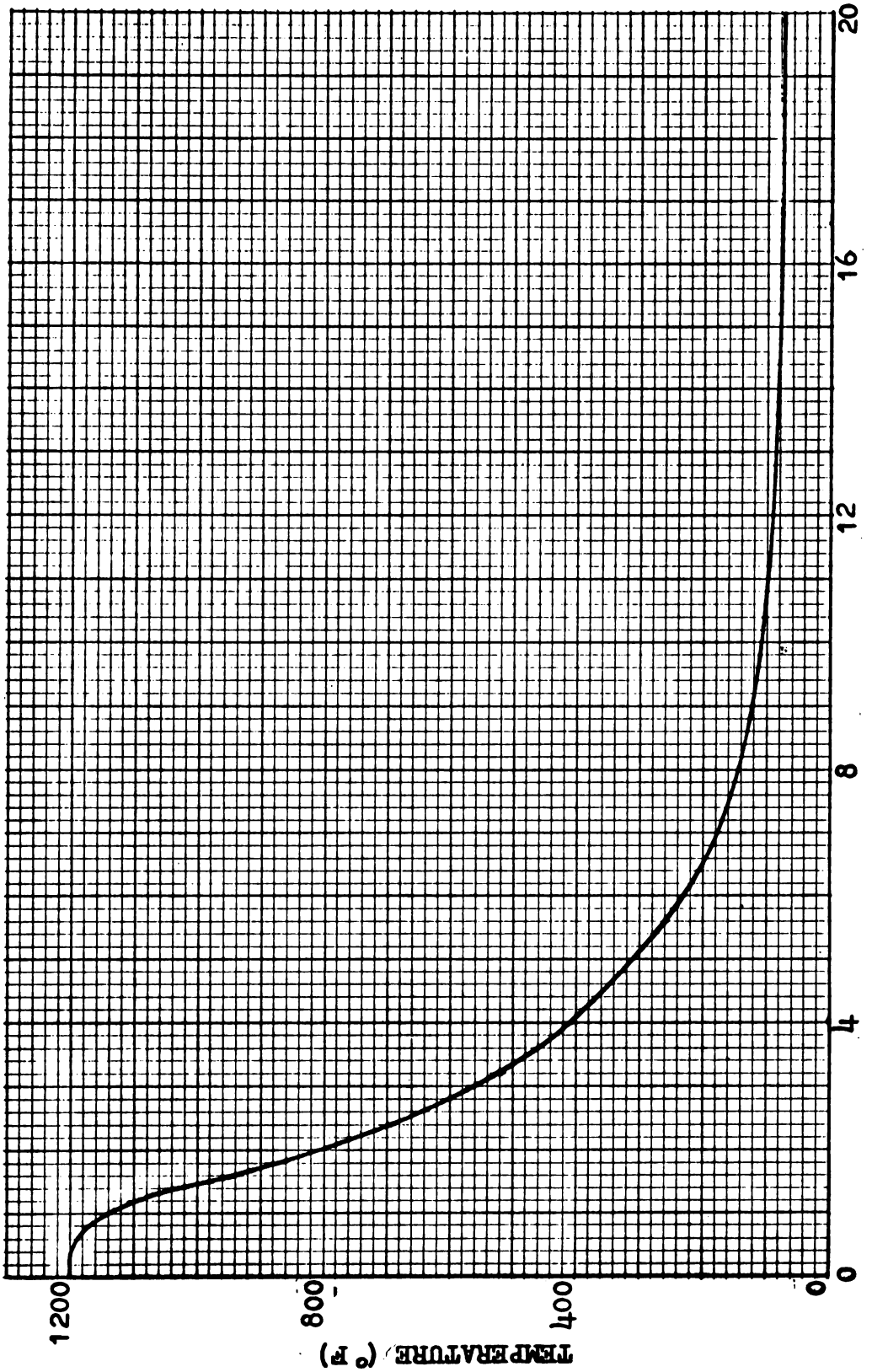

Fig. 3.2 Temperature Distribution for the 6-Foot-Long Bar Heated at the Middle

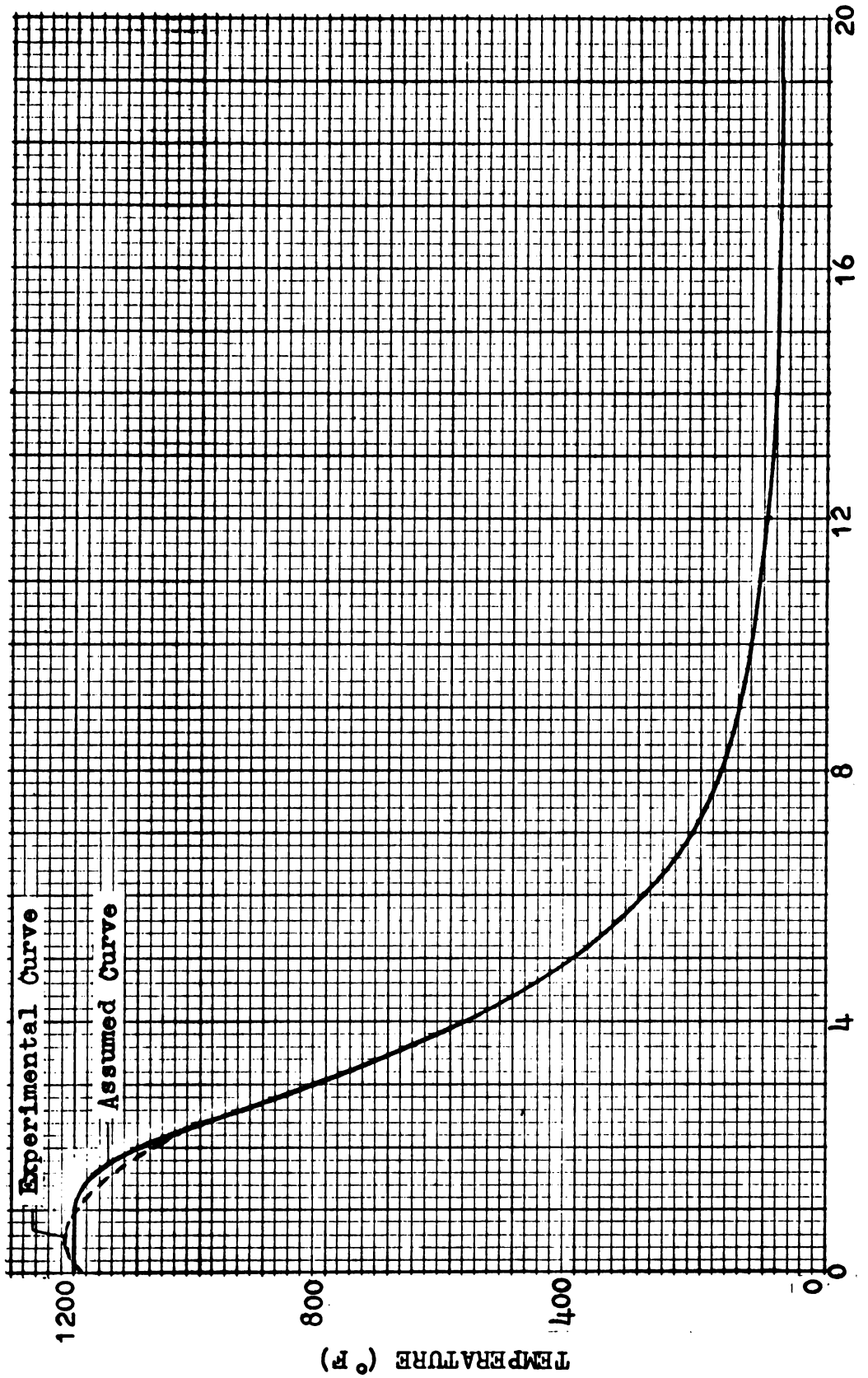

Fig. 3.3 Temperature Distribution for the 4-Foot-Long Bar Heated at the End

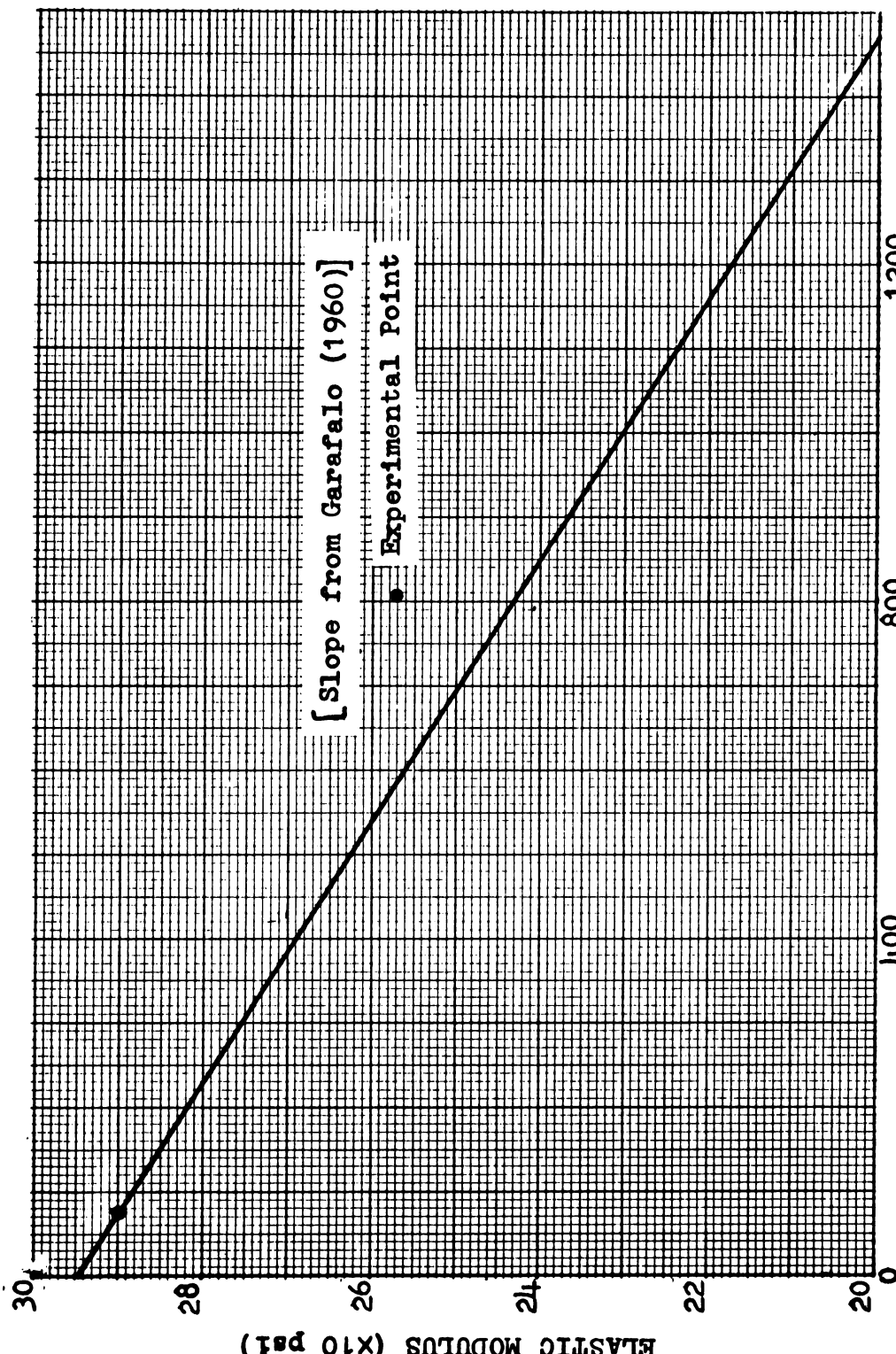

Fig. 3.4 Elastic Modulus Versus Temperature

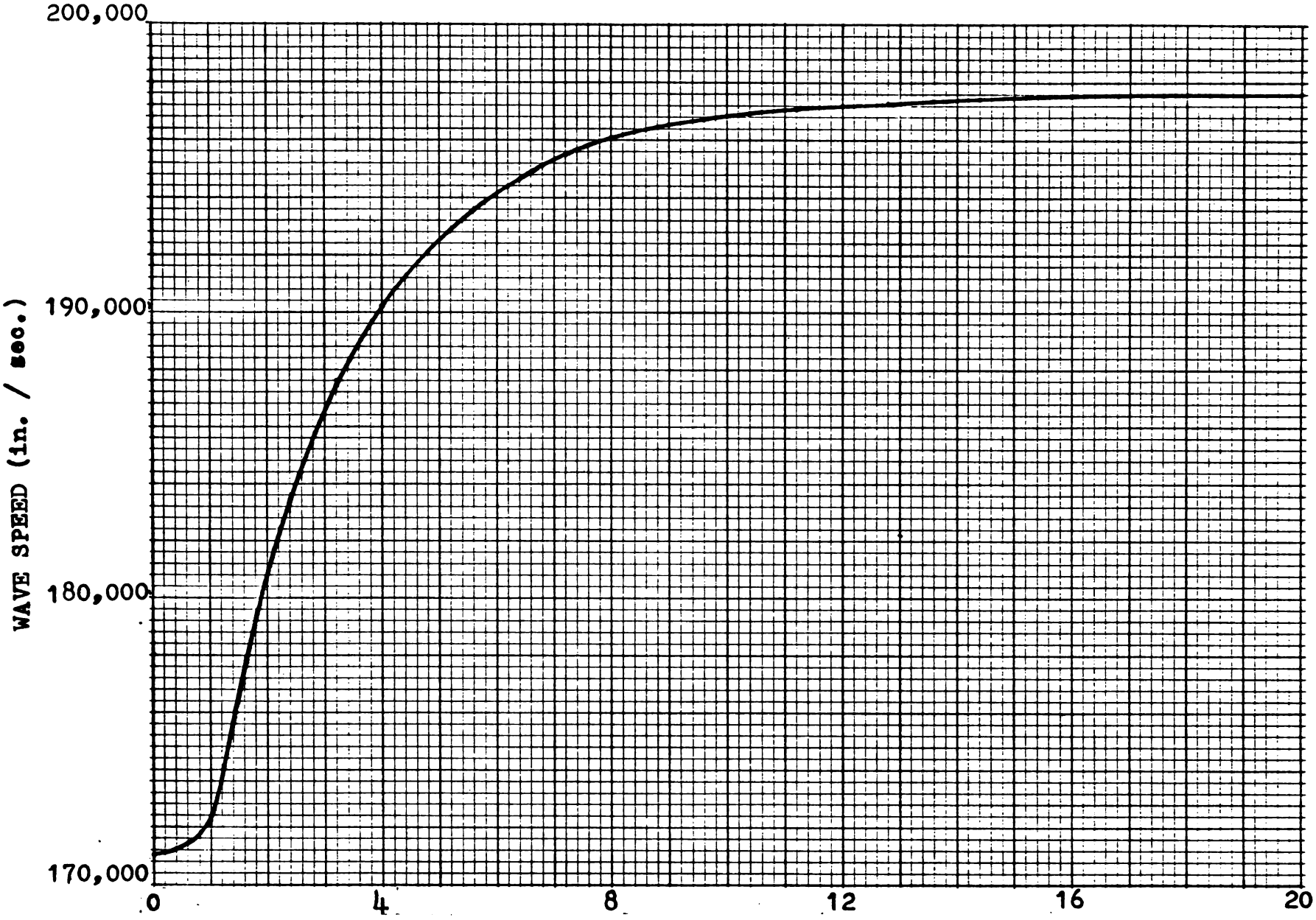

Fig. 3.5 Wave Speed versus Distance for the 6-Foot Bar Heated at the Middle

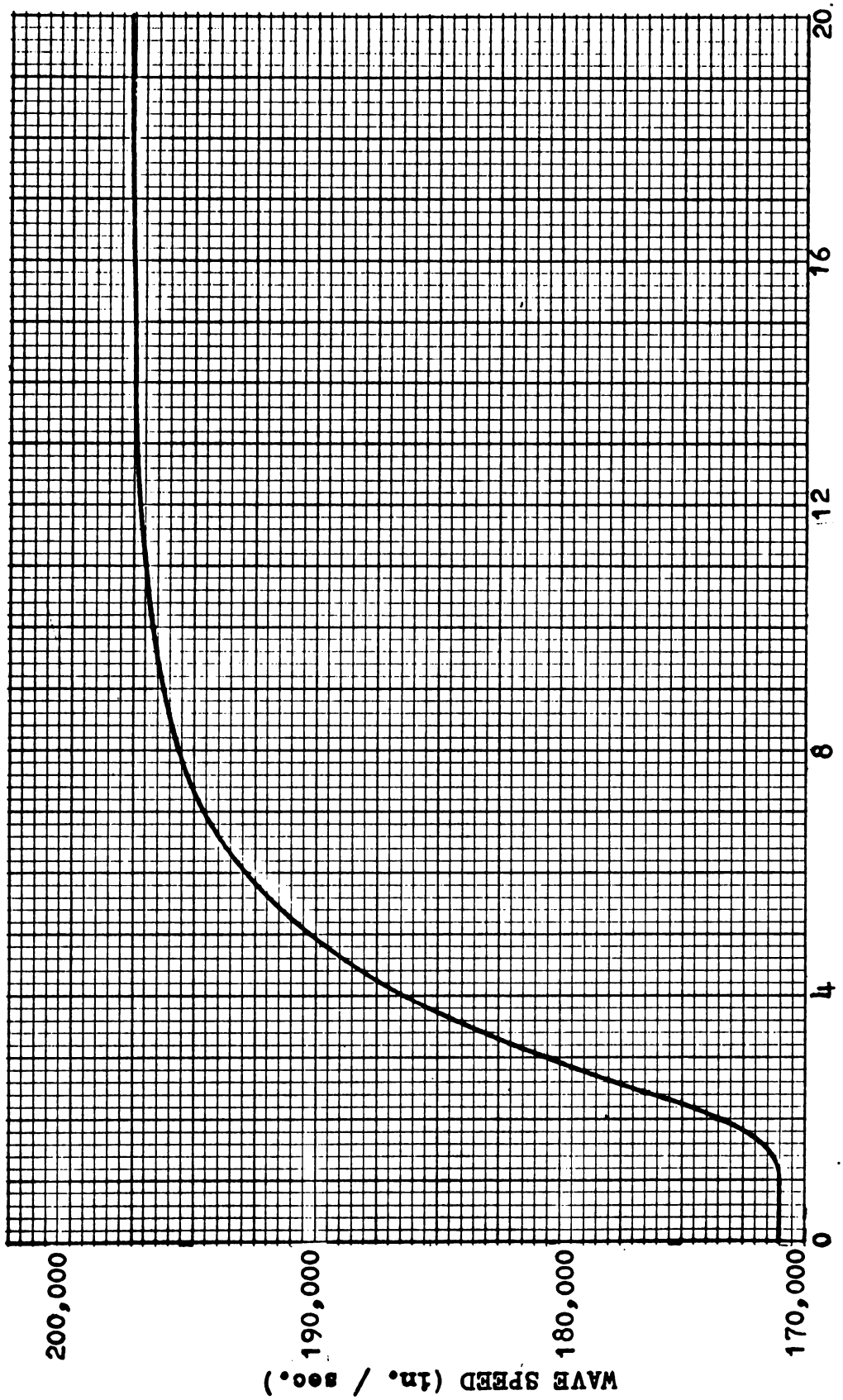

Fig. 3.6 Wave Speed versus Distance for the 4-Foot Bar Heated at the End

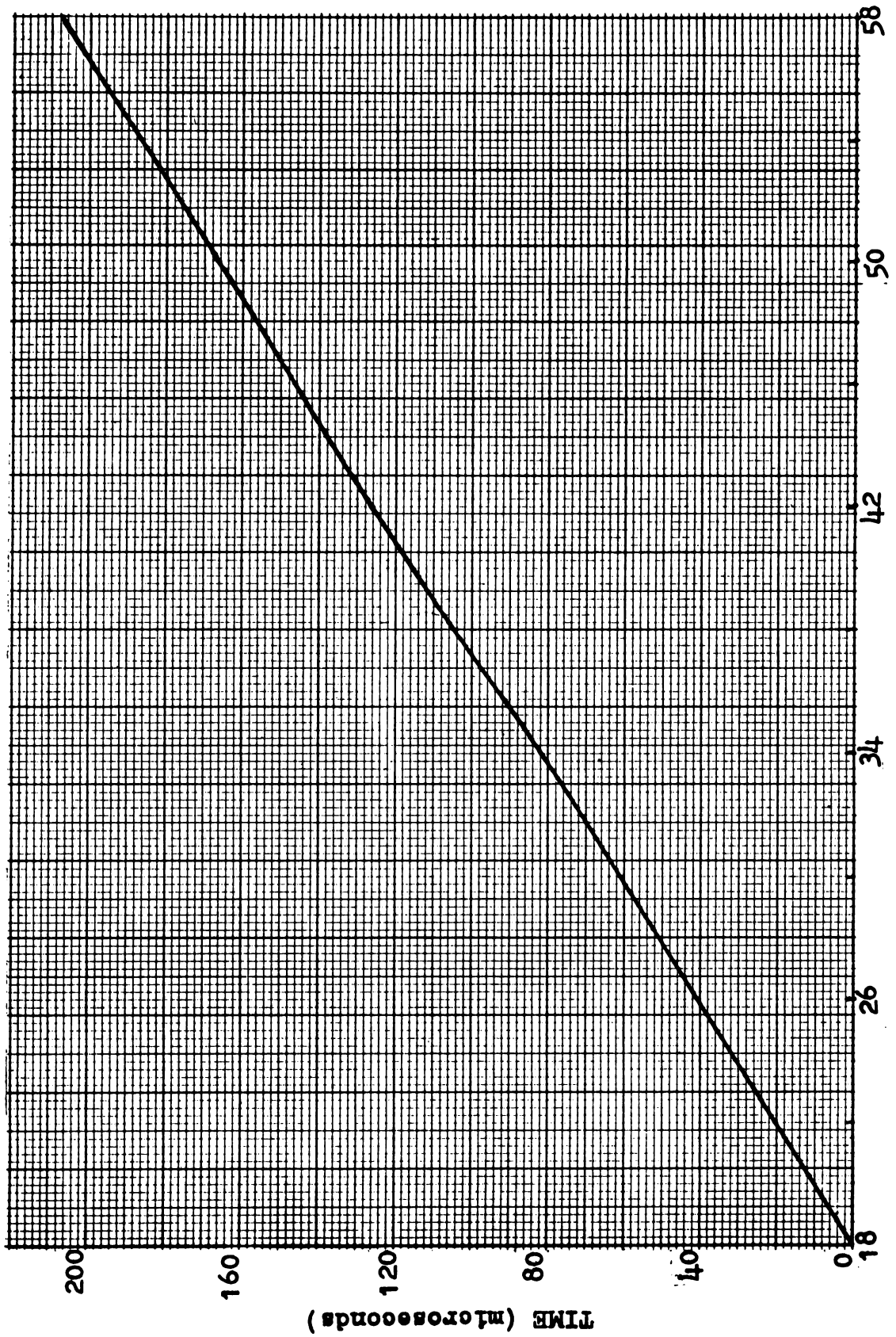

Fig. 3.7 Leading Wave Front Characteristic for the 6-Foot Bar Heated at the Middle

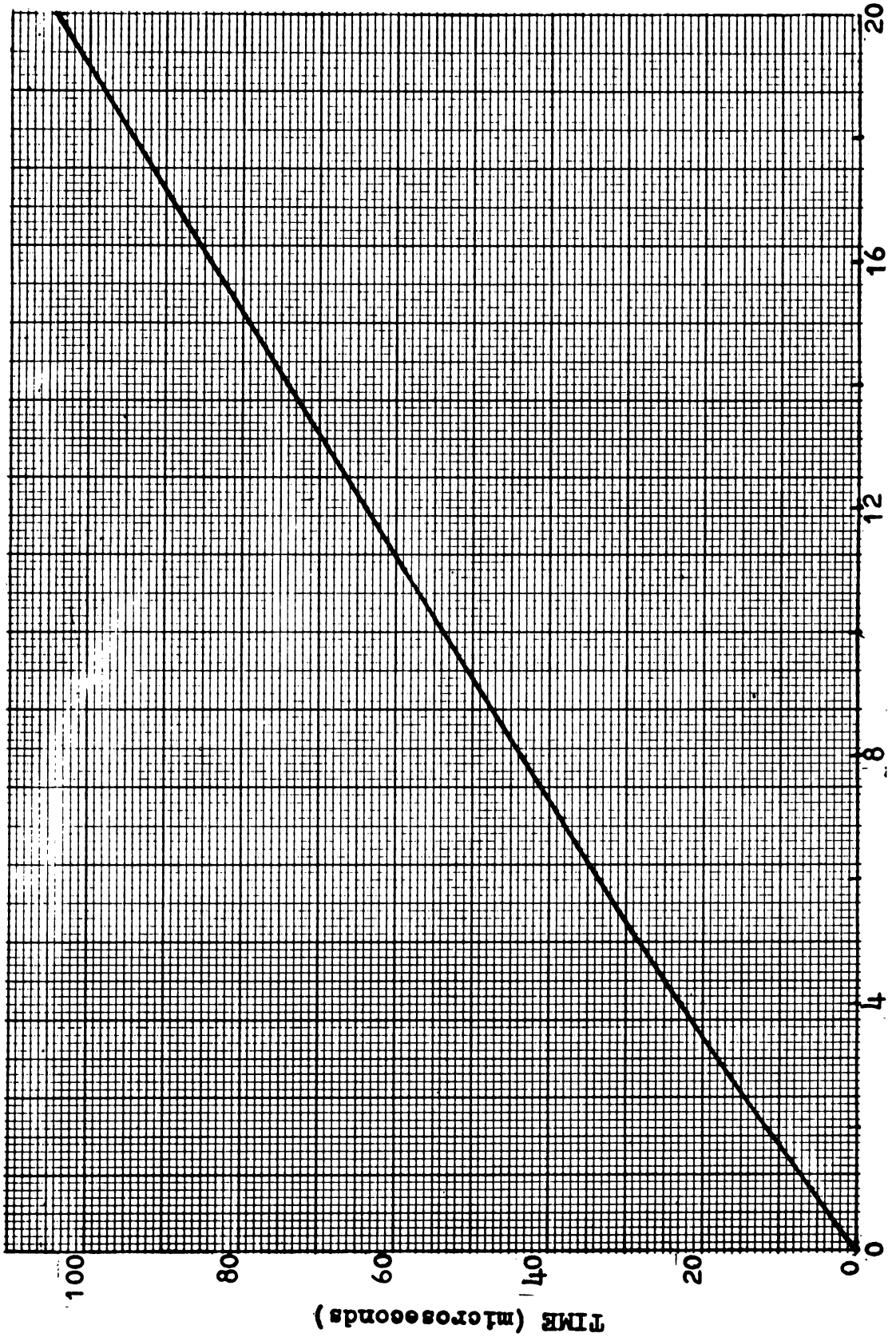

Fig. 3.8 Leading Wave Front Characteristic for the 4-Foot Bar Heated at the End

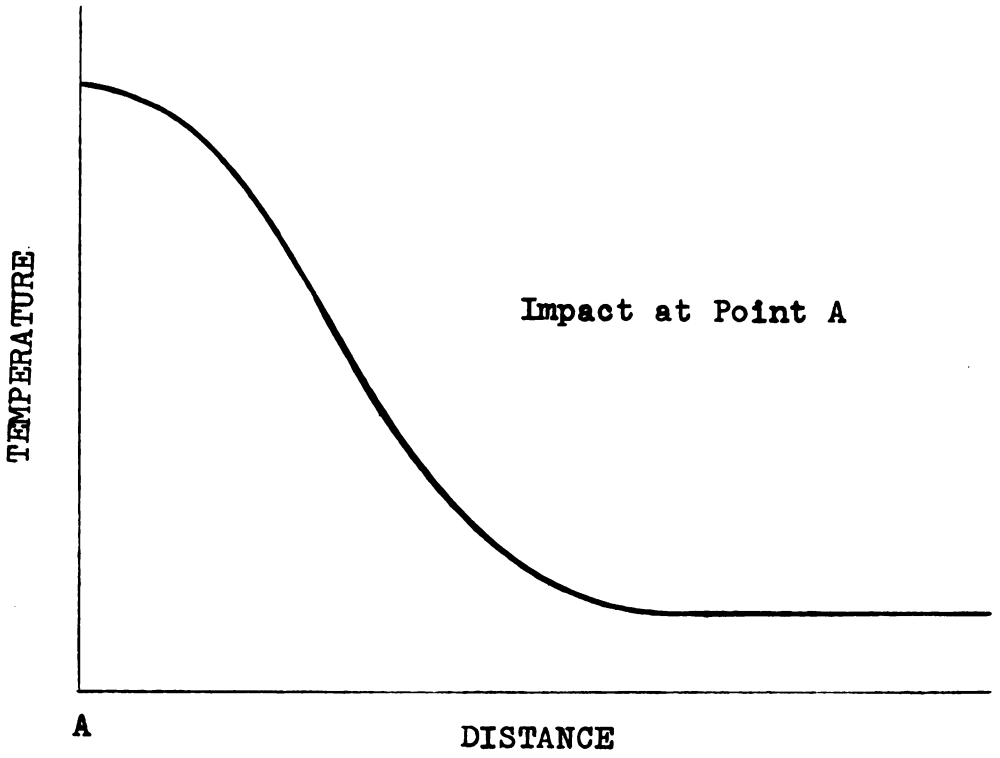

(a) Bar Impacted at the Hot End

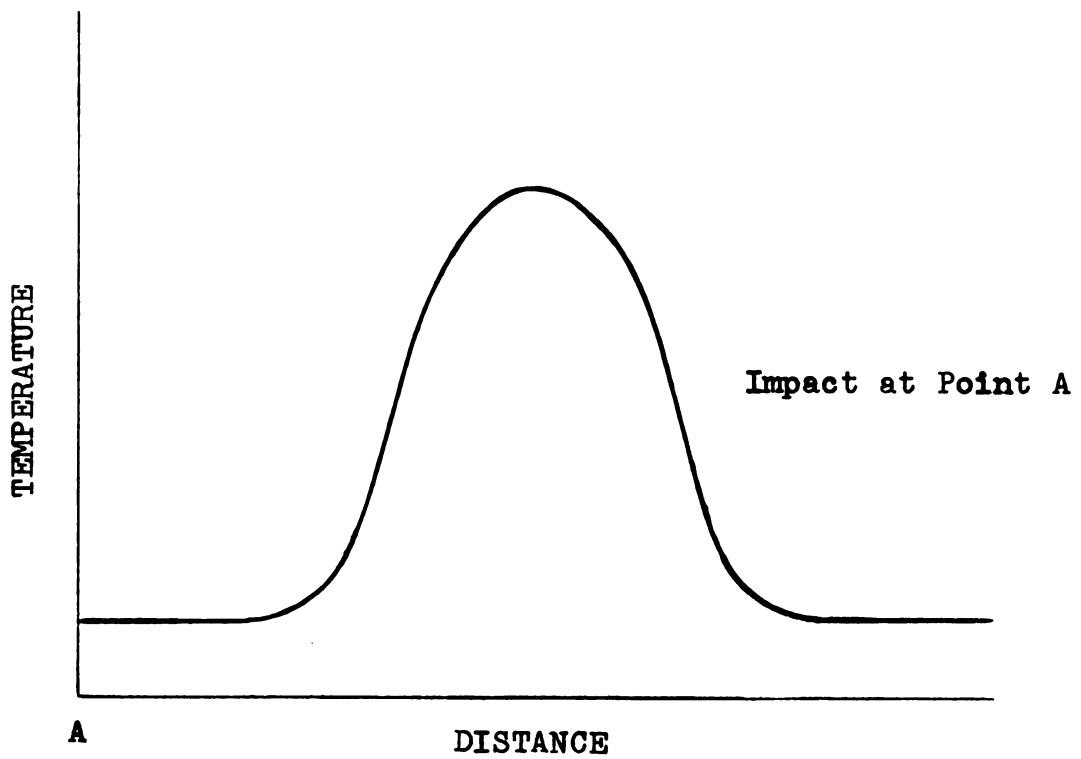

(b) Bar Heated at the Middle

Fig. 3.9 Types of Temperature Distribution Considered

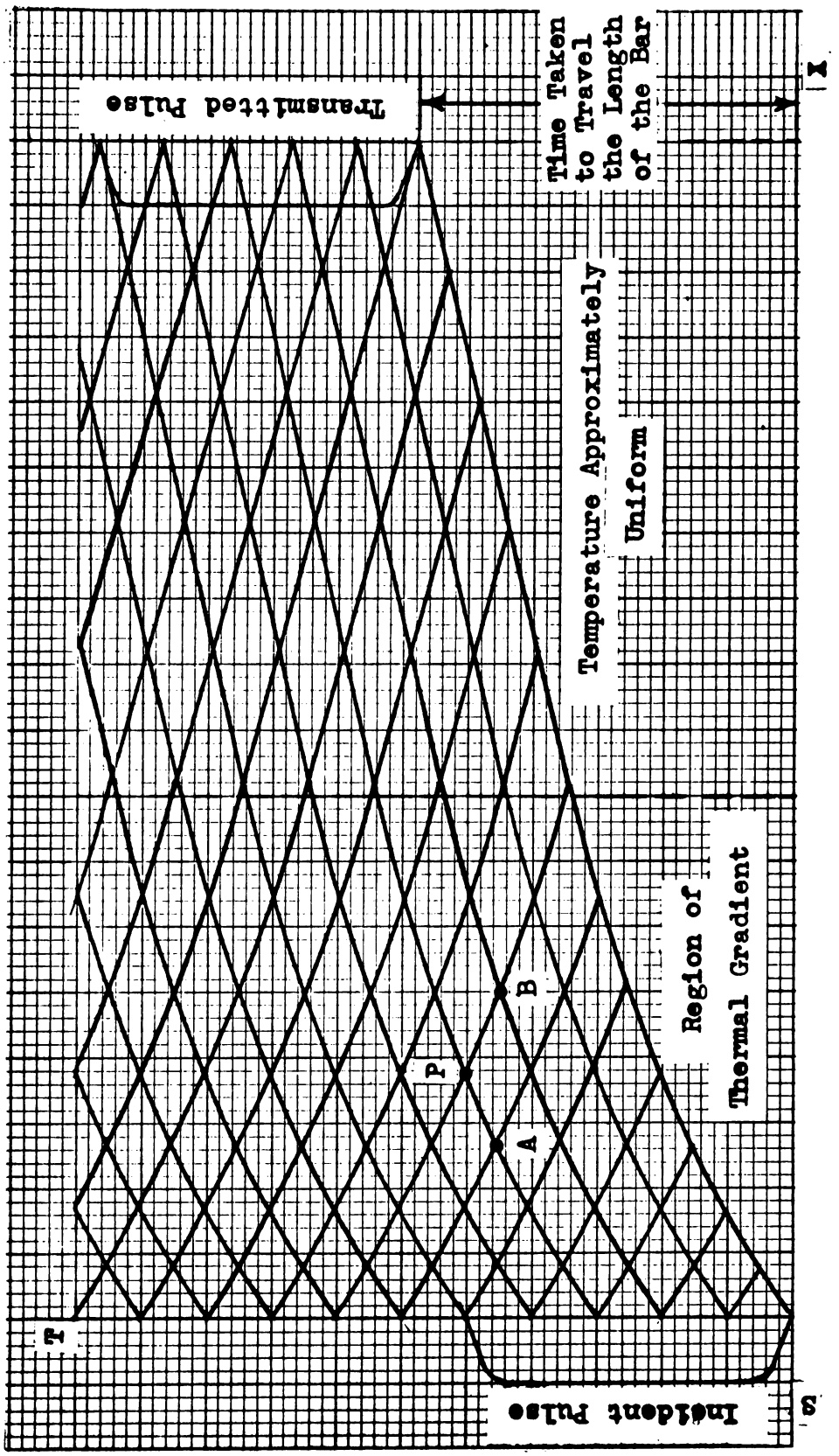

Fig. 3.10 Characteristic Field for the Bar with a Hot End (Schematic)

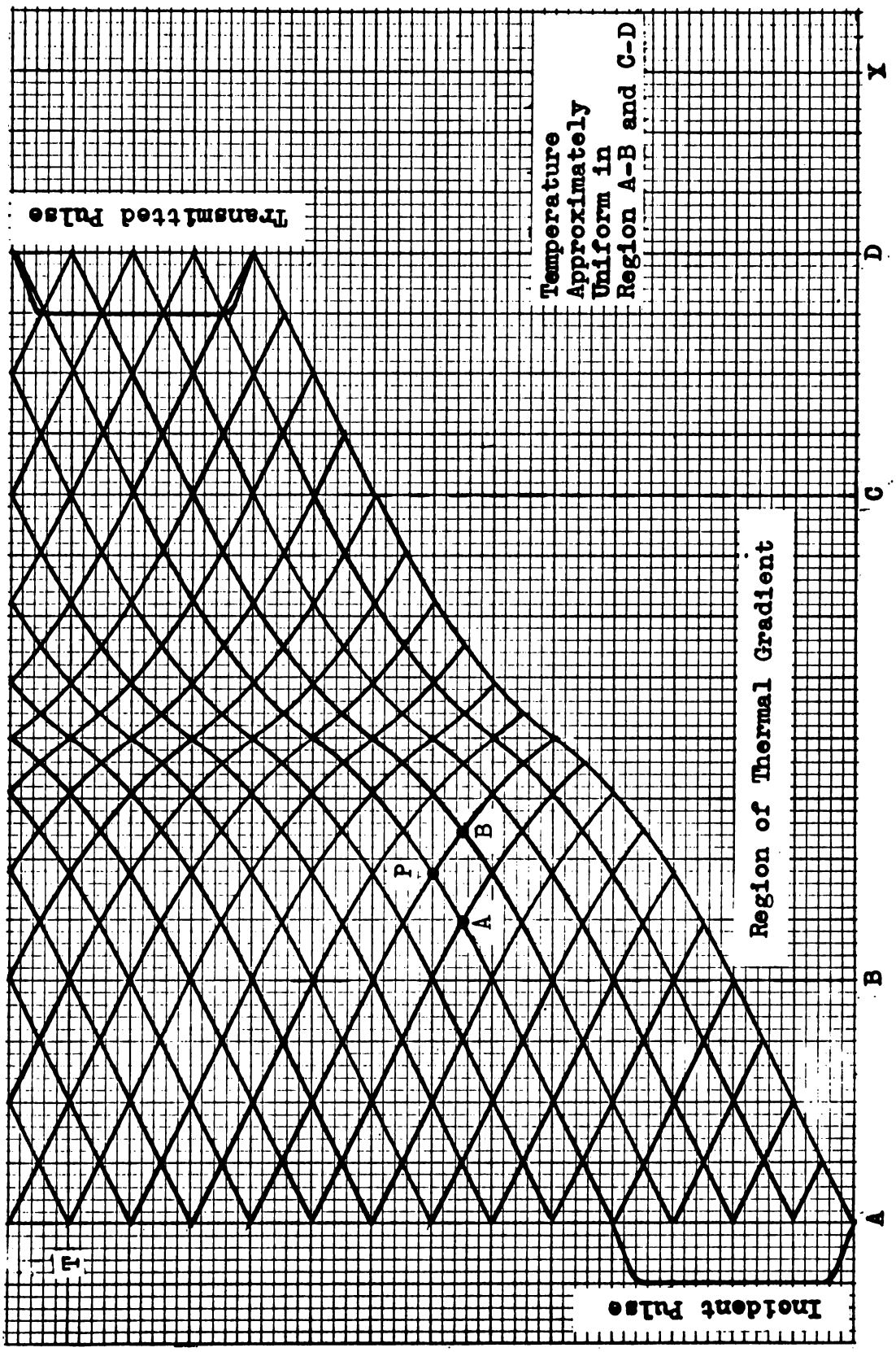

Fig. 3.11 Characteristic Field for a Bar Heated in the Middle (Schematic)

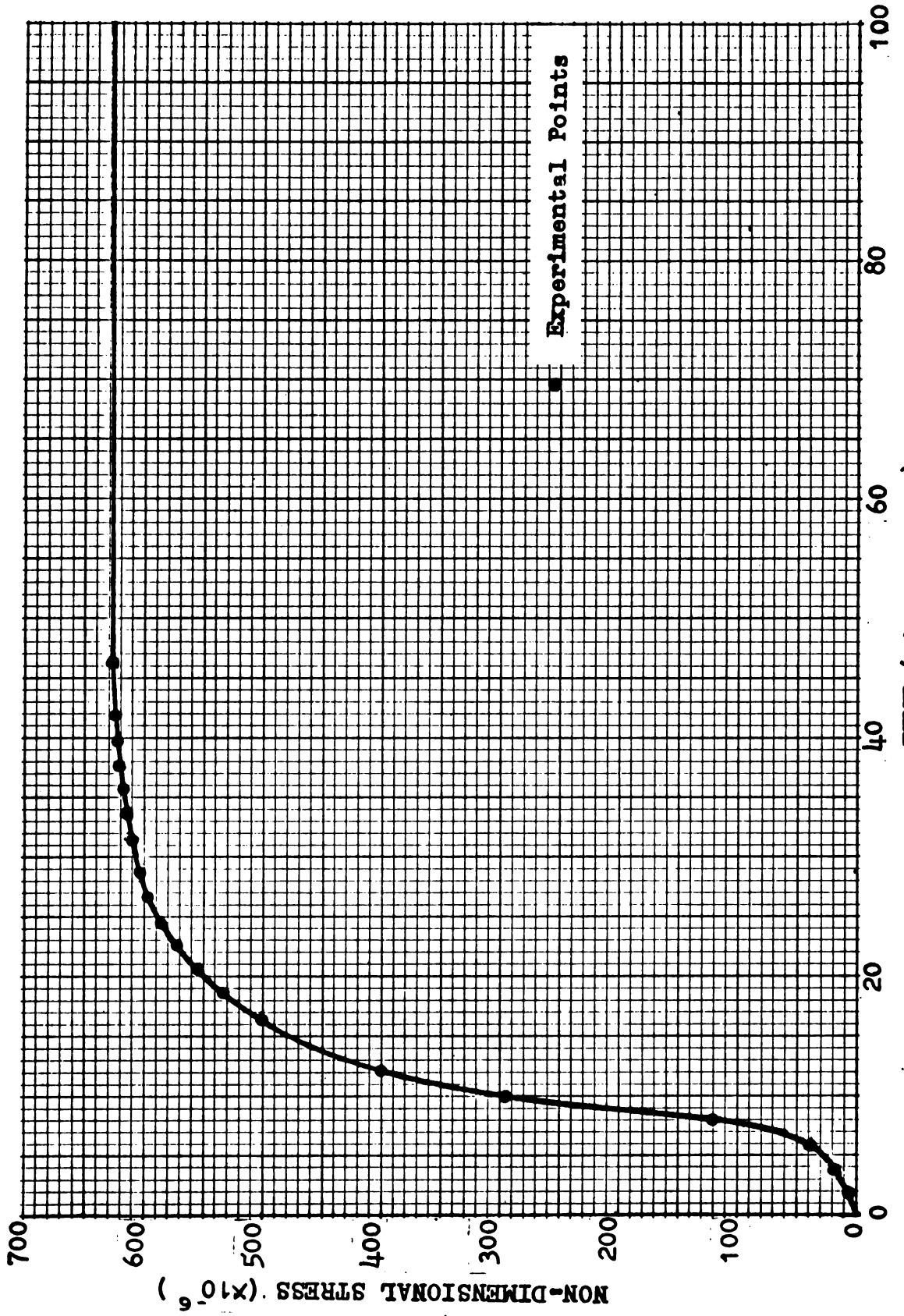

Fig. 3.12 Incident Pulse for the 6-Foot-Long Bar Heated in the Middle

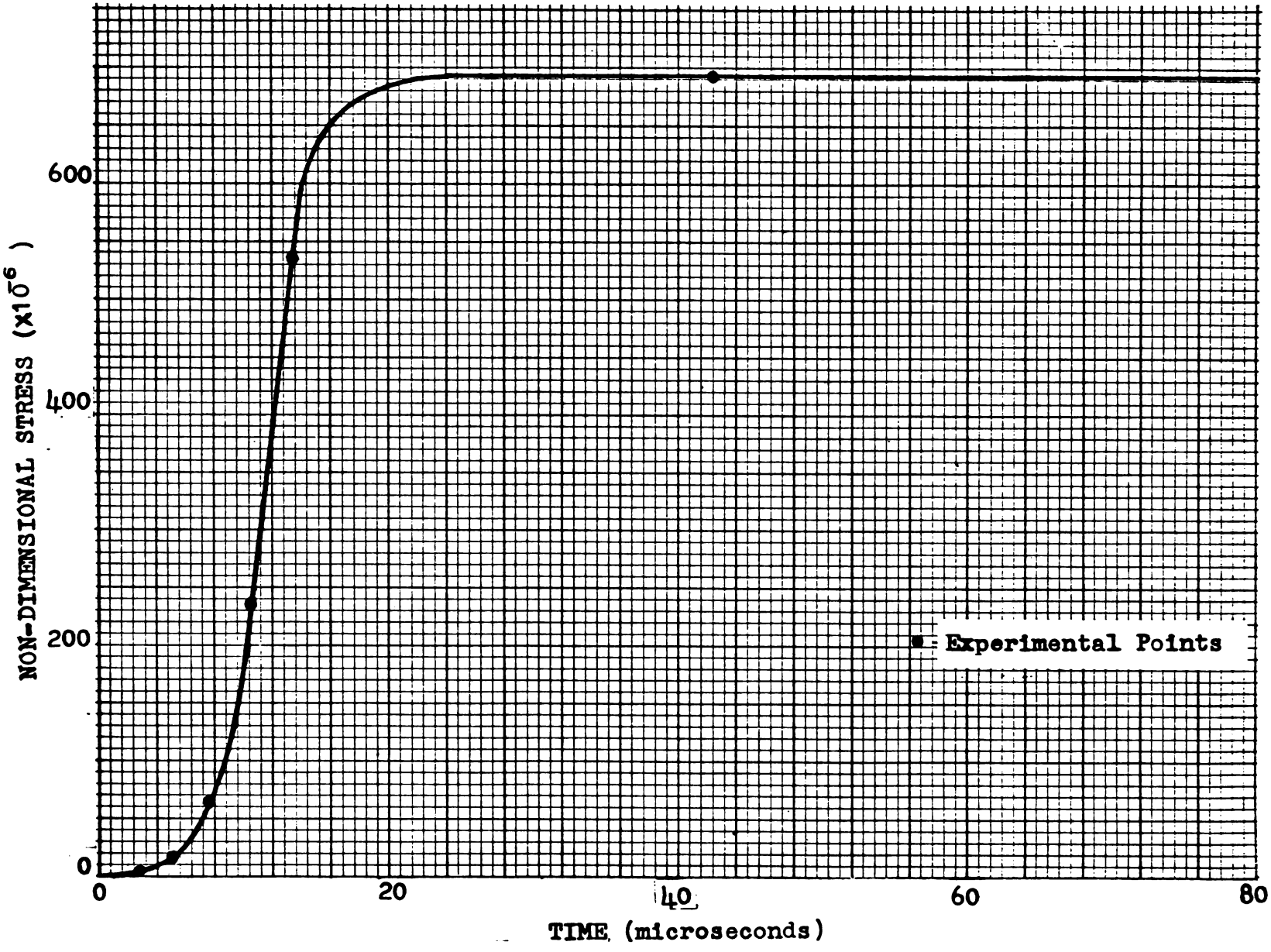

Fig. 3.13 Incident Pulse for the 4-Foot-Long Bar Heated at the End

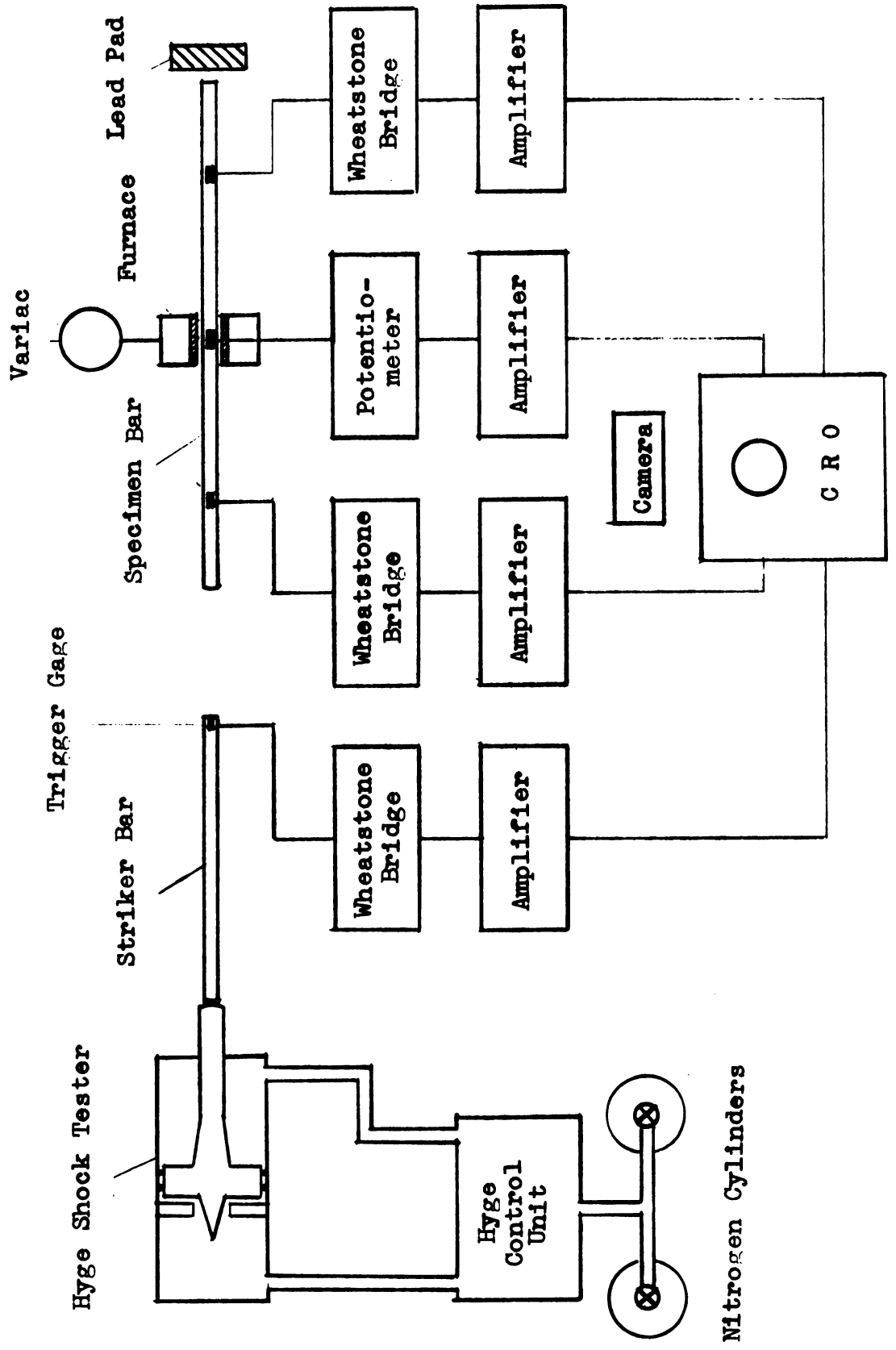

Fig. 5.1 Schematic Drawing of the Apparatus

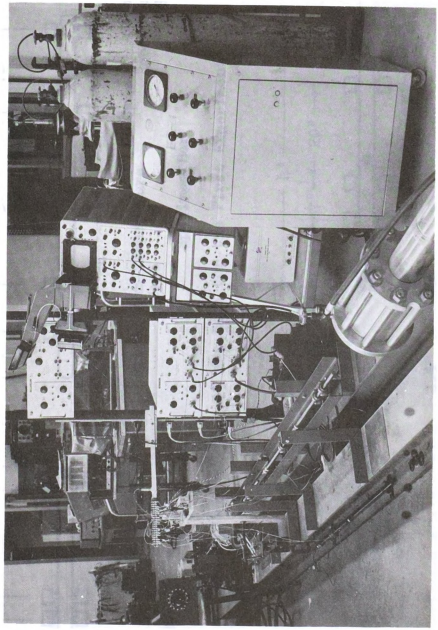

Fig. 5.2 A General View of the Test Set-Up

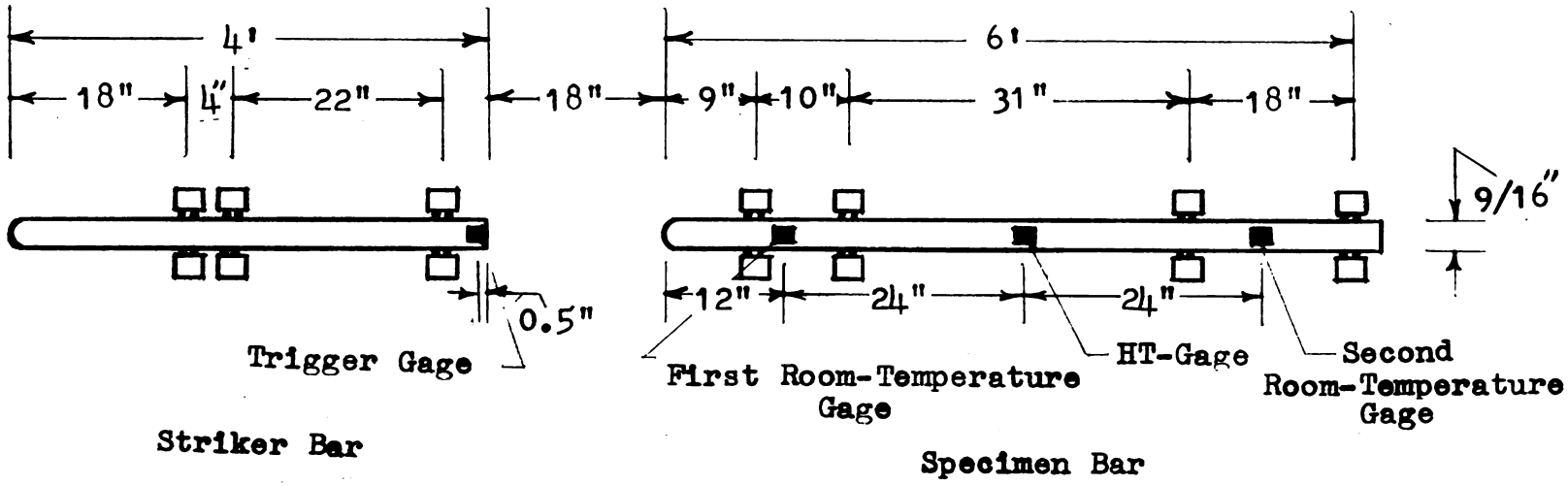

Fig. 5.3(a) Details of the Bars for the First Experiment

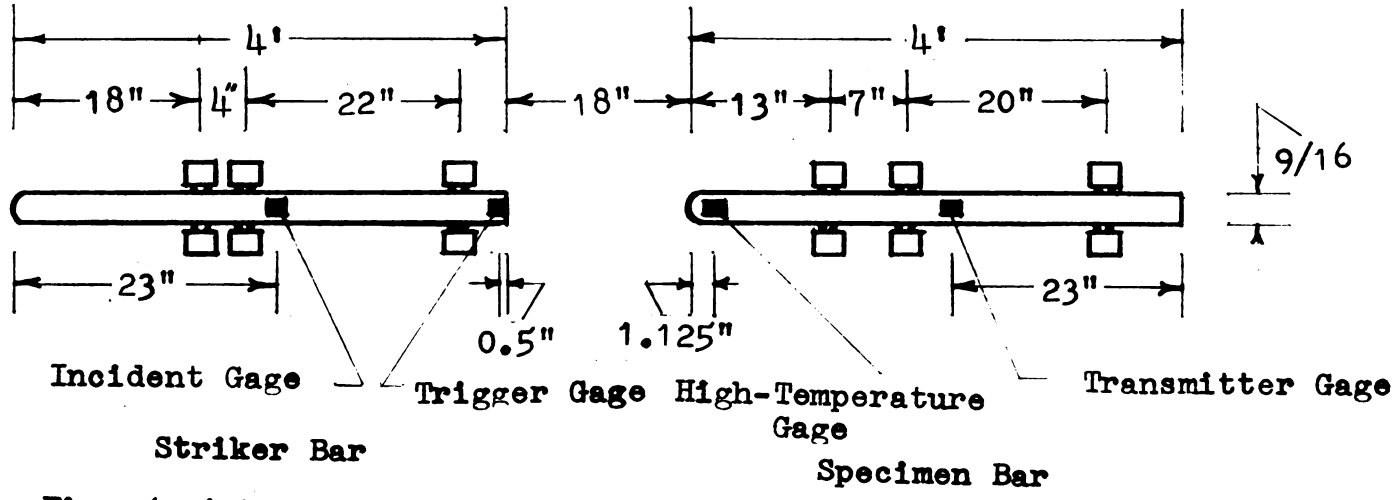

Fig. 5.3(b) Details of the Bars for the Second Experiment

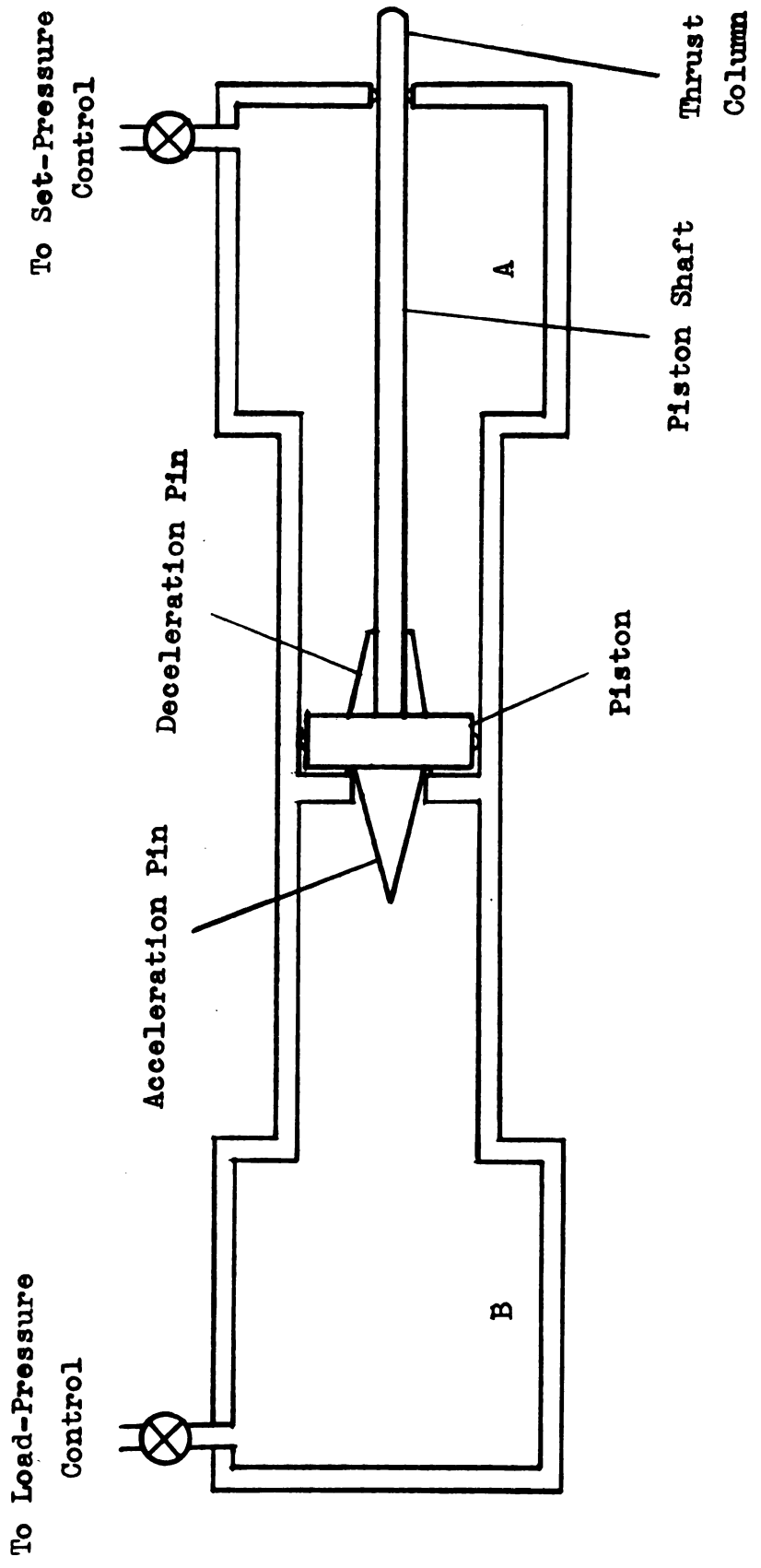

Fig. 5.4 Hyge Shock Tester (after Childister, 1961)

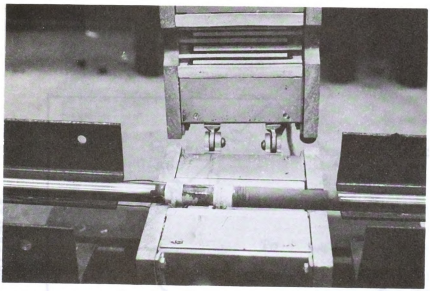

(a) Bar Heated at the Middle

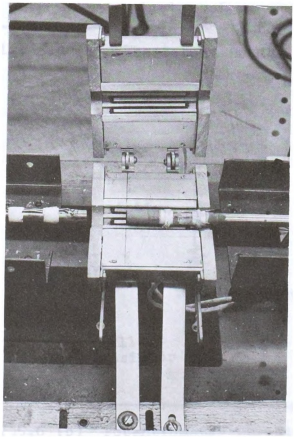

(b) Bar Heated at the End

Fig. 5.5 Close-Up of the Furnace and the High-Temperature Gage

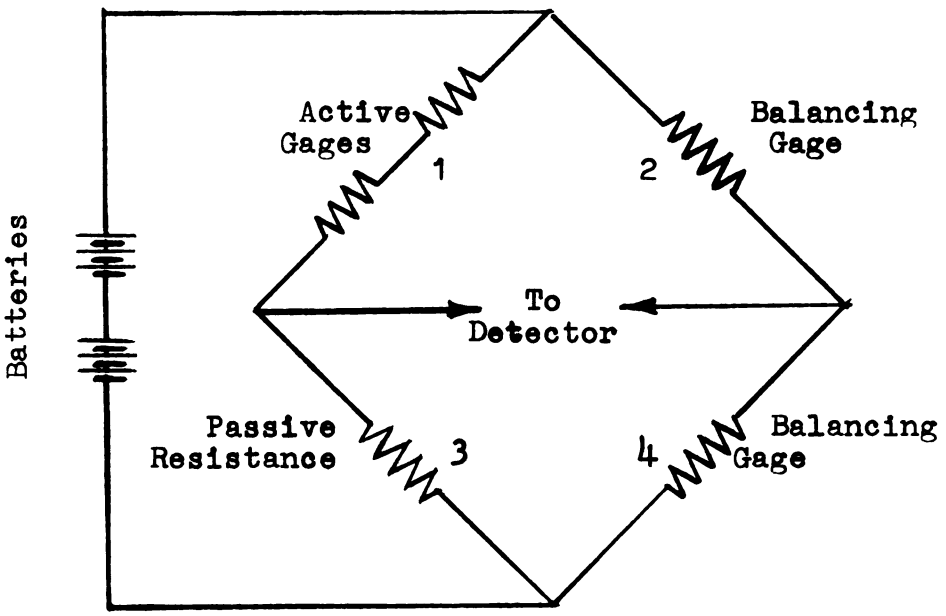

Fig. 5.6 (a) Wheatstone Bridge

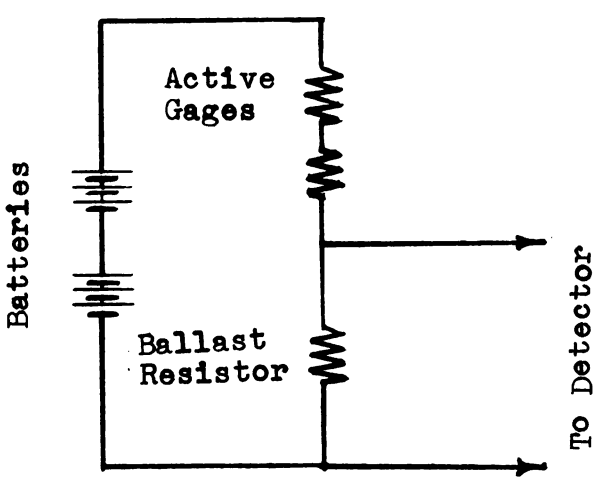

Fig. 5.6 (b) Potentiometer Circuit

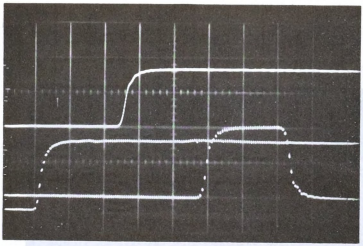

(a) At Room Temperature (Sweep Speed 50 microsec./c.m.)

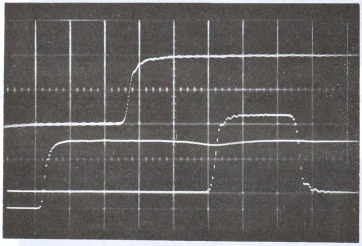

(b) At 1200° F (Sweep Speed 50 microsec./c.m.)

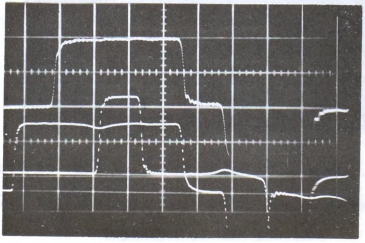

(c) At 1200° F (Sweep Speed 100 microsec./c.m.)

Fig. 7.1 Oscilloscope Records from the 6 Foot-Long Bar Heated in the Middle

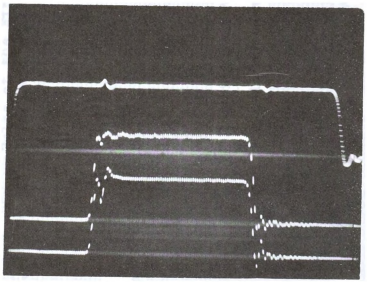

(a) At Room Temperature (Sweep Speed 50 microsec./c.m.)

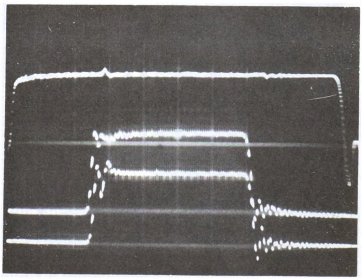

(b) At 1200° F (Sweep Speed 50 microsec./c.m.)

Fig. 7.2 Oscilloscope Records from the 4-Foot-Long Bar Impacted at the Hot End

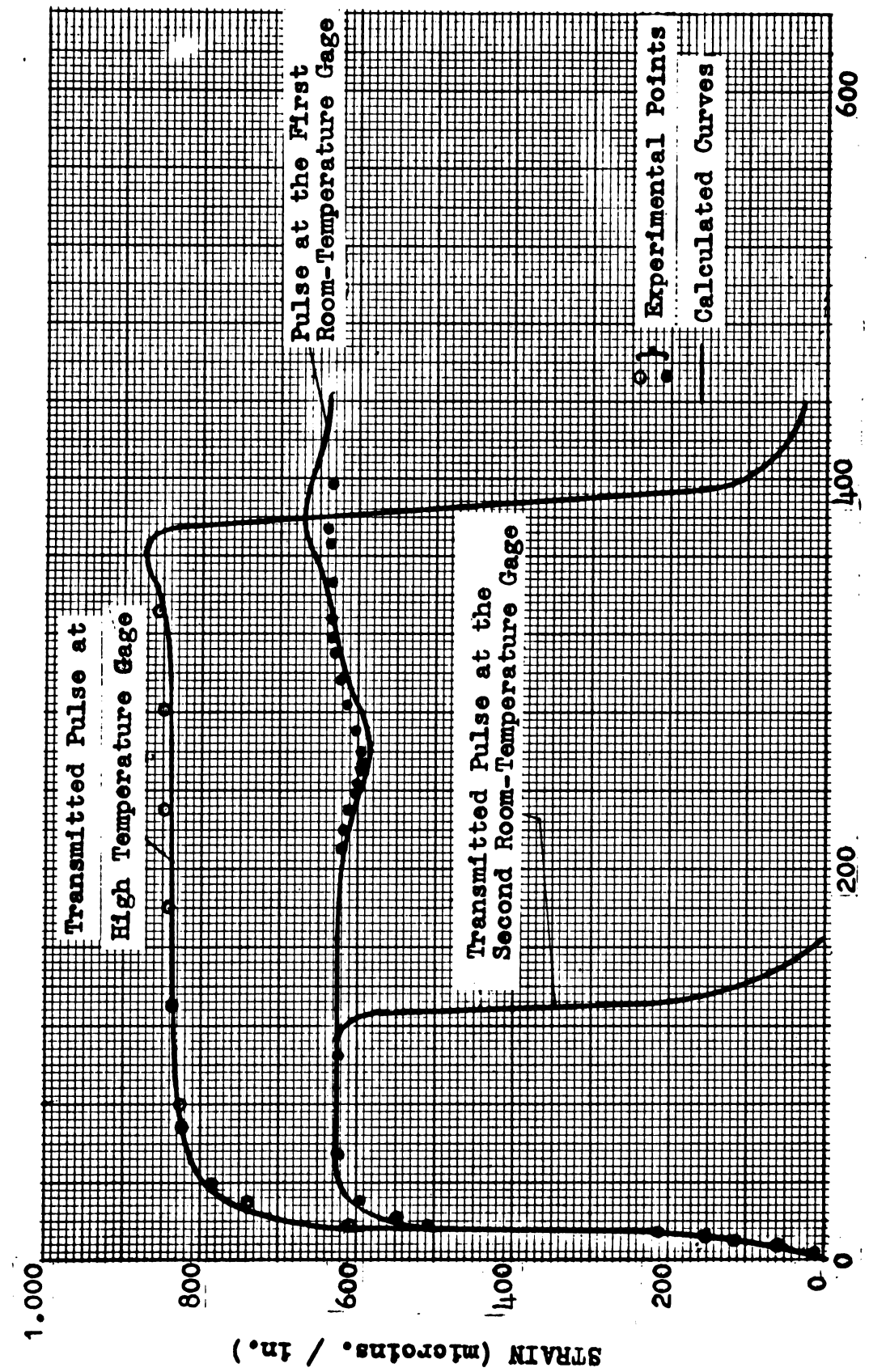

Fig. 7.3 Pulse at Various Points of the 6-Foot Bar Heated at the Middle

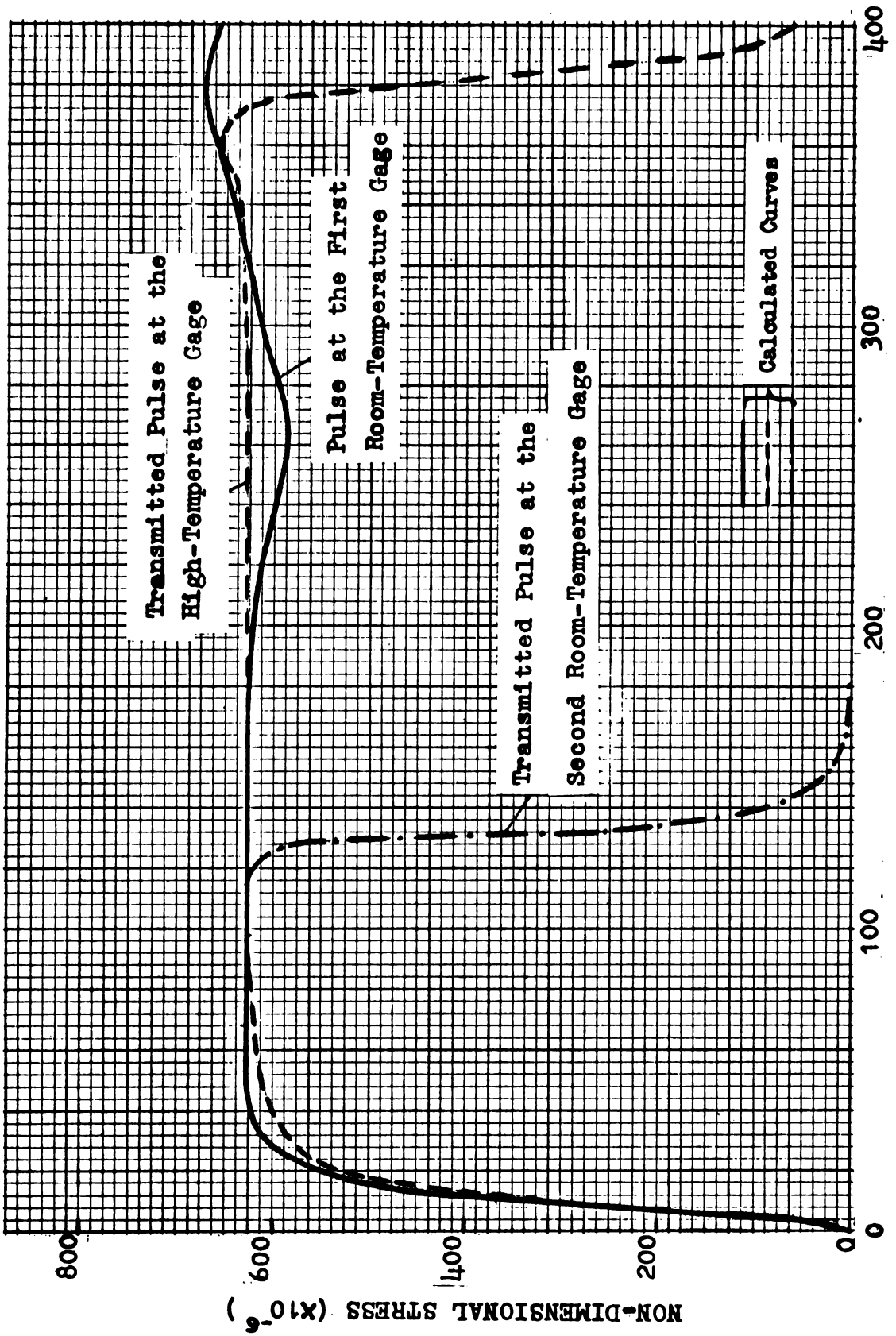

Fig. 7.4 Stress Pulse at Various Points of the 6-Foot Bar Heated at the Middle

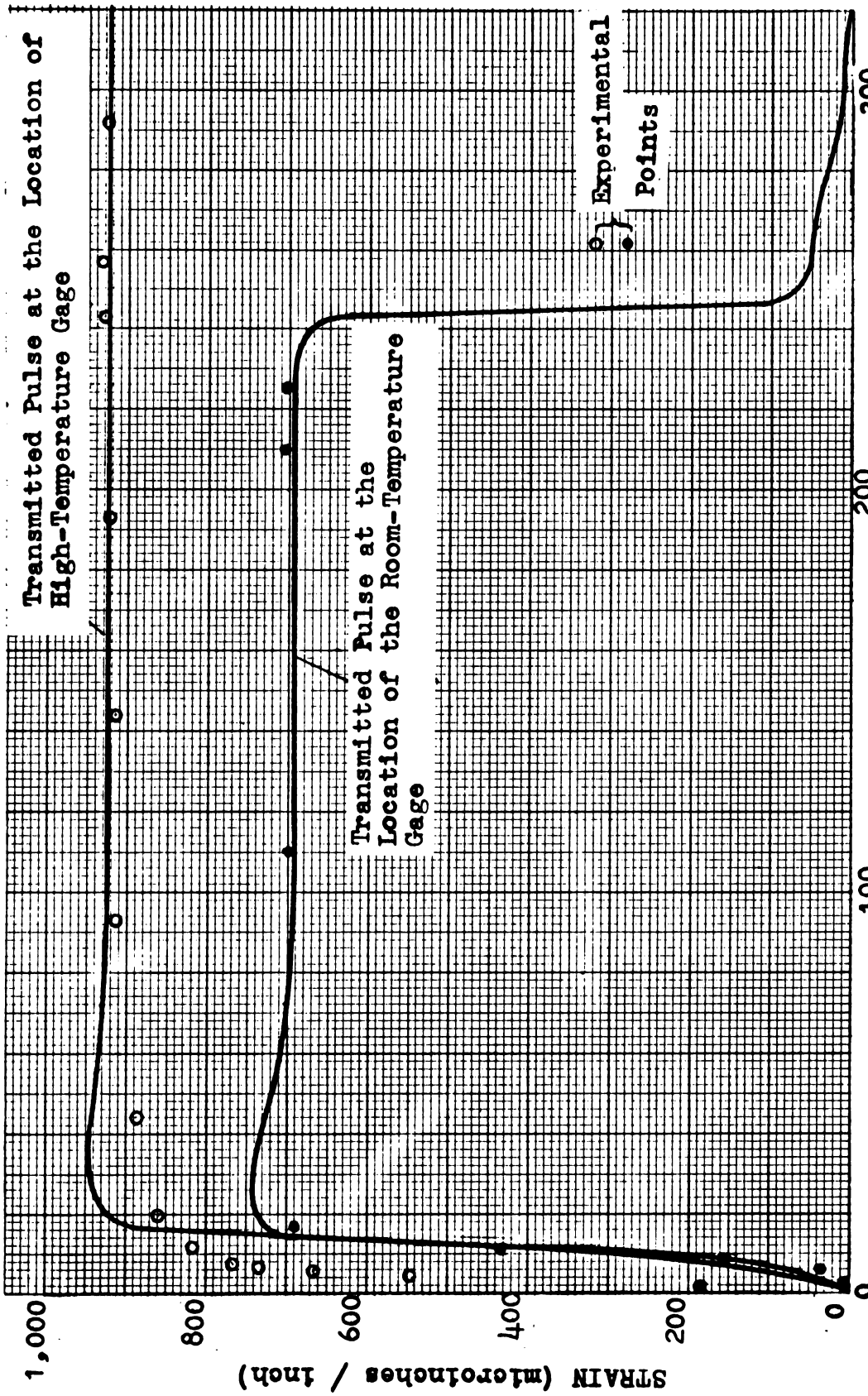

Fig. 7.5 The Transmitted Pulse in the 4-Foot-Long Bar Impacted at the Hot End

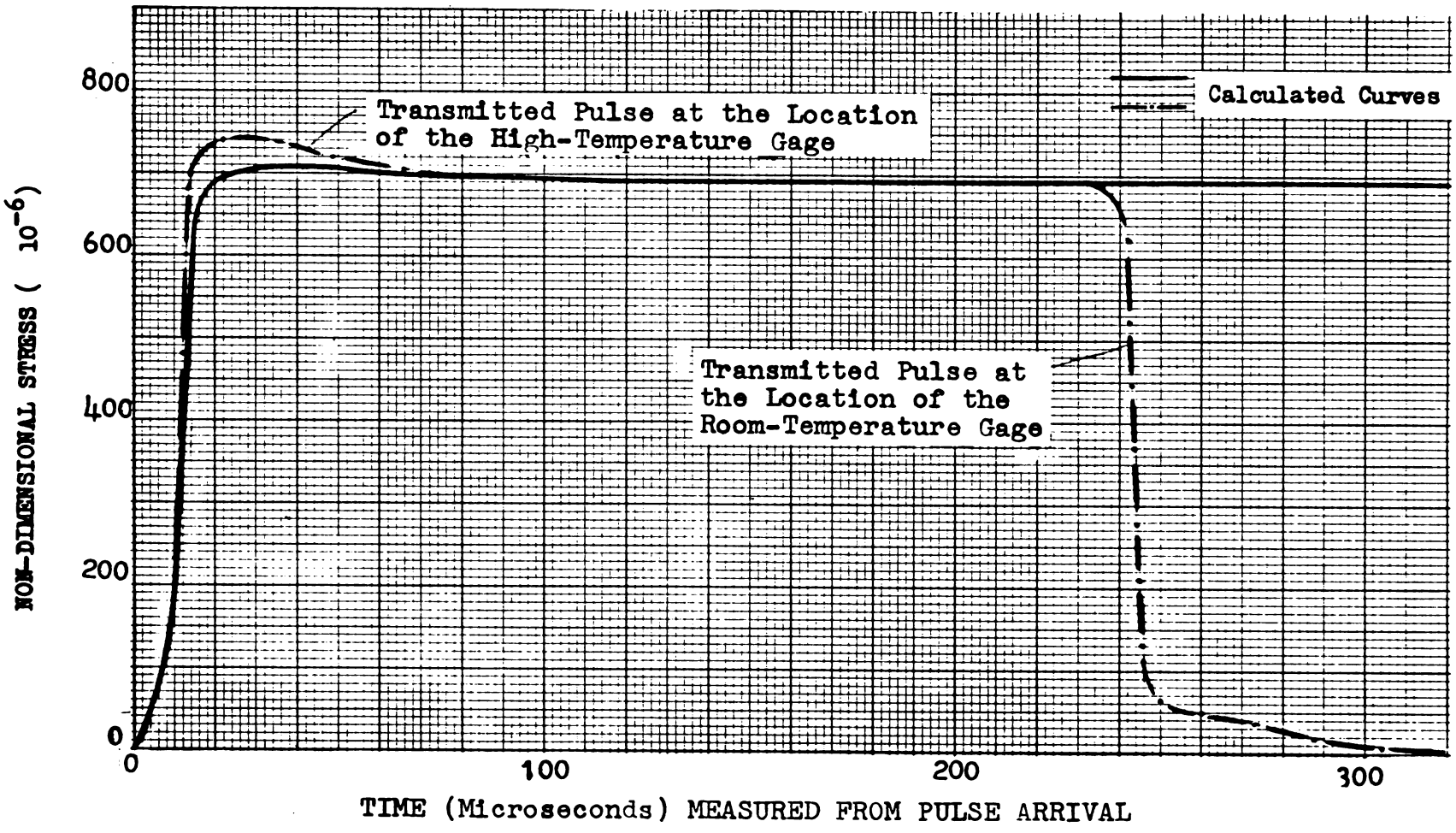

Fig. 7.6 The Transmitted Stress Pulse in the 4-Foot-Long Bar Impacted at the Hot End

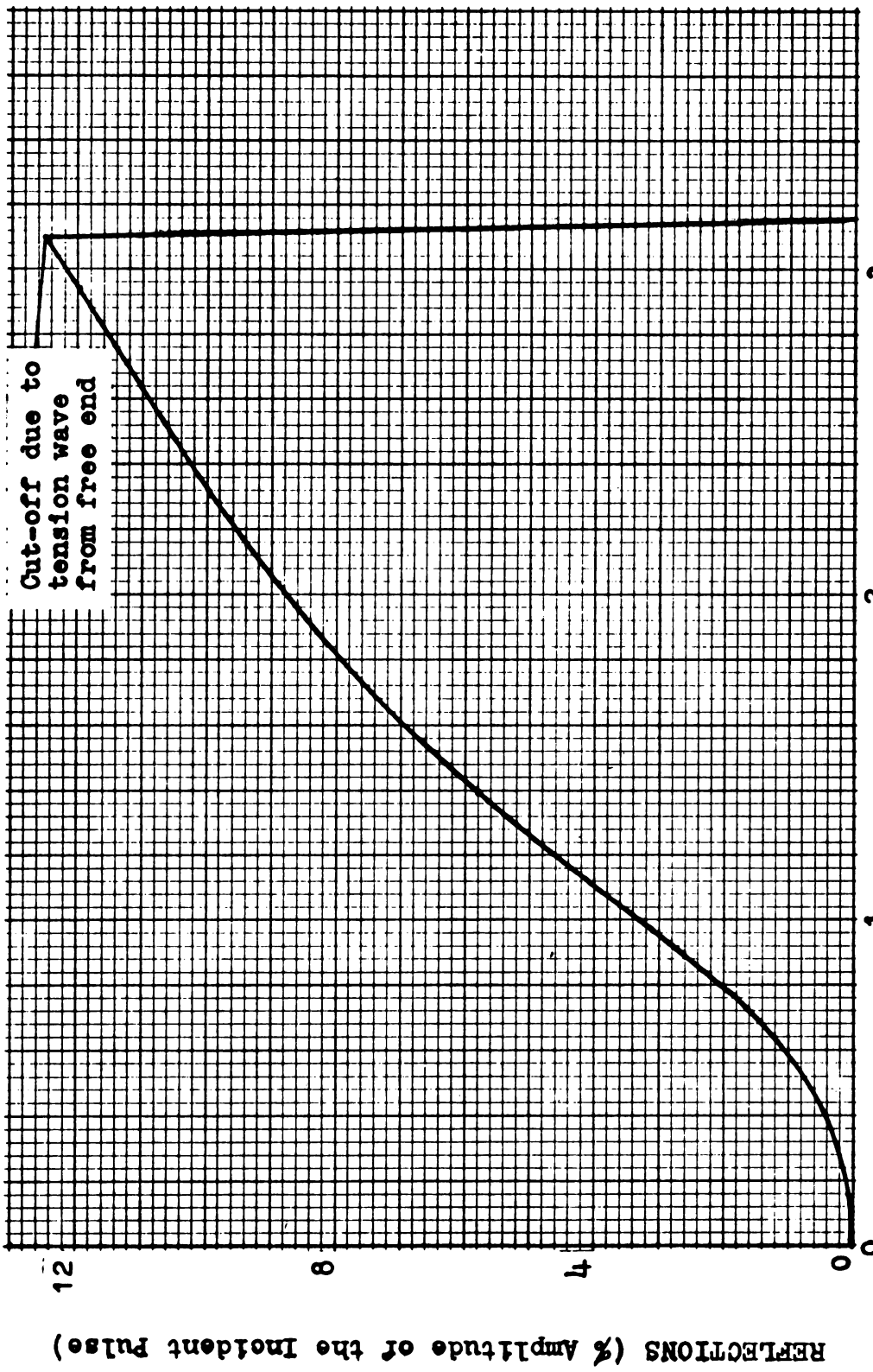

Fig. 7.7 Reflected Pulse in the Modified Lindholm Problem(Measured at the Middle of the Bar)

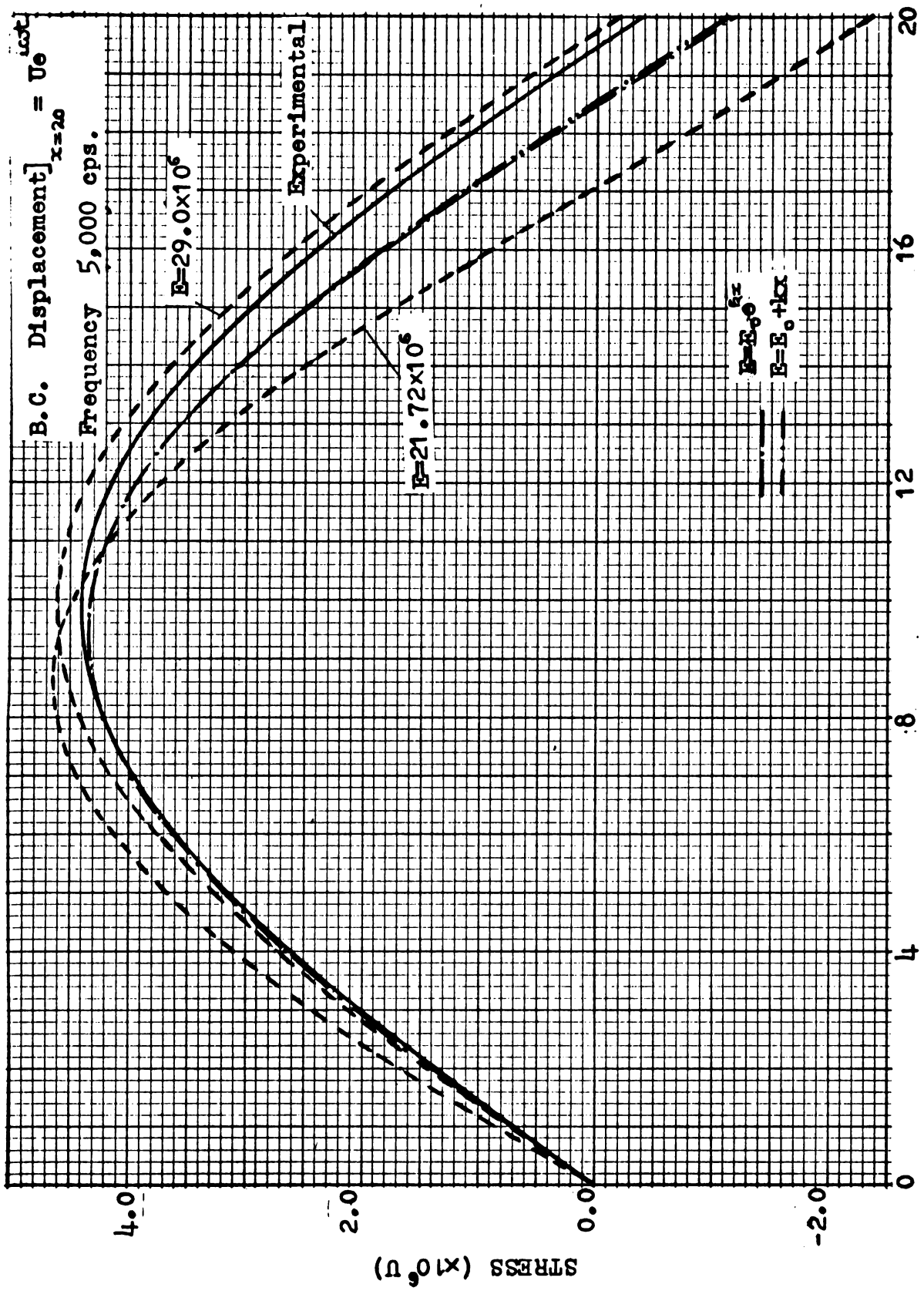

Fig. 7.8 Stress Amplitude for 5000 cps.

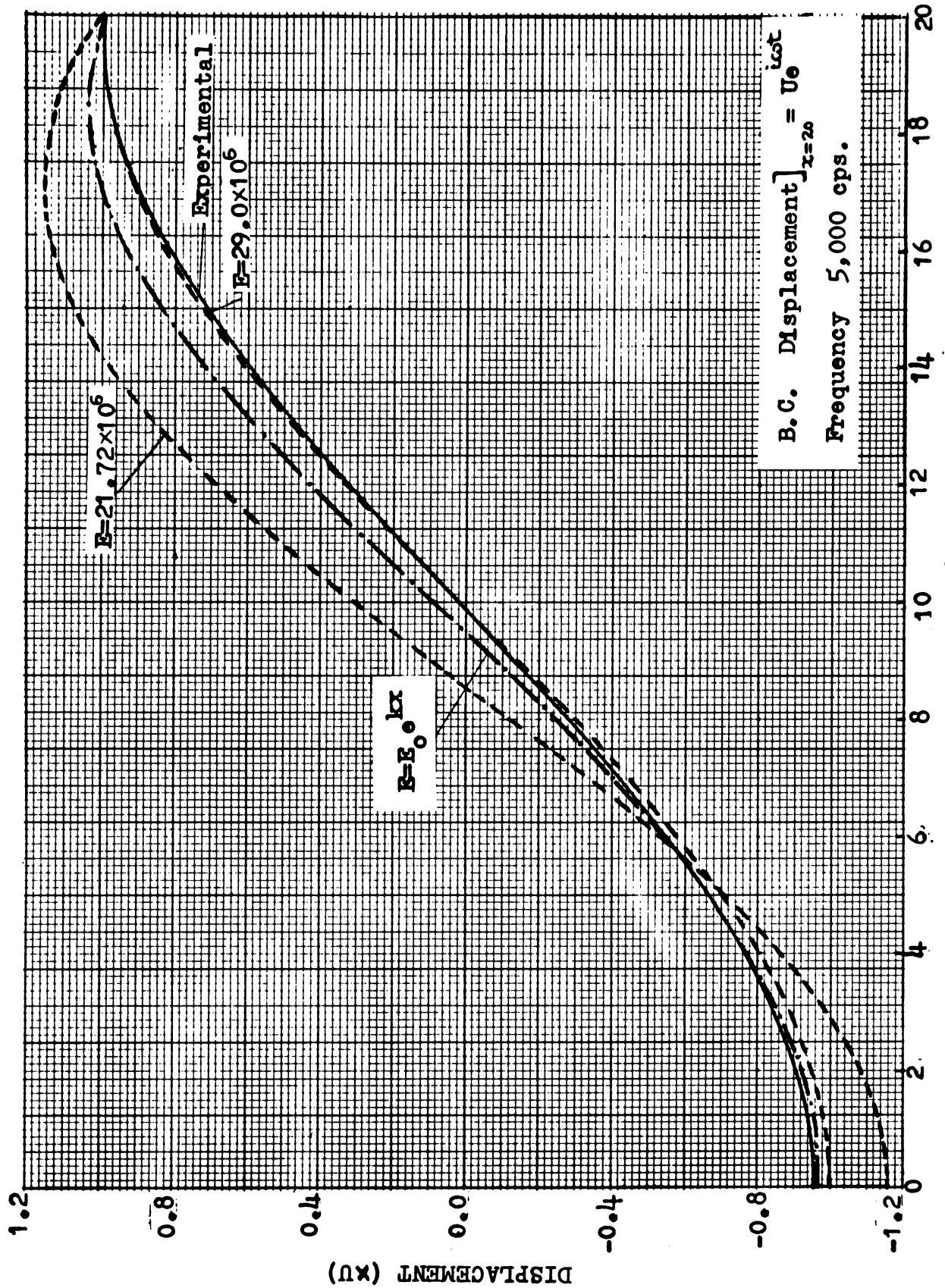

Fig. 7.9 Displacement Amplitude for 5000 cps.

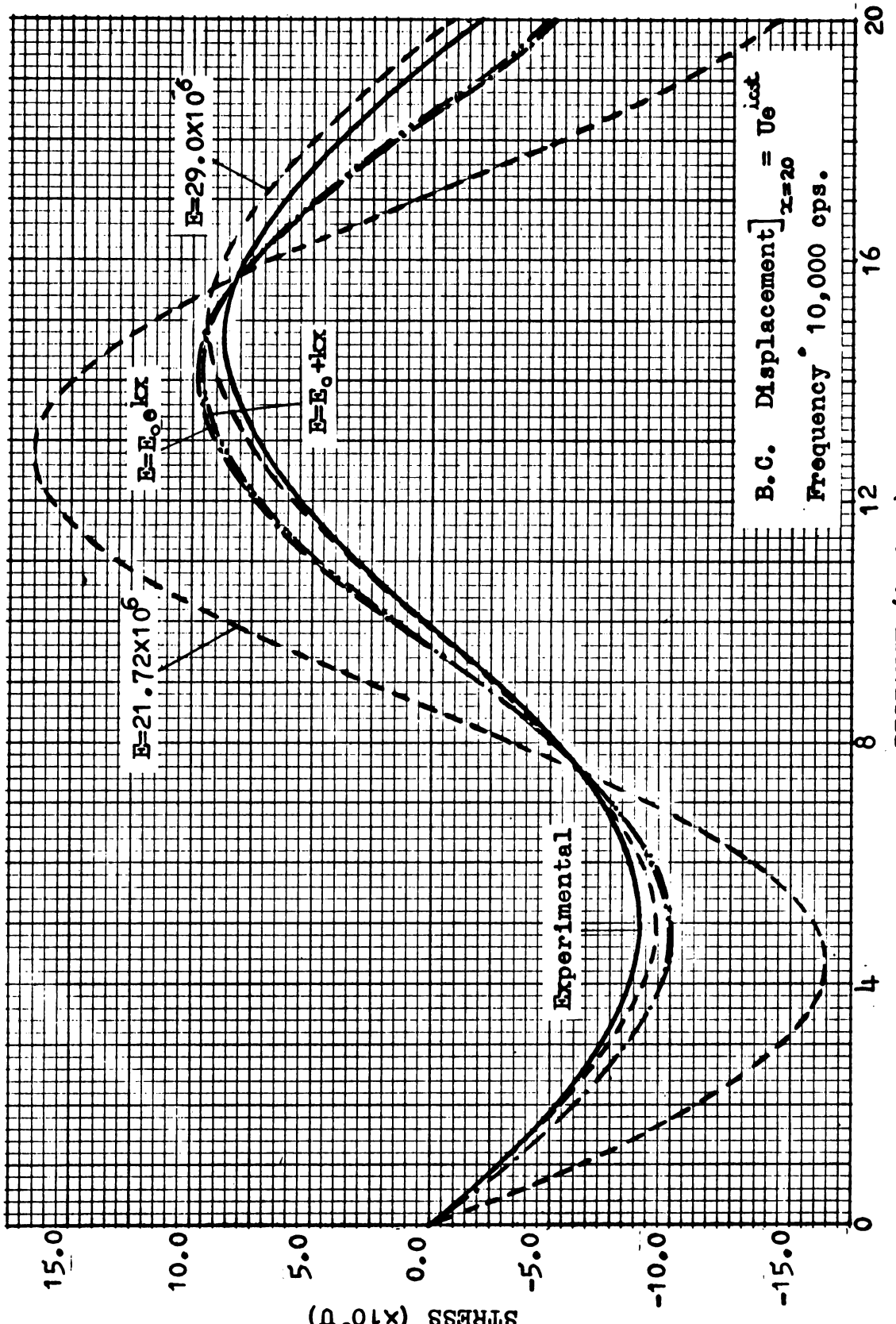

Fig. 7.10 Stress Amplitude for 10,000 cps.

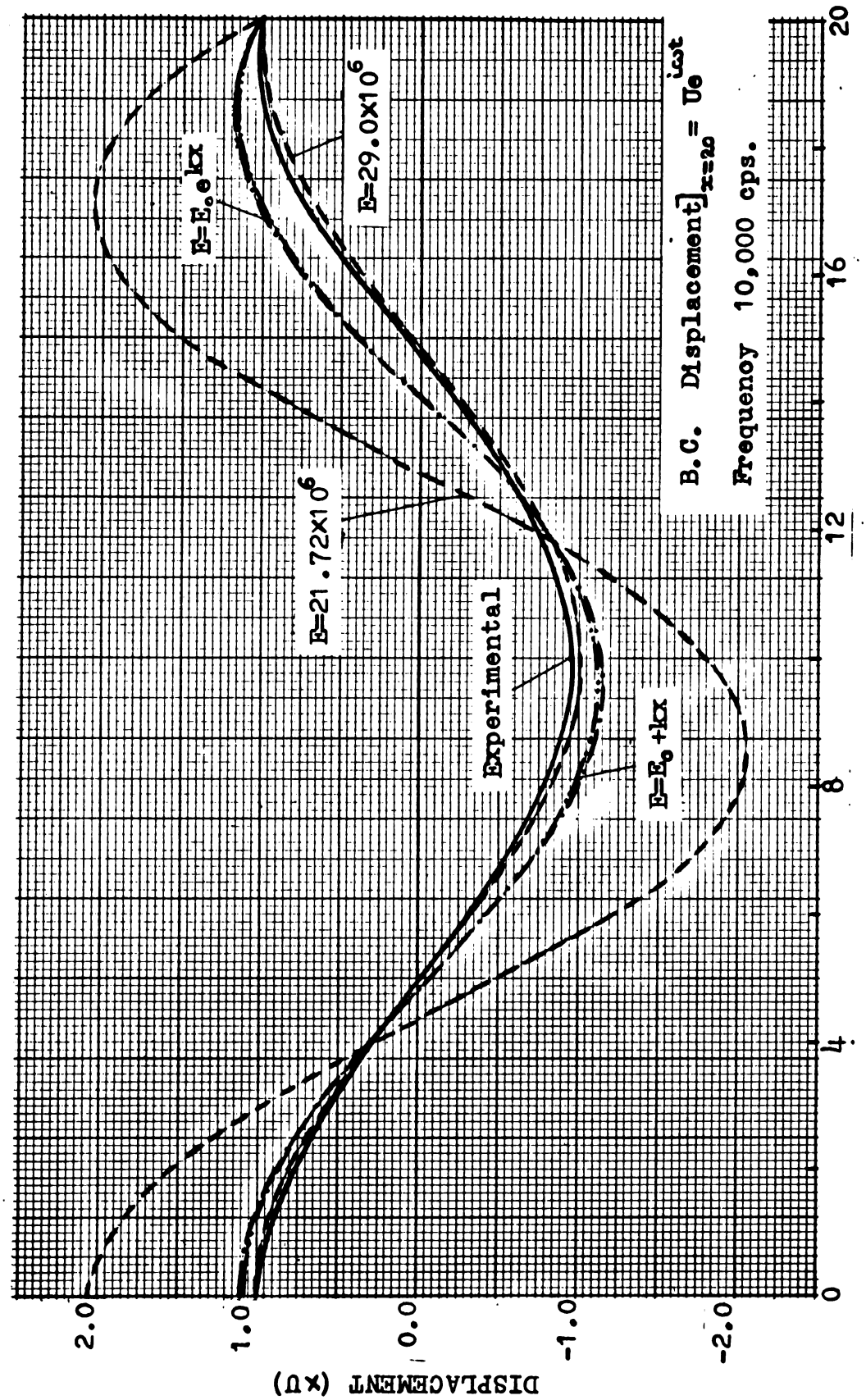

Fig. 7.11 Displacement Amplitude for 10,000 cps.

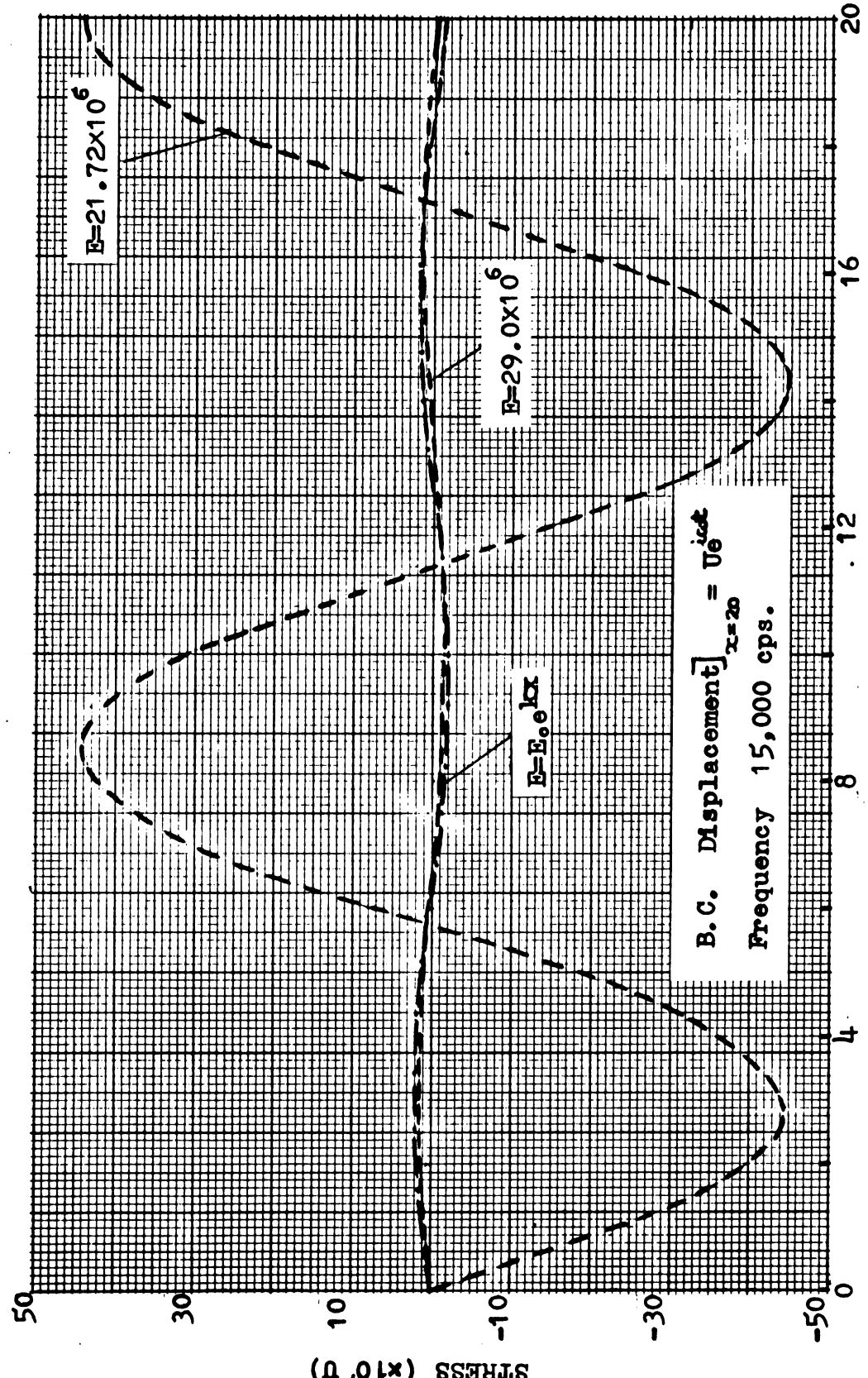

Fig. 7.12 Stress Amplitude for 15,000 cps.

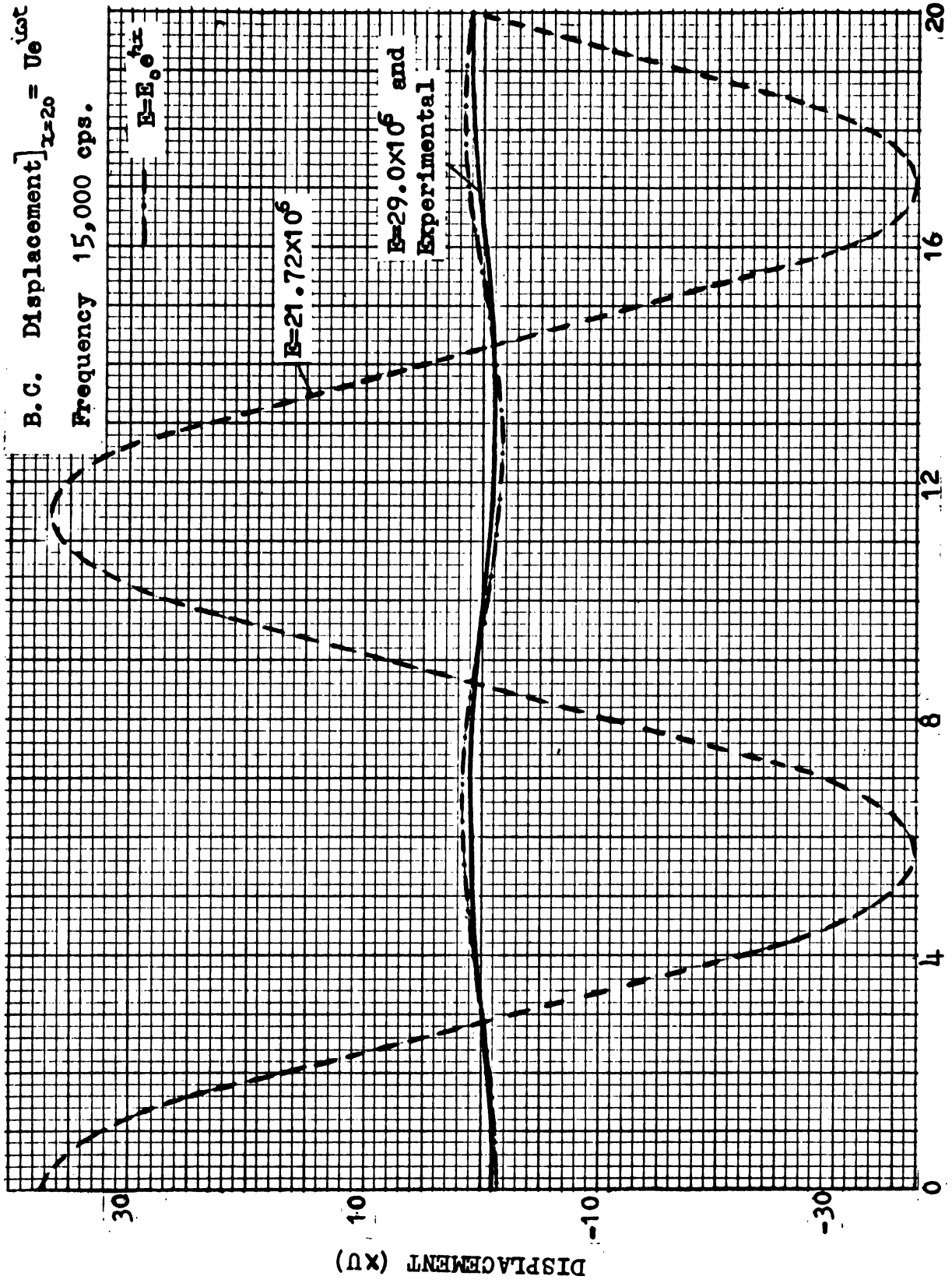

Fig. 7.13 Displacement Amplitude for 15,000 cps.

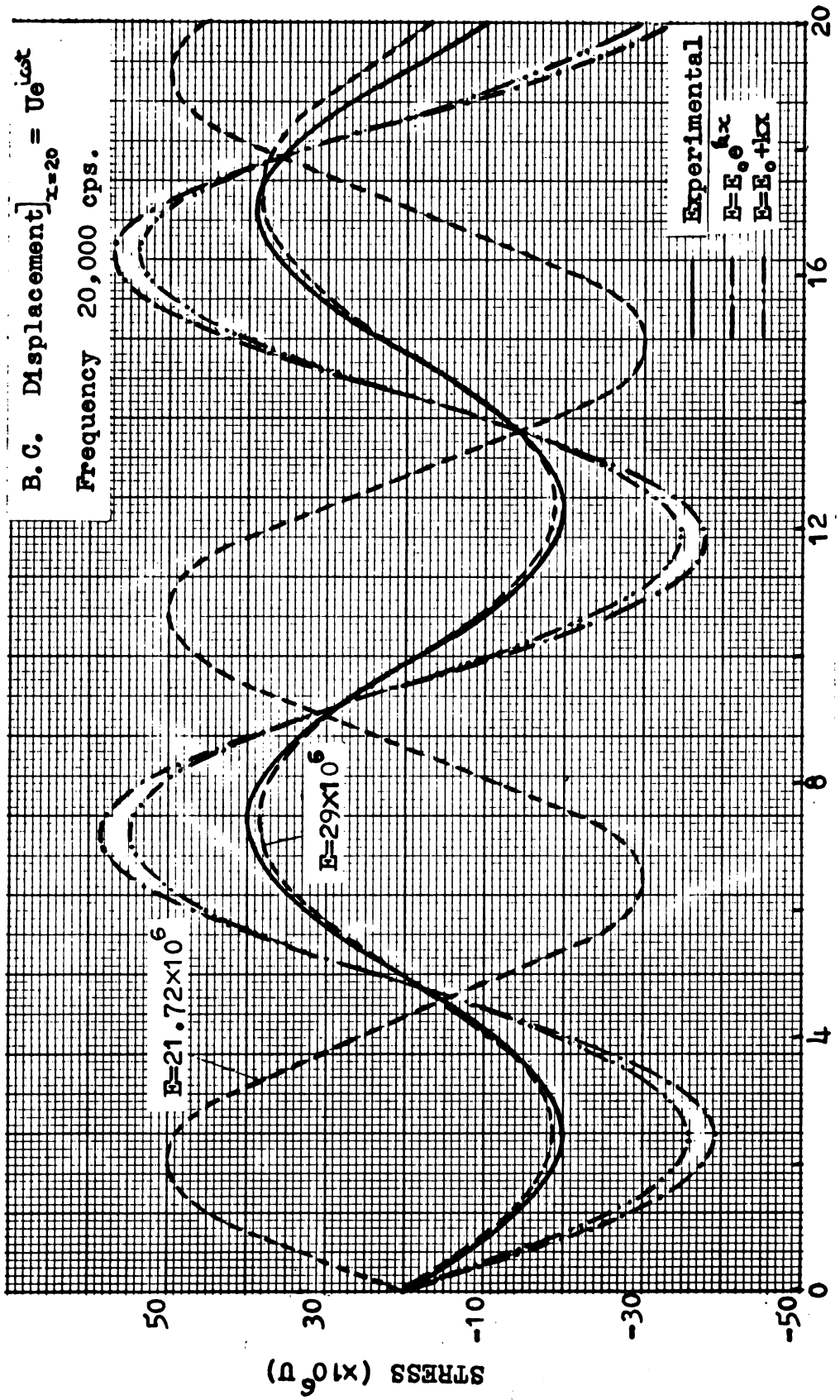

Fig. 7.14 Stress Amplitude for 20,000 cps.

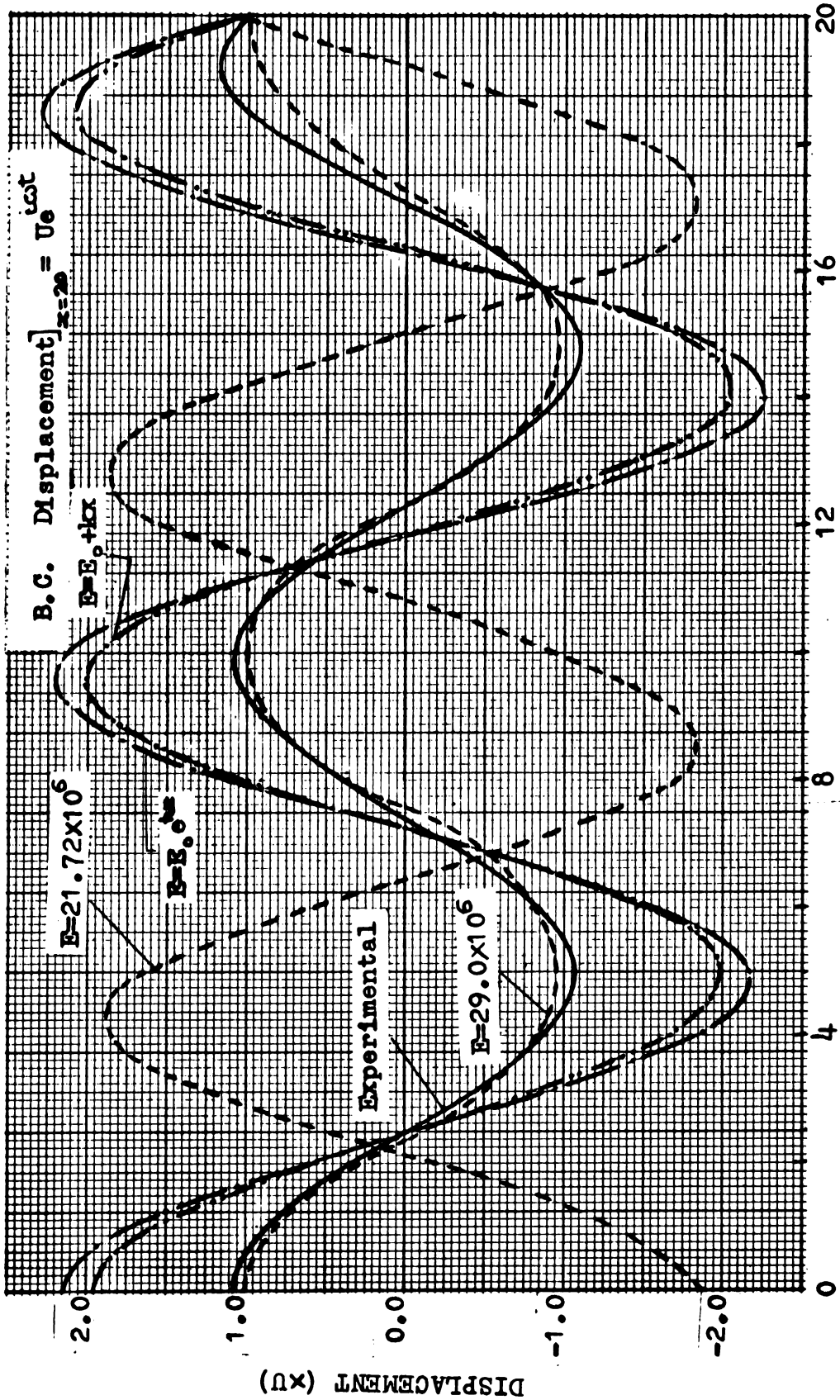

Fig. 7.15 Displacement Amplitude for 20,000 cps.

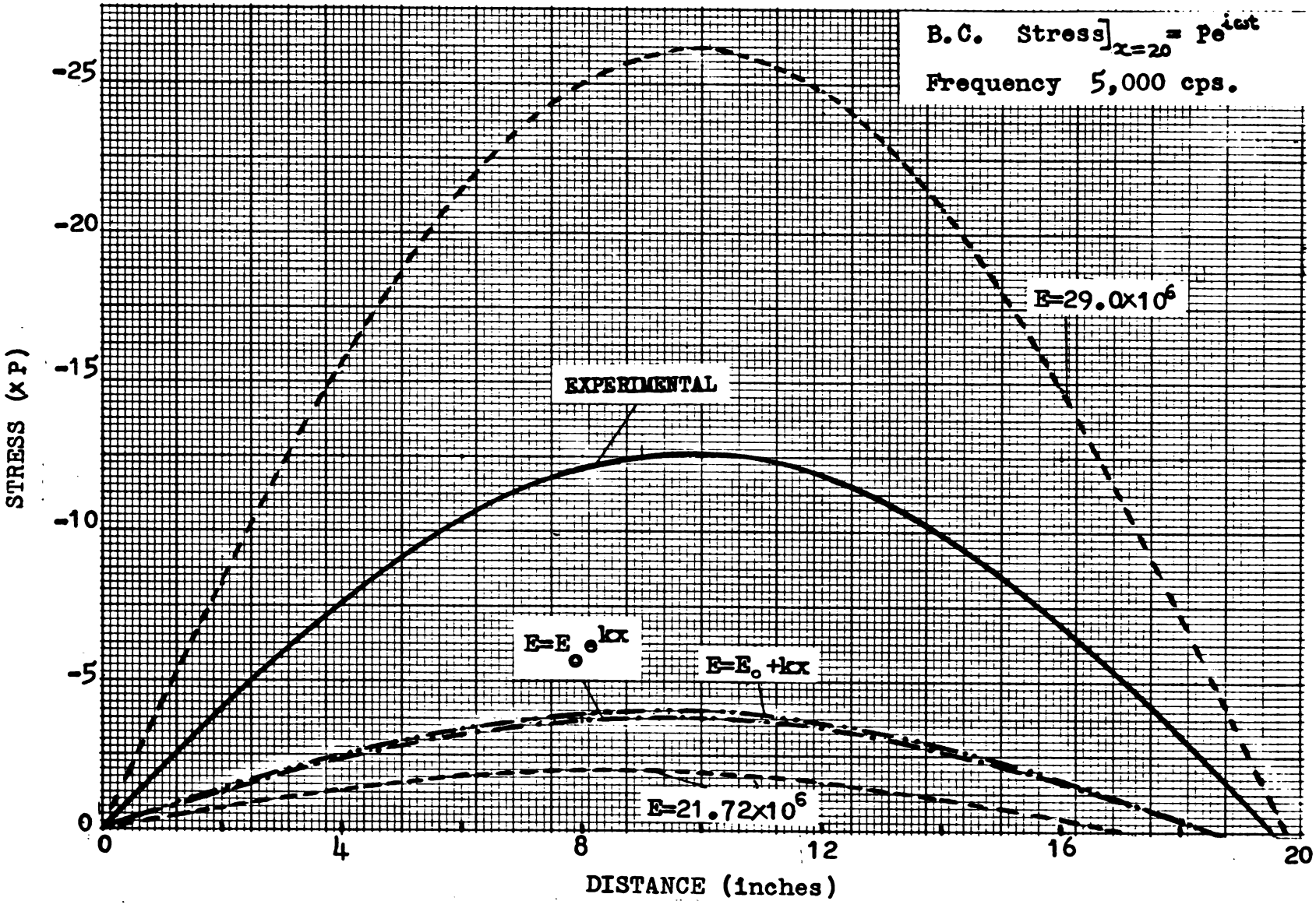

Fig. 7.16 Stress Amplitude for 5,000 cps.

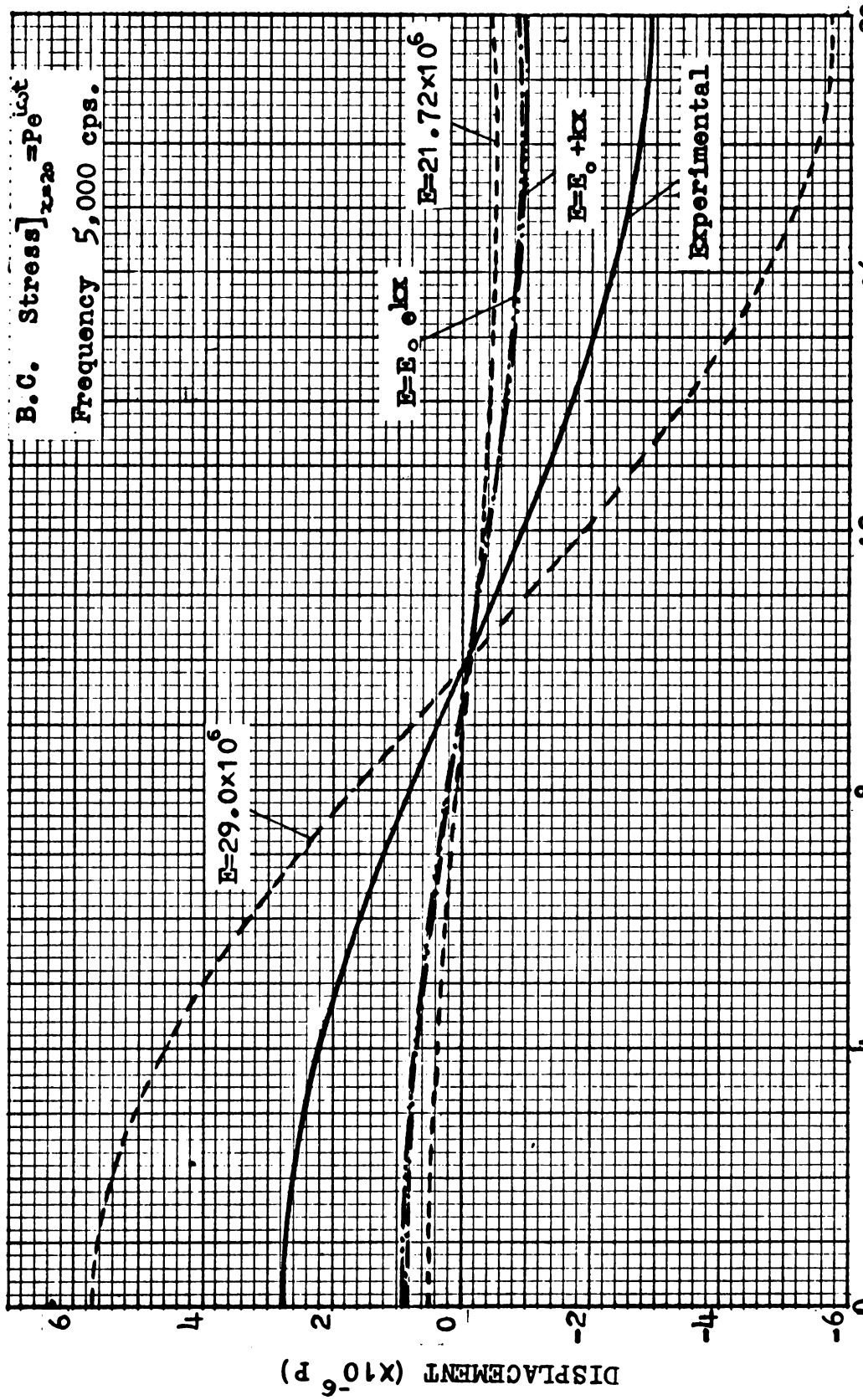

Fig. 7.17 Displacement Amplitude for 5,000 cps.

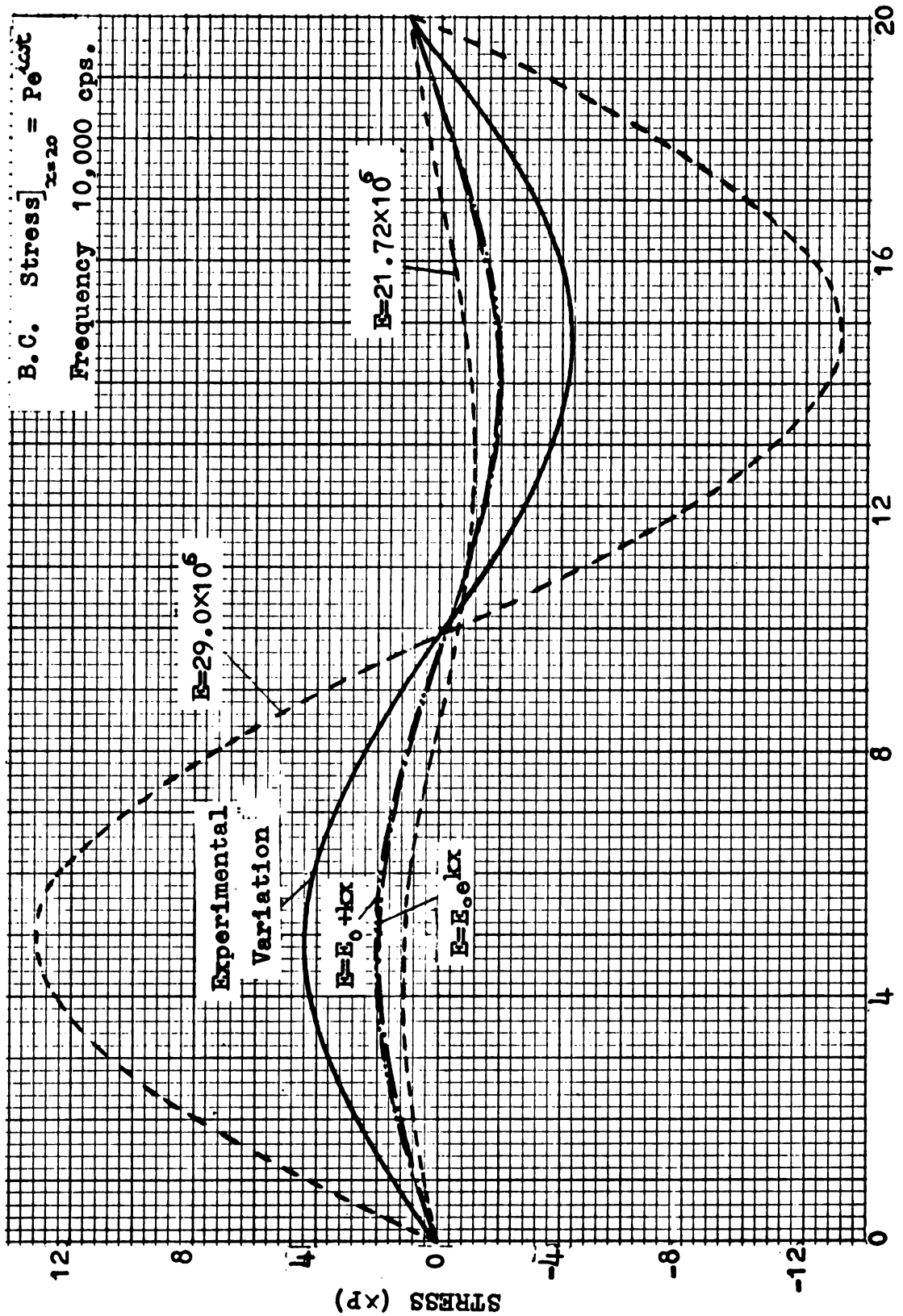

Fig. 7.18 Stress Amplitude for 10,000 cps.

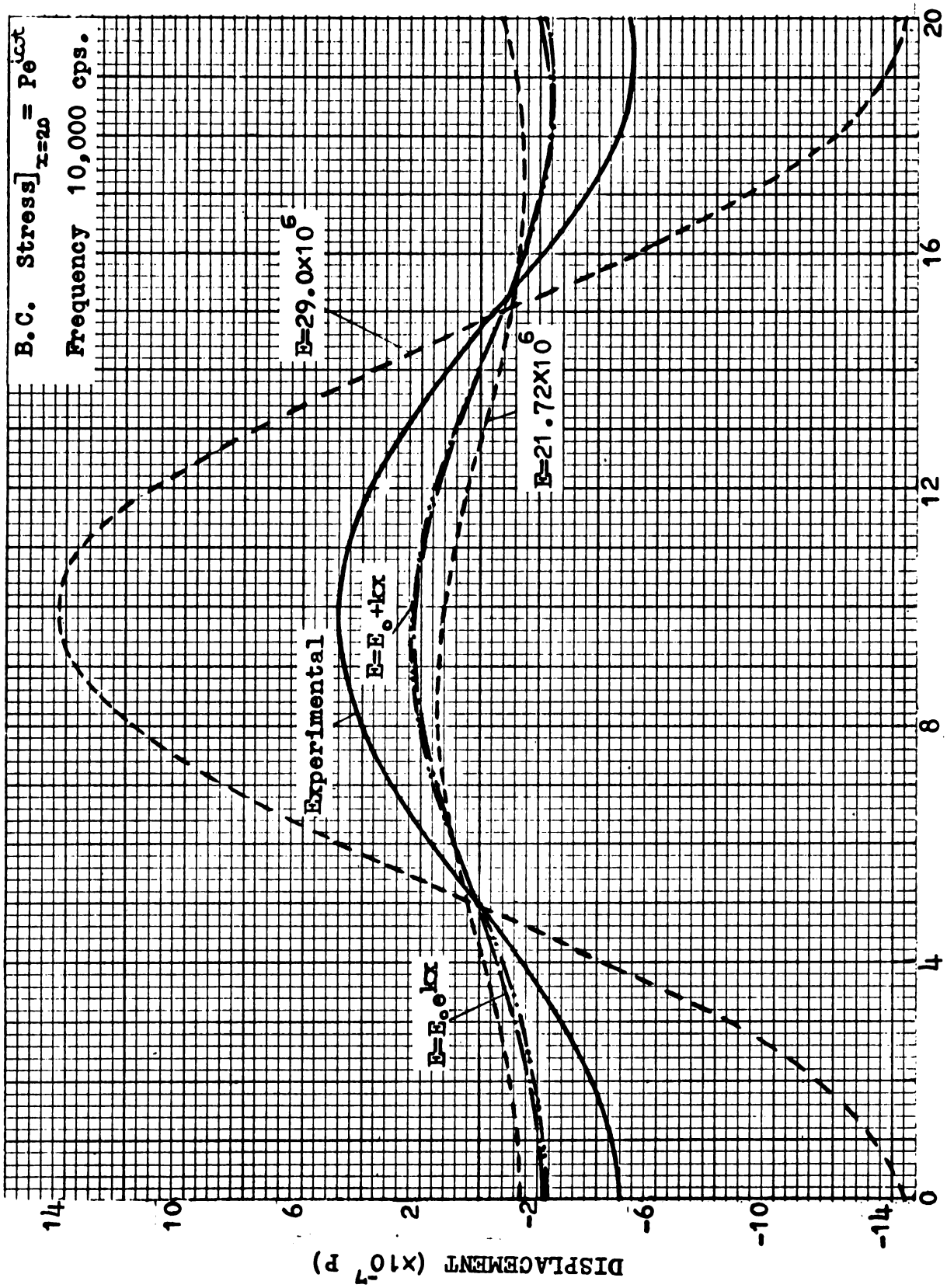

Fig. 7.19 Displacement Amplitude for 10,000 cps.

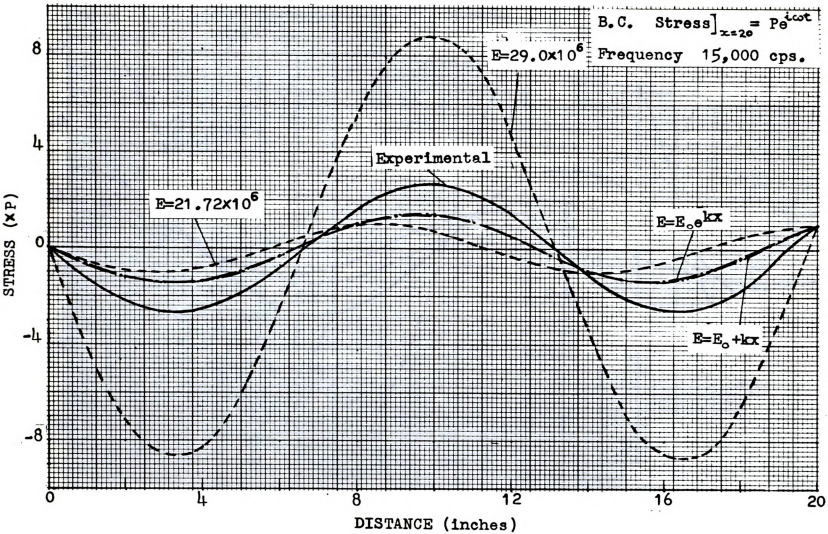

Fig. 7.20 Stress Amplitude for 15,000 cps.

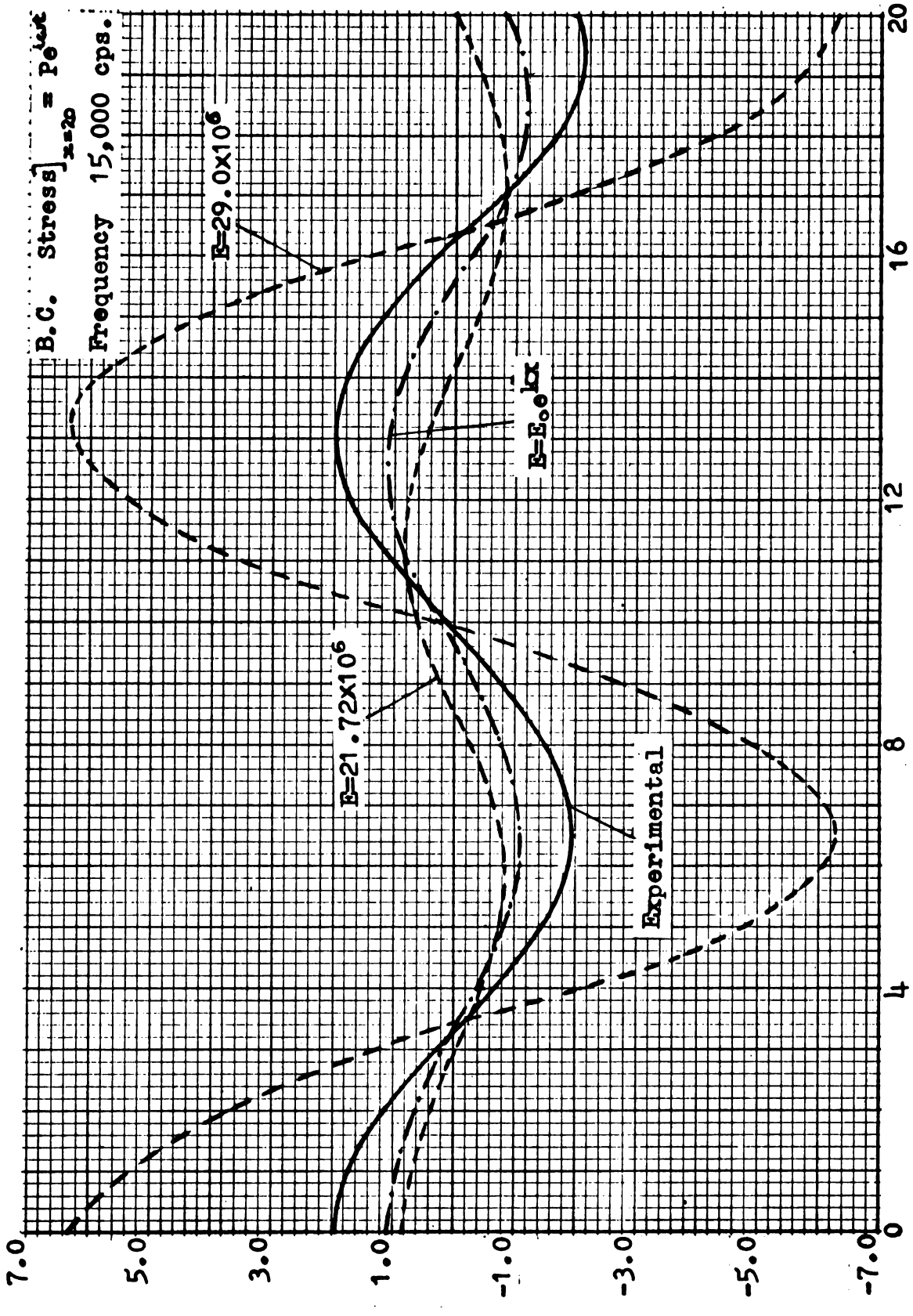

Fig. 7.21 Displacement Amplitude for 15,000 cps.

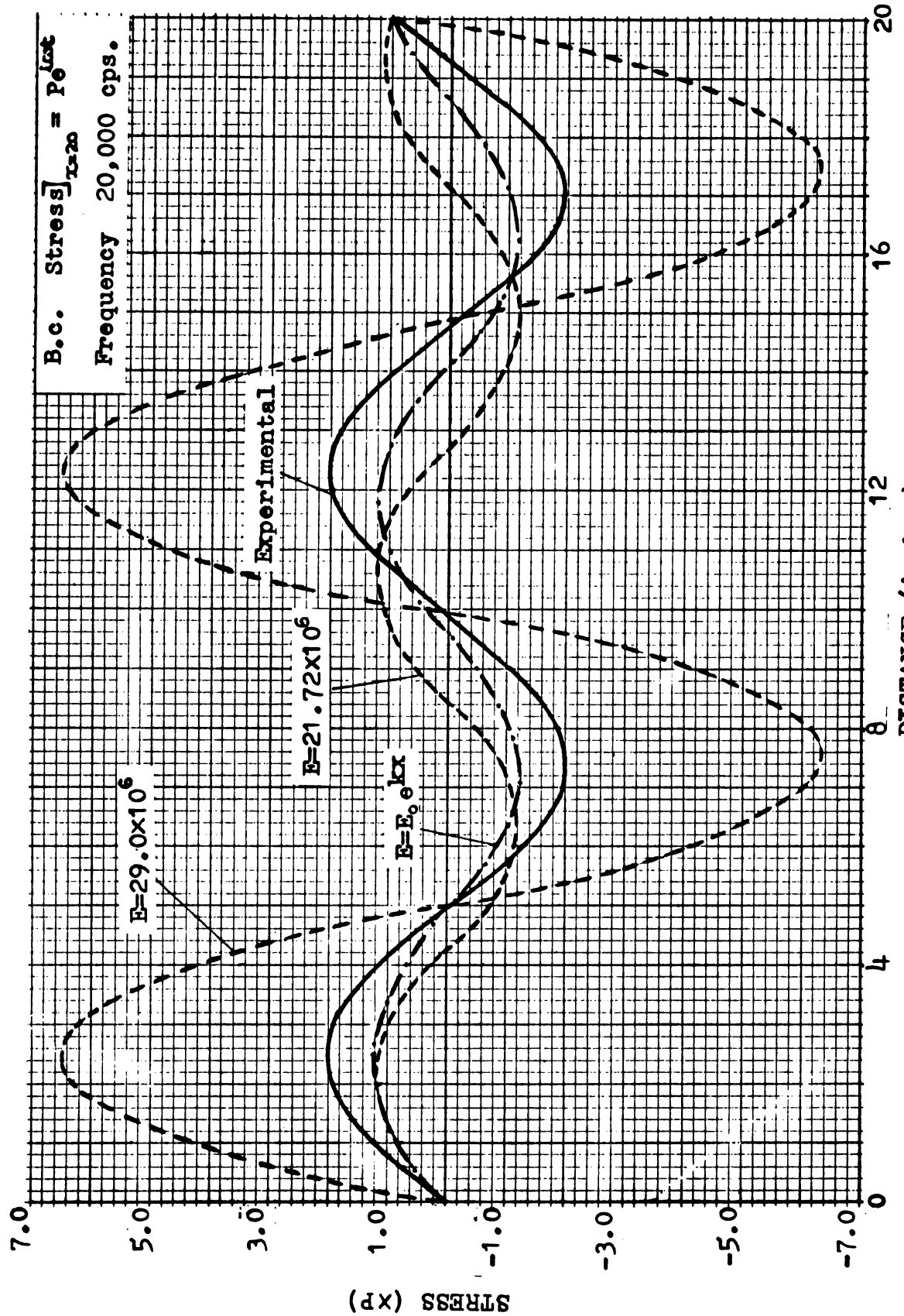

Fig. 7.22 Stress Amplitude for 20,000 cps.

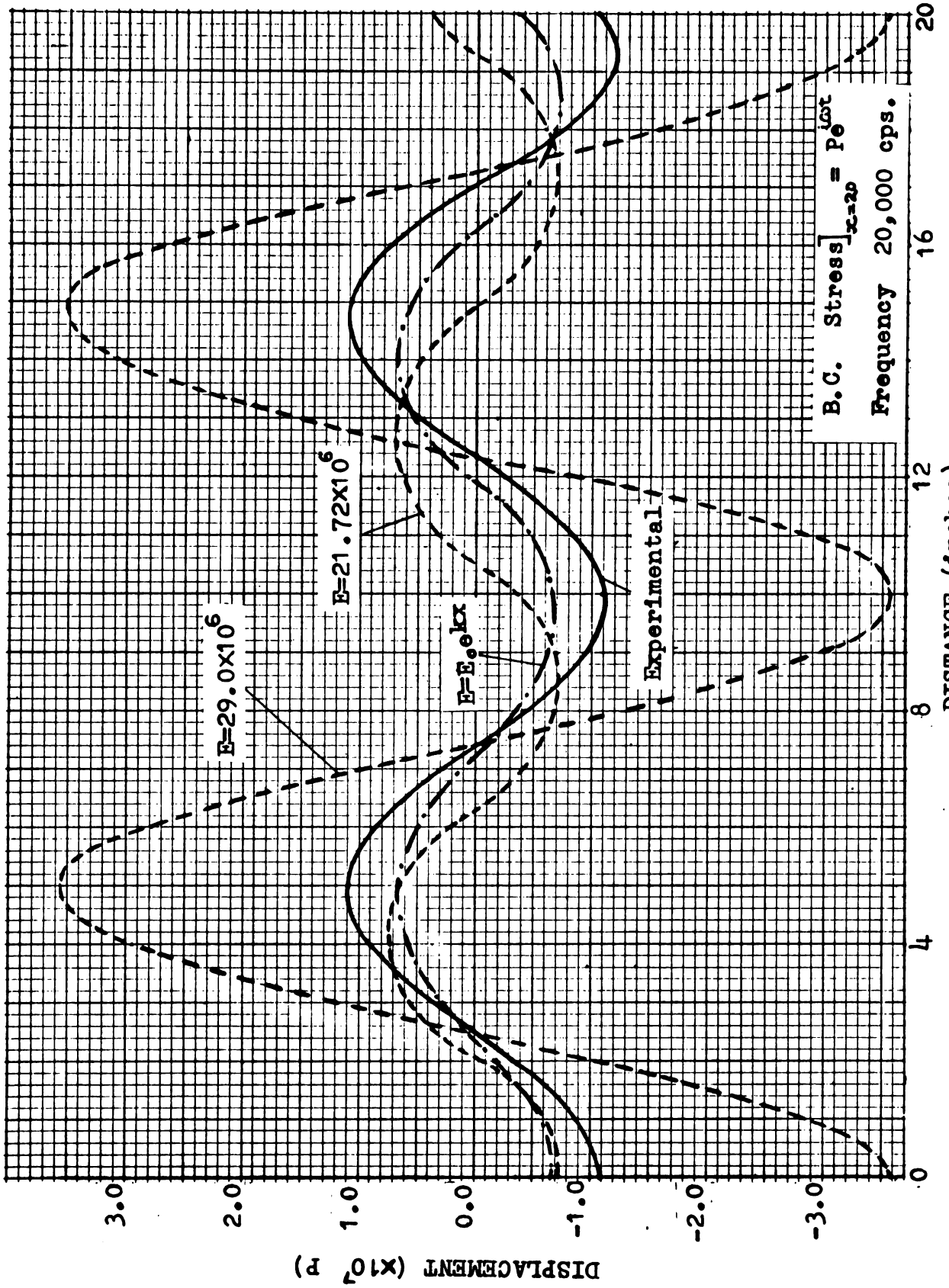

Fig. 7.23 Displacement Amplitude for 20,000 cps.

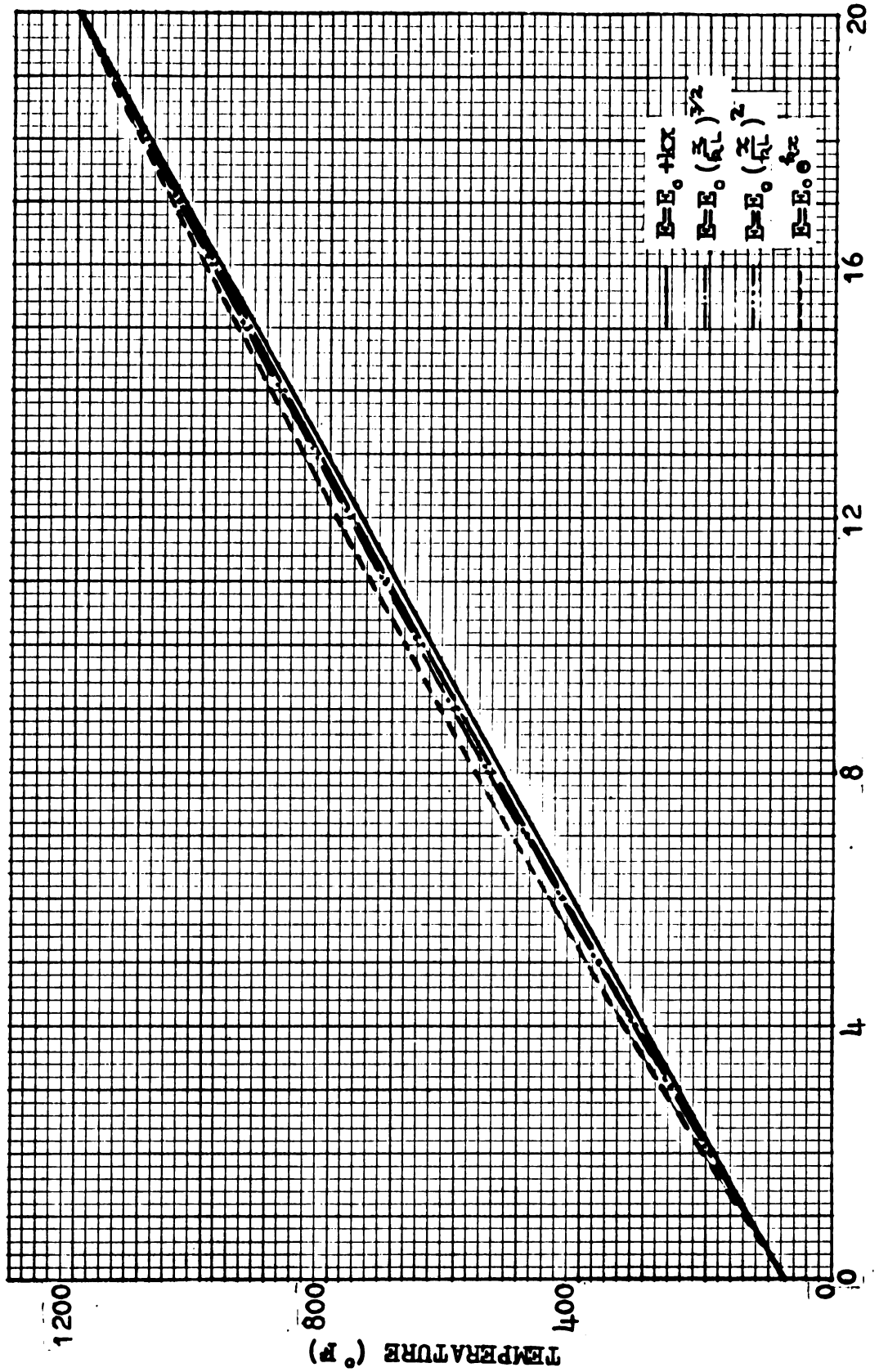

Fig. 7.24 Temperature versus Distance for the Assumed Distributions of E

APPENDIX A

INTERPOLATION

A.1. Introduction

Interpolation is a process for estimating the value y of a function $y = f(x)$ corresponding to any x, where the value of y is not to be computed directly from the function itself but is determined by means of certain values of the function which are already known, for example as experimental data at discrete points. An interpolating function may be defined as a function which contains in addition to the independent variable x, a number of arbitrary constants or parameters in such a way that by suitable choice of the parameters the function will assume assigned values for given values of the variable x (Milne, 1949; Nielsen, 1964).

The temperature distributions considered in this thesis were measured at 22 points in the first experiment and 16 in the second experiment. But both in the numerical solution of the pulse propagation by the method of characteristics and in the numerical solution of the periodic vibrations, it was desired to use the values at up to two thousand points. For the intermediate values of temperature or some other variable, such as the elastic wave speed or the elastic modulus, interpolation techniques were used.

There are three commonly used types of interpolating functions: polynomial, rational, and trignometric types. The choice depends upon the type of function being approximated. Only

polynomials will be discussed here, since polynomial interpolation gave good results for the temperature distributions.

There are many different polynomial interpolation formulas. A few of these are: Aitken's method; Neville's method; Newton's formula; Lagrange's formula; Bessel's formula; Stirling's formula; and Gauss' formula. Sometimes a combination of two or three formulas is used (see Milne, 1949). All nth-degree interpolating polynomial formulas based on the same $n+1$ points must give the same answer because there is a unique nth-degree polynomial taking on the $n+1$ prescribed values at the $n+1$ points. Therefore the choice of the interpolating polynomial formula to be used is based only on convenience. Because of the ease in programming, Aitken's method was used in this research.

A. 2. Aitken's Method of Interpolation

Aitken's method of interpolation can be considered as successive linear interpolation (Milne, 1949; Nielsen, 1964).

A. 2(a). Linear Interpolation

The simplest of all interpolation formulas is the linear interpolation formula. It is a special case of polynomial interpolation using two points and a polynomial of degree one. If we call the interpolating polynomial $I(x)$, the linear interpolation between i and j is

$$y = I(x) = \frac{1}{x_j - x_i} \begin{vmatrix} y_i & x_i - x \\ y_j & x_j - x \end{vmatrix}$$

A. 2(b). Aitken's Repeated Process

Using the notation of Nielsen (1964, pages 91 to 94)

$$y_{i1}(x) = \frac{1}{x_i - x_o} \begin{vmatrix} y_o & x_o - x \\ y_i & x_i - x \end{vmatrix}$$

This denotes linear interpolation between the values (x_o, y_o) and (x_i, y_i). If linear interpolation is exact, the values $y_{i1}(x)$, $(i=1, 2, \ldots, n)$ will be alike for any fixed x. If the function $y = f(x)$ is not linear, they will differ by some amount.

For a higher degree of accuracy, more points and an interpolating polynomial of a higher degree than the first, should be used. To achieve that, the linear interpolation formula can be applied to the values $y_{i1}(x)$, $(i=1, 2, \ldots, n)$. Thus with

$$I(x) = y_{i2}(x) = \frac{1}{x_i - x_1} \begin{vmatrix} y_{11}(x) & x_1 - x \\ y_{i1}(x) & x_i - x \end{vmatrix}$$

we now compute a set of values, $y_{i2}(x)$, $(i=2, \ldots, n)$. The process can be repeated and the general formula is given by

$$I(x) = y_{ik}(x) = \frac{1}{x_i - x_{k-1}} \begin{vmatrix} y_{k-1,\,k-1}(x) & x_{k-1} - x \\ y_{i,\,k-1}(x) & x_i - x \end{vmatrix}$$

in which k denotes the number of times linear interpolation has been applied and also the degree of the polynomial obtained. For each k, the sbuscript i assumes the values k, k+1, ..., n, where n is the degree of polynomial finally obtained.

The computational form for Aitken's repeated process is given below:

$$\begin{array}{c|ccccc|c} x_o & y_{00} & & & & & x_0 - x \\ x_1 & y_{10} & y_{11}(x) & & & & x_1 - x \\ x_2 & y_{20} & y_{21}(x) & y_{22}(x) & & & x_2 - x \\ x_3 & y_{30} & y_{31}(x) & y_{32}(x) & y_{33}(x) & & x_3 - x \\ x_4 & y_{40} & y_{41}(x) & y_{42}(x) & y_{43}(x) & y_{44}(x) & x_4 - x \end{array}$$

The computational form is constructed as follows: for a given x the columns between the vertical bars of the computational form are computed successively, each new entry being a linear interpolation between the first value in the preceding column and the value in the same row in the preceding column. For example, the value $y_{32}(x)$ is obtained by linear interpolation between $y_{11}(x)$ and $y_{31}(x)$ as

$$y_{32}(x) = \frac{1}{x_3 - x_1} \begin{vmatrix} y_{11}(x) & x_1 - x \\ y_{31}(x) & x_3 - x \end{vmatrix}$$

Aitken's process is a useful process, because the calculations are easily performed on a machine. Furthermore, it provides its own criterion of when the process has been carried far enough. This is judged by looking at the computational form on which, when the difference between $y_{k-1,\,k-1}$ and $y_{k,\,k}$ becomes less than the degree of accuracy desired, the process can be stopped. Sometimes the interpolated values appear to converge up to a certain value of k and after that appear to diverge. In such cases k is taken as the limiting value of the degree of polynomial which can be used for interpolating that particular data. To minimize round-off errors, the calculations are carried to at least one more decimal place than the required accuracy.

The same n-degree polynomial is obtained no matter which two n-1 degree polynomials are used to obtain it. For example

$$y_{55}(x) = \frac{1}{x_5 - x_4} \begin{vmatrix} y_{44}(x) & x_4 - x \\ y_{54}(x) & x_5 - x \end{vmatrix}$$

which in Milne's notation (pages 68 to 71) is written as

$$I_{0,1,2,3,4,5}(x) = \frac{\begin{vmatrix} I_{0,1,2,3,4}(x) & (x_4 - x) \\ I_{0,1,2,3,5}(x) & (x_5 - x) \end{vmatrix}}{x_5 - x_4}$$

can also be obtained by

$$I_{0,1,2,3,4,5}(x) = \frac{\begin{vmatrix} I_{0,1,2,3,5}(x) & (x_2 - x) \\ I_{0,1,3,4,5}(x) & (x_4 - x) \end{vmatrix}}{x_4 - x_2}$$

A. 2(c). Programming

In this research a fourth-degree polynomial was selected by the criterion mentioned above as giving optimum convergence for the values of temperature obtained experimentally in both of the experiments.

Except for the polynomial through the first five and the last five points, each polynomial was used only to obtain the interpolated values for the points lying in the middle quarter of the range covered by the five points as shown in Fig. A. 1, because of the fact that error in the interpolated value is minimum at the middle of the range of the polynomial and maximum at the ends (Milne, 1949, pages 167-168).

i-2 i-1 i i+1 i+2

Fig. A. 1. Range of Application of Interpolation Formula

The polynomial through the first five points was used to interpolate values from the first point to the middle of the interval between the third and fourth points. For a similar reason the polynomial using

the last five points was used to interpolate values from the middle of the interval between the second and third points to the fifth point.

The computational form for Aitken's repeated process was completed on the computer using each set of five points as input and the formula:

$$Y(I, J) = \frac{1}{X(J1) - X(I-1)}[\, Y(I-1, 1)\{ X(J1)-X\} - Y(I-1), J+1)\{ X(I-1) - X\}\,]$$

where

$I = 2, 3, \ldots, 5$

$I1 = 5-I$

$J = 1, 2, \ldots, I1$

$J1 = J+I-1$

$y(5, 1)$ was the last value computed and the required interpolated value of the function for the given x.

The same formula can be used to get higher-degree interpolation polynomials just by increasing the last value of I from 5 to $n+1$, where n is the degree of the required polynomial.

The computer program of this interpolation process is given in Appendix B along with other programs.

An accuracy of five to six digits was obtained when this program was used to interpolate between 20 values of $e^{-0.026904\, x^2}$, when the 20 values of x were entered at equal intervals of x between 0 and 19.

APPENDIX B

COMPUTER PROGRAMS

Four computer programs named TEMPWAV were written for the analysis of wave propagation in a bar with a thermally-induced inhomogeneity. This appendix includes a brief description of these programs, instructions for preparing input data for these programs and a description of the output in each case.

The two forms of wave propagation discussed earlier are:

1 - Pulse propagation

2 - Longitudinal periodic vibrations

The programs for each will be discussed separately.

B.1. Pulse Propagation

B.1(a). Description of the Blocks

Each program is divided into seven blocks, with block titles on the comment cards.

Block 1. CALCULATE E AND C FROM THE TEMPERATURE DATA

Read in the input temperature TEMP(J), for J = 1 to 24 in the first program (J = 1 to 20 in the second program). In the first program calculate TEMP(J) for J = 25 to 47 as mirror images of J = 1 to 24. Calculate the elastic modulus E(J) and the elastic wave speed C(J).

Block 2. INTERPOLATE TO GET ELASTIC WAVE SPEED C

Calculate the interpolated values of the elastic wave speed T5I(K), following the method described in Appendix A-3, of Kth interpolated temperature (K runs from 1 to 461 in the first program

and 1 to 381 in the second). X(K) is the distance from the point where temperature variation starts. Statements 900, 800 and 700 calculate various values of the Aitken's computational form.

Block 3. CALCULATE THE FIRST CHARACTERISTIC

Obtain the first characteristic by integrating the formula $t = \int_0^x \frac{1}{c(x)}\, dx$ by Simpsons rule, statement 23, described in Sec. 3.3. Calculate the time T(J) taken by the wave front to travel from the point where temperature variation starts to the point J (J runs from 1 to 47 points spaced at a distance of 0.8 inches in the first program, and in the second program J runs from 1 to 20 points spaced one inch apart). Calculate the total time TT taken by the wave front to travel the entire length of the bar by adding the values of time taken by the wave front to travel regions of uniform temperature, TR+TL, to the value required to travel the region of varying temperature, T(47) in the first program (T(20) in the second program). Divide TT by the number of mesh points on a characteristic (900 in the first program, 960 in the second) to give the time TS of travel between successive mesh points on a characteristic in a new mesh based on equal time intervals. Print the values of TR, TT, and TS (and TL in the first program).

Block 4. INTERPOLATE TO GET DISTANCE OF MESH POINTS

Calculate the distance X(K) from the point where the temperature variation starts to the Kth mesh point in the mesh spaced at equal time intervals. This calculation is done by interpolation between the values of the old mesh based on equal distances,

using statements 600, 300 and 730. (K = 1 to 466 in the first program, 1 to 388 in the second.)

Block 5. INTERPOLATE TO GET C AT THE MESH POINTS

Calculate the elastic wave speed T5I(K), by interpolation using the values of C and distance in Block 1, for the mesh points in the region of temperature variation located at distances X(K) of Block 4.

Block 6. INTERPOLATE TO GET THE NON DIMENSIONAL STRESS INPUT

Read in the input strain H(J), for J = 1 to 26 in the first program (J = 1 to 15 in the second program). Calculate the non-dimensional stress input U(K) by interpolation for the times G(K) spaced 2(TS) apart, where K runs from 1 to 58 in the first program (1 to 47 in the second).

Block 7. CALCULATE THE NON DIMENSIONAL STRESS AND VELOCITY

Calculate the non-dimensional elastic wave speed C(J) at each mesh point (J = 1 to 901 in the first program, 1 to 961 in the second). Calculate the non-dimensional stress S(2, J) and velocity V(2, J) in the next row (i. e. on the next characteristic) in terms of the values S(1, J) and V(1, J) in the previous row and the known end values. (S(1, J) and V(1, J) are zero the first time through.) Repeat this process to row 501 in the first program (801 in the second). For every 21st row, calculate the values of strain at the mesh points 149, 451, and 753 in the first program (26, 27, and 507 in the second program) by dividing the non-dimensional stress by the non-dimensional elastic modulus. For these mesh points print out the number of the

characteristic, the time after the arrival of the pulse, the non-dimensional stress, the strain, and the non-dimensional velocity.

B.1(b). Description of Symbols

The following list gives the description of various symbols used in the first two programs in the order they are encountered.

EO — Elastic modulus at room temperature, 29.0×10^6 psi.

EL — Elastic modulus at 1200°F, 21.72×10^6 psi.

TO — Room temperature, 75°F

TL — 1200°F

CO — Slope of the elastic modulus versus temperature line

TEMP(J) — Jth input temperature, J = 1 to 47 in first program (J = 1 to 20 in second program)

E(J) — Elastic modulus calculated at the point of TEMP(J)

ES — Square of elastic wave speed

C(J) — Elastic wave speed at point of TEMP(J)

Z(J) — In Block 1, distance from the point where temperature variation starts to the point of TEMP(J). In Block 6, time from beginning of incident pulse (J = 1 to 26 in first program, 1 to 15 in second.)

X(J) — In Block 1, distance from point where temperature variation starts to point of Jth interpolated temperature (J = 1 to 461 in first program, 1 to 381 in second.)

X(K) — In Block 4, distance from point where temperature variation starts to Kth mesh point on characteristic

(K = 1 to 466 in first program, 1 to 388 in second.)

P(1, M) Mth value in the first column inside the vertical bars of the Aitken's computational form (see Appendix A. 2)

Y(M) Mth value of the column outside the vertical bars on the left in the Aitkens computational form

P(I, J) Jth value in the Ith column inside the vertical bars of the Aitken's computational form

T5I(K) Kth interpolated value of the elastic wave speed obtained from a 5-point formula

In Block 2, K = 1 to 461 in first program, and 1 to 381 in second

In Block 5, K = 1 to 466 in first program and 1 to 388 in second

T(J) Time taken by the wave-front to travel distance Z(J) (of Block 1) from start of temperature gradient

TL or TR Time taken by the wave front to travel the region of uniform temperature on the left (or right)

TT Total time taken by the wave front to travel the entire length of the bar

TS Δt, time to travel between successive mesh points on a characteristic

G(J) In Block 3, time starting from the time when the wave-front reaches the point of varying temperature to the time it reaches the Jth mesh point on the characteristic (J = 1 to 466 in first program, J = 1 to 388 in second.)

G(J)	In Block 6, time interval between first and Jth characteristic, equal to 2(J-1)TS.(J = 1 to 501 in first program, 1 to 801 in second.)
H(J)	Jth varying incident strain input (J = 1 to 26 in first program, 1 to 15 in second.)
U(K)	Kth interpolated value of varying non-dimensional stress input (K = 1 to 58 in first program, 1 to 47 in second.)
U(J)	Jth value of non-varying non-dimensional stress input (J = 59 to 501 in first program, J = 47 to 801 in second.)
S(I, J)	Non-dimensional stress at the mesh point J of the Ith characteristic
V(I, J)	Non-dimensional stress at the mesh point J of the Ith characteristic
YS(1), YS(2), YS(3)	Strains printed out at points 1, 2, and 3 (In first program point 2 is at high-temperature gage. In second program 1 and 2 are at mesh points on either side of high-temperature gage.)

B.1(c). Input Data

Input data is provided on 80-column cards placed right after the "RUN" card in the main deck. Temperature cards are provided first with strain cards next.

The 24 temperature values (in degrees F) in the first program (20 in the second program) are provided on the first three cards with 8 values on each card; each value with its sign is punched in 10 columns.

The 26 strain values, in microinches per inch, in the first program (15 in the second program) are obtained from the incident pulse plot at time intervals of 2 microseconds. Eight values are punched on each card, and each value is punched in 10 columns.

B. 1(d). Output data

1. On one line TL(or TR), TT, and TS, labeled as T LEFT (or T RIGHT), T TOTAL, and T INTVL.
2. A series of groups arranged as follows:

   On first line, the number of the row from which values are printed (labeled POINT), and the time from the pulse arrival to the values printed below.

   On second line, non-dimensional stress at points 1, 2, and 3.

   On third line, strains at points 1, 2, and 3 (inches per inch).

   On fourth line, non-dimensional velocities at points 1, 2, and 3.

B. 2. Longitudinal Periodic Vibrations

Program 3 calculates displacement and stress amplitudes for excitation at the end $x = L$ by sinusoidal displacement of unit amplitude, while Program 4 is for excitation by sinusoidal stress of unit amplitude.

B. 2(a) Description of the Blocks

Each program is divided into four blocks, with block titles on the comment cards.

Block 1. CALCULATE ELASTIC MODULUS

Read in the input temperature TEMP(J), for J = 1 to 21. Calculate the elastic modulus D(J).

Block 2. INTERPOLATE FOR INTERMEDIATE VALUES OF ELASTIC MODULUS

Calculate the interpolated values of the elastic modulus E(K) at the points K, where X(K) is the distance from the stress-free end of the bar to the point of Kth interpolated temperature. (K runs from 1 to 2001.)

Block 3. CALCULATE DISPLACEMENT AMPLITUDE

Solve the finite difference equations written at each Jth point by the direct method (see Sec. 4.3) to obtain the displacement amplitude U(J) for J = 1 to 2001 for each frequency F(J). (For F(J) the index J = 1 to 7, and frequencies are read from the input data.) Print the frequency, and for every 50th point print the point number J, X(J), and U(J). With these values of U(J), obtain the iterated values V(J) of the displacement amplitude by the Gauss-Seidel method of Sec. 4.3. Iterate until either the change in successive values is less than 0.00001 or until 50 iteration cycles have been completed. Print the number of iterations and the maximum displacement change DAM in the last iteration.

Block 4. CALCULATE STRESS AMPLITUDE

Calculate the values of stress amplitude of the periodic vibrations S(J) from the iterated values of the displacement V(J1) following the method described in Sec. 4.3. Here J is every 10th point of the mesh in Block 2 and runs from 1 to 201 and J1 = (10J) - 9.

For each 50th point, print number J1, distance X(J1), stress S(J) and the final iterated value of the displacement V(J1).

B. 2(b). Description of Symbols

The following list gives the description of various symbols used in the programs:

Symbols EO, EL, TO, TL, CO, TEMP(J), P(1, M), Y(M), and P(I, J) are the same as in Appendix B. 2(b), and in addition:

D(J)	Elastic modulus calculated at the point J from temperature data, J = 1 to 21
G(J)	Distance from stress-free end to point of Jth input temperature
X(J)	Distance from stress-free end to point of Jth interpolated temperature, J = 1 to 2001
E(K)	Interpolated value of the elastic modulus at point K obtained from a 5-point formula, K = 1 to 2001
A(I, J)	The element of matrix A (Sec. 4. 3) situated on Ith row and Jth column
U(J)	Displacement amplitude at Jth point, J = 1 to 2001
V(J)	Iterated value of the displacement amplitude
K	The number of iterations
DAM	The maximum displacement change in the last iteration
S(J)	Jth stress amplitude (at point X(J1), where J1 = (10J)-9

B. 2(g). Input Data

Input data is provided on 80-column cards placed right after the "RUN" card in the main deck. The 7 frequencies (in cps.) are provided on one card; each value with its sign is punched in 11 columns. The 20 temperature values (in ^{o}F) are provided on the next three cards; each value with its sign is punched in 10 columns.

B. 2(h). Output Data

The output data comes in one group for each frequency. The first line in each group is the frequency in cps. Each line in the following subgroup gives for each 50th point three outputs: the point number J, X(J), and U(J).

The next subgroup gives on one line the number of iterations and the maximum displacement change DAM in the last iteration.

Each line in the following subgroup gives for each 50th point four outputs: the point number J, X(J), the stress amplitude and the iterated displacement amplitude (for end excitation of unit amplitude).

B.3 FORTRAN PROGRAMS

PULSE PROPAGATION SOLUTION BY THE METHOD OF CHARACTERISTICS

THERMAL GRADIENT AT THE MIDDLE OF THE BAR

```
      PROGRAM TEMPWAV
      TYPE DOUBLE TEMP,E,C,X,Z,P,T5I,T,Y,S,V,YS,U,H,G
      DIMENSION TEMP(47),E(47),T(47),X(466),Z(47),P(5,5),T5I(466),C(901)
      DIMENSION Y(5),S(2,901),V(2,901),YS(3),U(501),H(26),G(466)
    1 FORMAT (8(F10))
   11 FORMAT (3X,6HSTRESS,4X,D22.12,5X,D22.12,5X,D22.12)
   12 FORMAT (3X,6HSTRAIN,4X,D22.12,5X,D22.12,5X,D22.12)
   13 FORMAT (2X,8HVELOCITY,3X,D22.12,5X,D22.12,5X,D22.12)
   14 FORMAT (3X,5HPOINT,3X,I3,5X,5HTIME,3X,E15.8)
   26 FORMAT(12X,6H3 LEFT,22X,7HT TOTAL,22X,7HT INTVL)
   27 FORMAT (4X,D25.15,4X,D25.15,4X,D25.15)
  401 FORMAT (1H0)
C     CALCULATE E AND C FROM THE TEMPERATURE DATA
      E0=.290E+08
      EL= .2172E+08
      T0=75.
      TL=1200.
      C0=(EL-E0)/(TL-T0)
      READ 1,(TEMP(J),J=1,24)
      DO 2 J=1,23
    2 TEMP(48-J)=TEMP(J)
      DO 4 J=1,47
      E(J)=(C0*(TEMP(J)-T0))+E0
      ES=E(J)/(7.43E-04)
    4 C(J)=SQRTF(ES)
C     INTERPOLATE TO GET ELASTIC WAVE SPEED C
      Z(1)=0.0
      DO 5 J=2,47
    5 Z(J)=Z(J-1)+0.8
      X(1)=0.0
      DO 6 J=2,461
    6 X(J)=X(J-1)+.08
      L=1
      DO 907 M=1,5
      P(1,M)=C(M+L-1)
  907 Y(M)=Z(M+L-1)
      DO 905 K=1,26
      DO 900 I=2,5
      I1=6-I
      DO 900 J=1,I1
      J1=J+I-1
  900 P(I,J)=((P(I-1,1)*(Y(J1)-X(K)))-(P(I-1,J+1)*(Y(I-1)-X(K))))/(Y(J1)
```

```
     C-Y(I-1))
 905 T5I(K)=P(5,1)
     L=2
     DO 804 K1=26,430,10
     K2=K1+10
     DO 802 M=1,5
     P(1,M)=C(M+L-1)
 802 Y(M)=Z(M+L-1)
     DO 805 K=K1,K2
     DO 800 I=2,5
     I1=6-I
     DO 800 J=1,I1
     J1=J+I-1
 800 P(I,J)=((P(I-1,1)*(Y(J1)-X(K)))-(P(I-1,J+1)*(Y(I-1)-X(K))))/(Y(J1)
    C-Y(I-1))
 805 T5I(K)=P(5,1)
 804 L=L+1
     L=43
     DO 703 M=1,5
     P(1,M)=C(M+L-1)
 703 Y(M)=Z(M+L-1)
     DO 705 K=436,461
     DO 700 I=2,5
     I1=6-I
     DO 700 J=1,I1
     J1=J+I-1
 700 P(I,J)=((P(I-1,1)*(Y(J1)-X(K)))-(P(I-1,J+1)*(Y(I-1)-X(K))))/(Y(J1)
    C-Y(I-1))
 705 T5I(K)=P(5,1)
C      CALCULATE THE FIRST CHARACTERISTIC
       T(1)=0.0
       DO 23 J=2,47
       I=(J*10)-9
       I1=I-1
       I2=I-2
       A=1./T5I(2)
       DO 21 K=4,I1,2
  21   A=A+(1./T5I(K))
       Q=1./T5I(3)
       DO 22 K=5,I2,2
  22   Q=Q+(1./T5I(K))
  23   T(J)=((1./T5I(1))+(1./T5I(I))+(4.*A)+(2.*Q))*(.08/3.)
       TL=17.6/C(1)
       TR=17.6/C(47)
       TT=TL+TR+T(47)
       TS=TT/900.0
       PRINT 26
       PRINT 27,(TL,TT,TS)
C      INTERPOLATE TO GET DISTANCE OF MESH POINTS
       G(1)=(TS*218. )-TR
       DO 7 J=2,466
```

```
    7 G(J)=G(J-1)+TS
      L=1
      DO 607 M=1,5
      P(1,M)=Z(M+L-1)
  607 Y(M)=T(M+L-1)
      DO 605 K=1,28
      DO 600 I=2,5
      I1=6-I
      DO 600 J=1,I1
      J1=J+I-1
  600 P(I,J)=((P(I-1,1)*(Y(J1)-G(K)))-(P(I-1,J+1)*(Y(I-1)-G(K))))/(Y(J1)
     C-Y(I-1))
  605 X(K)=P(5,1)
      L=2
      DO 304 K1=29,430,10
      K2=K1+9
      DO 302 M=1,5
      P(1,M)=Z(M+L-1)
  302 Y(M)=T(M+L-1)
      DO 305 K=K1,K2
      DO 300 I=2,5
      I1=6-I
      DO 300 J=1,I1
      J1=J+I-1
  300 P(I,J)=((P(I-1,1)*(Y(J1)-G(K)))-(P(I-1,J+1)*(Y(I-1)-G(K))))/(Y(J1)
     C-Y(I-1))
  305 X(K)=P(5,1)
  304 L=L+1
      L=43
      DO 733 M=1,5
      P(1,M)=Z(M+L-1)
  733 Y(M)=T(M+L-1)
      DO 735 K=439,466
      DO 730 I=2,5
      I1=6-I
      DO 730 J=1,I1
      J1=J+I-1
  730 P(I,J)=((P(I-1,1)*(Y(J1)-G(K)))-(P(I-1,J+1)*(Y(I-1)-G(K))))/(Y(J1)
     C-Y(I-1))
  735 X(K)=P(5,1)
C     INTERPOLATE TO GET C AT THE MESH POINTS
      L=1
      DO 107 M=1,5
      P(1,M)=C(M+L-1)
  107 Y(M)=Z(M+L-1)
      DO 105 K=1,28
      DO 100 I=2,5
      I1=6-I
      DO 100 J=1,I1
      J1=J+I-1
  100 P(I,J)=((P(I-1,1)*(Y(J1)-X(K)))-(P(I-1,J+1)*(Y(I-1)-X(K))))/(Y(J1)
     C-Y(I-1))
```

```
  105 TSI(K)=P(5,1)
      L=2
      DO 114 K1=29,430,10
      K2=K1+9
      DO 112 M=1,5
      P(1,M)=C(M+L-1)
  112 Y(M)=Z(M+L-1)
      DO 115 K=K1,K2
      DO 110 I=2,5
      I1=6-I
      DO 110 J=1,I1
      J1=J+I-1
  110 P(I,J)=((P(I-1,1)*(Y(J1)-X(K)))-(P(I-1,J+1)*(Y(I-1)-X(K))))/(Y(J1)
     C-Y(I-1))
  115 TSI(K)=P(5,1)
  114 L=L+1
      L=43
      DO 123 M=1,5
      P(1,M)=C(M+L-1)
  123 Y(M)=Z(M+L-1)
      DO 125 K=439,466
      DO 120 I=2,5
      I1=6-I
      DO 120 J=1,I1
      J1=J+I-1
  120 P(I,J)=((P(I-1,1)*(Y(J1)-X(K)))-(P(I-1,J+1)*(Y(I-1)-X(K))))/(Y(J1)
     C-Y(I-1))
  125 TSI(K)=P(5,1)
C     INTERPOLATE TO GET NON DIMENSIONAL STRESS INPUT
      READ 1,(H(J),J=1,26)
      Z(1)=0.0
      DO 99 J=2,26
   99 Z(J)=Z(J-1)+(+.2E-05)
      G(1)=0.0
      DO 299 J=2,58
  299 G(J)=G(J-1)+(2.0*TS)
      L=1
      DO 137 M=1,5
      P(1,M)=H(M+L-1)
  137 Y(M)=Z(M+L-1)
      DO 135 K=1,6
      DO 130 I=2,5
      I1=6-I
      DO 130 J=1,I1
      J1=J+I-1
  130 P(I,J)=((P(I-1,1)*(Y(J1)-G(K)))-(P(I-1,J+1)*(Y(I-1)-G(K))))/(Y(J1)
     C-Y(I-1))
  135 U(K)=P(5,1)*(+.1E-05)
      L=2
      DO 144 K1=7,58,5
      K2=K1+1
```

```
      DO 142 M=1,5
      P(1,M)=H(M+L-1)
  142 Y(M)=Z(M+L-1)
      DO 145 K=K1,K2
      DO 140 I=2,5
      I1=6-I
      DO 140 J=1,I1
      J1=J+I-1
  140 P(I,J)=((P(I-1,1)*(Y(J1)-G(K)))-(P(I-1,J+1)*(Y(I-1)-G(K))))/(Y(J1)
     C-Y(I-1))
  145 U(K)=P(5,1)*( .1E-05)
  144 L=L+2
      L=3
      DO 154 K1=9,58,5
      K2=K1+2
      DO 152 M=1,5
      P(1,M)=H(M+L-1)
  152 Y(M)=Z(M+L-1)
      DO 155 K=K1,K2
      DO 150 I=2,5
      I1=6-I
      DO 150 J=1,I1
      J1=J+I-1
  150 P(I,J)=((P(I-1,1)*(Y(J1)-G(K)))-(P(I-1,J+1)*(Y(I-1)-G(K))))/(Y(J1)
     C-Y(I-1))
  155 U(K)=P(5,1)*(+.1E-05)
  154 L=L+2
      DO 771 J=59,501
  771 U(J)=+.62727E-03
C     CALCULATE NON DIMENSIONAL STRESS AND VELOCITY
      DO 500 I=1,2
      DO 500 J=1,901
      S(I,J)=0.0
  500 V(I,J)=0.0
      DO 502 J=219,684
  502 C(J)=(T5I(J-218)/C(1))
      DO 501 J=1,218
  501 C(J)=1.0
      DO 503 J=684,901
  503 C(J)=1.0
      Q=1.0
      DO 508 L=1,25
      DO 507 K=2,21
      K1=((L*20)-20)+K
      S(2,1)=U(K1)
      V(2,1)=V(1,2)-((S(2,1)-S(1,2))/C(1))
      DO 506 J=2,90
      CA=C(J)+C(J+1)
      CB=C(J)+C(J-1)
      CT=CA+CB
      S(2,J)=(((CA*S(2,J-1))+(CB*S(1,J+1))+(CA*CB*(V(1,J+1)-V(2,J-1))/2.0
```

```
     C))/CT
  506 V(2,J)=((CB*V(2,J-1))+(CA*V(1,J+1))-(2.*S(2,J-1))+(2.*S(1,J+1)))/C
     CT
      S(2,901)=0.0
      V(2,901)=V(2,900)-(S(2,900)/C(900))
      DO 507 JAC=1,901
      S(1,JAC)=S(2,JAC)
  507 V(1,JAC)=V(2,JAC)
      L1=(L*20)+1
      TIME=Q*20.0*TS*2.0
      PRINT 14,L1,TIME
      YS(1)=S(1,149)
      YS(2)=S(1,451)/(E(24)/E(1))
      YS(3)=S(1,753)
      PRINT 11,S(1,149),S(1,451),S(1,753)
      PRINT 12,YS(1),YS(2),YS(3)
      PRINT 13,V(1,149),V(1,451),V(1,753)
      PRINT 401
  508 Q=Q+1.
      STOP
      END
         SCOPE
*LOAD
*RUN,20,4000
```

PULSE PROPAGATION SOLUTION BY THE METHOD OF CHARACTERISTICS

BAR STRUCK AT THE HOT END

```
      PROGRAM TEMPWAV
      TYPE DOUBLE TEMP,E,C,X,Z,P,T5I,T,Y,S,V,YS,U,H,G
      DIMENSION TEMP(20),E(20),T(20),X(388),Z(20),P(5,5),T5I(388),C(961)
      DIMENSION Y(5),S(2,961),V(2,961),YS(3),U(801),H(26),G(388)
    1 FORMAT (8(F10))
   11 FORMAT (3X,6HSTRESS,4X,D22.12,5X,D22.12,5X,D22.12)
   12 FORMAT (3X,6HSTRAIN,4X,D22.12,5X,D22.12,5X,D22.12)
   13 FORMAT (2X,8HVELOCITY,3X,D22.12,5X,D22.12,5X,D22.12)
   14 FORMAT (3X,5HPOINT,3X,I3,5X,5HTIME,3X,E15.8)
   26 FORMAT(12X,7HT RIGHT,22X,7HT TOTAL,22X,7HT INTVL)
   27 FORMAT (4X,D25.15,4X,D25.15,4X,D25.15)
  401 FORMAT (1H0)
C     CALCULATE E AND C FROM THE TEMPERATURE DATA
      E0=.290E+08
      EL= .2172E+08
      T0=75.
      TL=1200.
      C0=(EL-E0)/(TL-T0)
      READ 1,(TEMP(J),J=1,20)
      DO 4 J=1,20
      E(J)=(C0*(TEMP(J)-T0))+E0
      ES=E(J)/(7.43E-04)
    4 C(J)=SQRTF(ES)
C     INTERPOLATE TO GET ELASTIC WAVE SPEED C
      Z(1)=0.0
      DO 5 J=2,20
    5 Z(J)=Z(J-1)+1.0
      X(1)=0.0
      DO 6 J=2,388
    6 X(J)=X(J-1)+.05
      L=1
      DO 907 M=1,5
      P(1,M)=C(M+L-1)
  907 Y(M)=Z(M+L-1)
      DO 905 K=1,50
      DO 900 I=2,5
      I1=6-I
      DO 900 J=1,I1
      J1=J+I-1
  900 P(I,J)=((P(I-1,1)*(Y(J1)-X(K)))-(P(I-1,J+1)*(Y(I-1)-X(K))))/(Y(J1)
     C-Y(I-1))
  905 T5I(K)=P(5,1)
      L=2
```

```
      DO 804 K1=51,320,20
      K2=K1+19
      DO 802 M=1,5
      P(1,M)=C(M+L-1)
  802 Y(M)=Z(M+L-1)
      DO 805 K=K1,K2
      DO 800 I=2,5
      I1=6-I
      DO 800 J=1,I1
      J1=J+I-1
  800 P(I,J)=((P(I-1,1)*(Y(J1)-X(K)))-(P(I-1,J+1)*(Y(I-1)-X(K))))/(Y(J1)
     C-Y(I-1))
  805 T5I(K)=P(5,1)
  804 L=L+1
      L=16
      DO 703 M=1,5
      P(1,M)=C(M+L-1)
  703 Y(M)=Z(M+L-1)
      DO 705 K=331,381
      DO 700 I=2,5
      I1=6-I
      DO 700 J=1,I1
      J1=J+I-1
  700 P(I,J)=((P(I-1,1)*(Y(J1)-X(K)))-(P(I-1,J+1)*(Y(I-1)-X(K))))/(Y(J1)
     C-Y(I-1))
  705 T5I(K)=P(5,1)
C     CALCULATE THE FIRST CHARACTERISTIC
      T(1)=0.0
      DO 23 J=2,20
      I=(J*20)-19
      I1=I-1
      I2=I-2
      A=1./T5I(2)
      DO 21 K=4,I1,2
   21 A=A+(1./T5I(K))
      Q=1./T5I(3)
      DO 22 K=5,I2,2
   22 Q=Q+(1./T5I(K))
   23 T(J)=((1./T5I(1))+(1./T5I(I))+(4.*A)+(2.*Q))*(.05/3.)
      TR=29.0/C(20)
      TT=TR+T(20)
      TS=TT/960.0
      PRINT 26
      PRINT 27,(TR,TT,TS)
C     INTERPOLATE TO GET DISTANCE OF MESH POINTS
      G(1)=0.0
      DO 7 J=2,388
    7 G(J)=G(J-1)+TS
      L=1
      DO 607 M=1,5
      P(1,M)=Z(M+L-1)
```

```
  607 Y(M)=T(M+L-1)
      DO 605 K=1,56
      DO 600 I=2,5
      I1=6-I
      DO 600 J=1,I1
      J1=J+I-1
  600 P(I,J)=((P(I-1,1)*(Y(J1)-G(K)))-(P(I-1,J+1)*(Y(I-1)-G(K))))/(Y(J1)
     C-Y(I-1))
  605 X(K)=P(5,1)
      L=2
      DO 304 K1=57,320,20
      K2=K1+20
      DO 302 M=1,5
      P(1,M)=Z(M+L-1)
  302 Y(M)=T(M+L-1)
      DO 305 K=K1,K2
      DO 300 I=2,5
      I1=6-I
      DO 300 J=1,I1
      J1=J+I-1
  300 P(I,J)=((P(I-1,1)*(Y(J1)-G(K)))-(P(I-1,J+1)*(Y(I-1)-G(K))))/(Y(J1)
     C-Y(I-1))
  305 X(K)=P(5,1)
  304 L=L+1
      L=16
      DO 733 M=1,5
      P(1,M)=Z(M+L-1)
  733 Y(M)=T(M+L-1)
      DO 735 K=338,388
      DO 730 I=2,5
      I1=6-I
      DO 730 J=1,I1
      J1=J+I-1
  730 P(I,J)=((P(I-1,1)*(Y(J1)-G(K)))-(P(I-1,J+1)*(Y(I-1)-G(K))))/(Y(J1)
     C-Y(I-1))
  735 X(K)=P(5,1)
C     INTERPOLATE TO GET C AT THE MESH POINTS
      L=1
      DO 107 M=1,5
      P(1,M)=C(M+L-1)
  107 Y(M)=Z(M+L-1)
      DO 105 K=1,56
      DO 100 I=2,5
      I1=6-I
      DO 100 J=1,I1
      J1=J+I-1
  100 P(I,J)=((P(I-1,1)*(Y(J1)-X(K)))-(P(I-1,J+1)*(Y(I-1)-X(K))))/(Y(J1)
     C-Y(I-1))
  105 TSI(K)=P(5,1)
      L=2
      DO 114 K1=57,320,20
```

```
      K2=K1+20
      DO 112 M=1,5
      P(1,M)=C(M+L-1)
  112 Y(M)=Z(M+L-1)
      DO 115 K=K1,K2
      DO 110 I=2,5
      I1=6-I
      DO 110 J=1,I1
      J1=J+I-1
  110 P(I,J)=((P(I-1,1)*(Y(J1)-X(K)))-(P(I-1,J+1)*(Y(I-1)-X(K))))/(Y(J1)
     C-Y(I-1))
  115 T5I(K)=P(5,1)
  114 L=L+1
      L=16
      DO 123 M=1,5
      P(1,M)=C(M+L-1)
  123 Y(M)=Z(M+L-1)
      DO 125 K=338,388
      DO 120 I=2,5
      I1=6-I
      DO 120 J=1,I1
      J1=J+I-1
  120 P(I,J)=((P(I-1,1)*(Y(J1)-X(K)))-(P(I-1,J+1)*(Y(I-1)-X(K))))/(Y(J1)
     C-Y(I-1))
  125 T5I(K)=P(5,1)
C     INTERPOLATE TO GET NON DIMENSIONAL STRESS INPUT
      READ 1,(H(J),J=1,15)
      Z(1)=0.0
      DO 99 J=2,15
   99 Z(J)=Z(J-1)+(+.2E-05)
      G(1)=0.0
      DO 299 J=2,50
  299 G(J)=G(J-1)+(2.0*TS)
      L=1
      DO 137 M=1,5
      P(1,M)=H(M+L-1)
  137 Y(M)=Z(M+L-1)
      DO 135 K=1,10
      DO 130 I=2,5
      I1=6-I
      DO 130 J=1,I1
      J1=J+I-1
  130 P(I,J)=((P(I-1,1)*(Y(J1)-G(K)))-(P(I-1,J+1)*(Y(I-1)-G(K))))/(Y(J1)
     C-Y(I-1))
  135 U(K)=P(5,1)*(+.1E-05)
      L=2
      DO 144 K1=11,48,4
      K2=K1+3
      DO 142 M=1,5
      P(1,M)=H(M+L-1)
  142 Y(M)=Z(M+L-1)
      DO 145 K=K1,K2
```

```
      DO 140 I=2,5
      I1=6-I
      DO 140 J=1,I1
      J1=J+I-1
  140 P(I,J)=((P(I-1,1)*(Y(J1)-G(K)))-(P(I-1,J+1)*(Y(I-1)-G(K))))/(Y(J1)
     C-Y(I-1))
  145 U(K)=P(5,1)*(+.1E-05)
  144 L=L+1
      DO 771 J=48,801
  771 U(J)=+.693E-03
C     CALCULATE NON DIMENSIONAL STRESS AND VELOCITY
      DO 500 I=1,2
      DO 500 J=1,961
      S(I,J)=0.0
  500 V(I,J)=0.0
      CAT=C(20)
      DO 502 J=1,388
  502 C(J)=(T5I(J)/CAT)
      DO 501 J=389,961
  501 C(J)=1.0
      Q=1.0
      DO 508 L=1,40
      DO 507 K=2,21
      K1=((L*20)-20)+K
      S(2,1)=U(K1)
      V(2,1)=V(1,2)-((S(2,1)-S(1,2))/((C(1)+C(2))/2.0))
      DO 506 J=2,960
      CA=C(J)+C(J+1)
      CB=C(J)+C(J-1)
      CT=CA+CB
      S(2,J)=((CA*S(2,J-1))+(CB*S(1,J+1))+(CA*CB*(V(1,J+1)-V(2,J-1))/2.0
     C))/CT
  506 V(2,J)=((CB*V(2,J-1))+(CA*V(1,J+1))-(2.*S(2,J-1))+(2.*S(1,J+1)))/C
     CT
      S(2,961)=0.0
      V(2,961)=V(2,960)-(S(2,960)/C(960))
      DO 507 JAC=1,961
      S(1,JAC)=S(2,JAC)
  507 V(1,JAC)=V(2,JAC)
      L1=(L*20)+1
      TIME=Q*20.0*TS*2.0
      PRINT 14,L1,TIME
      YS(1)=S(1,26)/(C(26)*C(26))
      YS(2)=S(1,27)/(C(27)*C(27))
      YS(3)=S(1,507)
      PRINT 11,S(1,26),S(1,27),S(1,507)
      PRINT 12,YS(1),YS(2),YS(3)
      PRINT 13,V(1,26),V(1,27),V(1,507)
      PRINT 401
  508 Q=Q+1.
      STOP
      END
```

SAMPLE INPUT DATA OF TEMPERATURE

+75.0	+76.0	+77.0	+78.0	+80.0	+82.0	+84.0	+87.0
+92.0	+97.0	+105.0	+115.0	+126.0	+143.0	+169.0	+207.0
+258.0	+323.0	+404.0	+518.0	+695.0	+940.0	+1170.0	+1200.0

SAMPLE INPUT DATA OF THE NON DIMENSIONAL STRESS

+00.0	+7.00	+20.0	+42.0	+130.0	+290.0	+395.0	+454.0
+495.0	+526.0	+549.0	+568.0	+583.0	+594.0	+602.0	+607.0
+612.0	+616.0	+618.0	+621.0	+623.0	+625.0	+626.2	+627.27
+627.27	+627.27						

PERIODIC VIBRATIONS SOLUTION FOR A GENERAL TEMPERATURE DISTRIBUTION

BOUNDARY CONDITION
AT X=L. DISPLACEMENT=U $e^{i\omega t}$

```
      PROGRAM TEMPWAV
      DIMENSION A(2000,3),U(2001),X(2001),E(2001),Z(2000,2),S(201)
      DIMENSION V(2001),F(7),TEMP(21),D(21),G(21),P(5,5),Y(5)
  101 FORMAT (7(E10.3,1X))
  120 FORMAT (10X,11HFREQUENCY =,2X,E10.3)
  255 FORMAT (2X,I4,3X,E10.3,7X,E15.8)
  256 FORMAT (2X,I4,3X,E10.3,7X,E15.8,5X,E15.8)
  410 FORMAT (1H0)
  420 FORMAT (10X,16HNO OF ITERATIONS,3X,I3,6X,4HDAM=,2X,E15.8)
  801 FORMAT (3X,1HJ,5X,5HPOINT,10X,12HDISPLACEMENT)
  901 FORMAT (3X,1HJ,5X,5HPOINT,13X,6HSTRESS,13X,15HIT DISPLACEMENT)
      READ 101, (F(J),J=1,7)
      R=7.43E-04
      TL=20.
      H=TL/2000.0
      U(2001)=1.0
C     CALCULATE ELASTIC MODULUS
      E0=.290E+08
      EL= .2172E+08
      T0=75.
      TL=1200.
      C0=(EL-E0)/(TL-T0)
    1 FORMAT (8(F10))
      TEMP(1)=75.0
      READ 1,(TEMP(J),J=2,21)
      DO 4 J=1,21
    4 D(J)=(C0*(TEMP(J)-T0))+E0
C     INTERPOLATE FOR INTERMEDIATE VALUES OF ELASTIC MODULUS
      G(1)=0.0
      DO 5 J=2,21
    5 G(J)=G(J-1)+1.0
      X(1)=0.0
      DO 6 J=2,2001
    6 X(J)=X(J-1)+.01
      L=1
      DO 907 M=1,5
      P(1,M)=D(M+L-1)
  907 Y(M)=G(M+L-1)
      DO 905 K=102,250
      DO 931 I=2,5
      I1=6-I
      DO 931 J=1,I1
      J1=J+I-1
  931 P(I,J)=((P(I-1,1)*(Y(J1)-X(K)))-(P(I-1,J+1)*(Y(I-1)-X(K))))/(Y(J1)
     C-Y(I-1))
```

```
  905 E(K)=P(5,1)
      L=2
      DO 804 K1=251,1730,100
      K2=K1+99
      DO 818 M=1,5
      P(1,M)=D(M+L-1)
  818 Y(M)=G(M+L-1)
      DO 805 K=K1,K2
      DO 819 I=2,5
      I1=6-I
      DO 819 J=1,I1
      J1=J+I-1
  819 P(I,J)=((P(I-1,1)*(Y(J1)-X(K)))-(P(I-1,J+1)*(Y(I-1)-X(K))))/(Y(J1)
     C-Y(I-1))
  805 E(K)=P(5,1)
  804 L=L+1
      L=17
      DO 703 M=1,5
      P(1,M)=D(M+L-1)
  703 Y(M)=G(M+L-1)
      DO 705 K=1751,2001
      DO 700 I=2,5
      I1=6-I
      DO 700 J=1,I1
      J1=J+I-1
  700 P(I,J)=((P(I-1,1)*(Y(J1)-X(K)))-(P(I-1,J+1)*(Y(I-1)-X(K))))/(Y(J1)
     C-Y(I-1))
  705 E(K)=P(5,1)
      DO 706 J=1,101
  706 E(J)=E0
C     CALCULATE DISPLACEMENT AMPLITUDE
      A(1,1)=0.0
      DO 200 J=2,2000
  200 A(J,1)=(1.-((E(J+1)-E(J-1))/(4.*E(J))))
      B=-(1.+((E(2001)-E(1999))/(4.*E(2000))))
      DO 202 J=2,1999
  202 A(J,3)=(1.+((E(J+1)-E(J-1))/(4.*E(J))))
      A(1,3)=2.0
      A(2000,3)=0.0
      DO 210 J=1,2000
  210 Z(J,2)=A(J,3)
      DO 300 I=1,7
      W=6.28319*F(I)
      DO 201 J=1,2000
  201 A(J,2)=((R*((W*H)**2.))/E(J))-2.
      Z(1,1)=A(1,2)
      DO 211 J=2,2000
  211 Z(J,1)=A(J,2)-((A(J,1)/Z(J-1,1))*A(J-1,3))
      U(2000)=B/Z(2 00,1)
      DO 212 J=1,1999
      J1=2000-J
```

```
  212 U(J1)=-((Z(J1,2)/Z(J1,1))*U(J1+1))
      PRINT 120,F(1)
      PRINT 410
      PRINT 801
      PRINT 255,(J,X(J),U(J),J=1,2001,50)
      PRINT 410
      K=1
  660 V(1)=-((A(1,3)/A(1,2))*U(2))
      DO 600 J=2,1999
  600 V(J)=-(((A(J,1)*V(J-1))+(A(J,3)*U(J+1)))/A(J,2))
      V(2000)=(B-(A(2000,1)*V(1999)))/A(2000,2)
      V(2001)=U(2001)
      DAM =(U(1)-V(1))
      J=1
  670 IF(J-2000)680,680,690
  680 DIF=U(J)-V(J)
      IF(DAM-DIF)671,672,672
  671 DAM=DIF
      J=J+1
      GO TO 670
  672 J=J+1
      GO TO 670
  690 IF(DAM-.00001)803,800,800
  800 DO 802 J=1,2001
  802 U(J)=V(J)
      K=K+1
      IF(K-50)660,660,803
C     CALCULATE STRESS AMPLITUDE
  803 S(1)=0.
      DO 900 J=2,200
      J1=((J*10)-9)
  900 S(J)=E(J1)*((V(J1+1)-V(J1-1))/(2.*H))
      S(201)=E(2001)*((V(2001)-V(2000))/H)
      PRINT 420,K,DAM
      PRINT 410
      PRINT 901
      DO 902 J=1,201,5
      J1=((J*10)-9)
  902 PRINT 256,(J1,X(J1),S(J),V(J1))
  300 PRINT 410
      STOP
      END
         SCOPE
'LOAD
'RUN,2,3000
```

PERIODIC VIBRATIONS SOLUTION FOR A GENERAL TEMPERATURE DISTRIBUTION

BOUNDARY CONDITION
AT X=L, STRESS=$Pe^{i\omega t}$

```
      PROGRAM TEMPWAV
      DIMENSION A(2 01,3),U(2001),X(2001),E(2001),Z(2001,2),S(201)
      DIMENSION V(2 01),F(7),TEMP(21),D(21),G(21),P(5,5),Y(5)
  101 FORMAT (7(E10.3,1X))
  120 FORMAT (10X,11HFREQUENCY =,2X,E10.3)
  255 FORMAT (2X,I4,3X,E10.3,7X,E15.8)
  256 FORMAT (2X,I4,3X,E10.3,7X,E15.8,5X,E15.8)
  410 FORMAT (1H0)
  420 FORMAT (10X,16HNO OF ITERATIONS,3X,I3,6X,4HDAM=,2X,E15.8)
  801 FORMAT (3X,1HJ,5X,5HPOINT,10X,12HDISPLACEMENT)
  901 FORMAT (3X,1HJ,5X,5HPOINT,13X,6HSTRESS,13X,15HIT DISPLACEMENT)
      READ 101, (F(J),J=1,7)
      TL=20.
      H=.01
      R=7.43E-04
C     CALCULATE ELASTIC MODULUS
      EO=.290E+08
      EL= .2172E+08
      TO=75.
      TL=1200.
      CO=(EL-EO)/(TL-TO)
    1 FORMAT (8(F10))
      TEMP(1)=75.0
      READ 1,(TEMP(J),J=2,21)
      DO 4 J=1,21
    4 D(J)=(CO*(TEMP(J)-TO))+EO
C     INTERPOLATE FOR INTERMEDIATE VALUES OF ELASTIC MODULUS
      G(1)=0.0
      DO 5 J=2,21
    5 G(J)=G(J-1)+1.0
      X(1)=0.0
      DO 6 J=2,2001
    6 X(J)=X(J-1)+.01
      L=1
      DO 907 M=1,5
      P(1,M)=D(M+L-1)
  907 Y(M)=G(M+L-1)
      DO 905 K=102,250
      DO 931 I=2,5
      I1=6-I
      DO 931 J=1,I1
      J1=J+I-1
  931 P(I,J)=((P(I-1,1)*(Y(J1)-X(K)))-(P(I-1,J+1)*(Y(I-1)-X(K))))/(Y(J1)
     C-Y(I-1))
  905 E(K)=P(5,1)
```

```
      L=2
      DO 804 K1=251,1730,100
      K2=K1+99
      DO 818 M=1,5
      P(1,M)=D(M+L-1)
  818 Y(M)=G(M+L-1)
      DO 805 K=K1,K2
      DO 819 I=2,5
      I1=6-I
      DO 819 J=1,I1
      J1=J+I-1
  819 P(I,J)=((P(I-1,1)*(Y(J1)-X(K)))-(P(I-1,J+1)*(Y(I-1)-X(K))))/(Y(J1)
     C-Y(I-1))
  805 E(K)=P(5,1)
  804 L=L+1
      L=17
      DO 703 M=1,5
      P(1,M)=D(M+L-1)
  703 Y(M)=G(M+L-1)
      DO 705 K=1751,2001
      DO 700 I=2,5
      I1=6-I
      DO 700 J=1,I1
      J1=J+I-1
  700 P(I,J)=((P(I-1,1)*(Y(J1)-X(K)))-(P(I-1,J+1)*(Y(I-1)-X(K))))/(Y(J1)
     C-Y(I-1))
  705 E(K)=P(5,1)
      DO 706 J=1,101
  706 E(J)=E0
C     CALCULATE DISPLACEMENT AMPLITUDE
      A(1,1)=0.0
      DO 200 J=2,20 0
  200 A(J,1)=(1.-((E(J+1)-E(J-1))/(4.*E(J))))
      A(2001,1)=2.
      B=-((2.*H*(1. ((E(2001)-E(2000))/(2.*E(2001)))))/E(2001))
      DO 202 J=2,2000
  202 A(J,3)=(1.+((E(J+1)-E(J-1))/(4.*E(J))))
      A(1,3)=2.
      A(2001,3)=0.0
      DO 210 J=1,2001
  210 Z(J,2)=A(J,3)
      DO 300 I=1,7
      W=6.28319*F(I)
      DO 201 J=1,2001
  201 A(J,2)=((R*((W*H)**2.))/E(J))-2.
      Z(1,1)=A(1,2)
      DO 211 J=2,2001
  211 Z(J,1)=A(J,2) ((A(J,1)/Z(J-1,1))*A(J-1,3))
      U(2001)=B/Z(2001,1)
      DO 212 J=1,2000
      J1=2001-J
```

```
  212 U(J1)=-((Z(J1,2)/Z(J1,1))*U(J1+1))
      PRINT 120,F(I)
      PRINT 410
      PRINT 801
      PRINT 255,(J,X(J),U(J),J=1,2001,50)
      PRINT 410
      K=1
  660 V(1)=-((A(1,3)/A(1,2))*U(2))
      DO 600 J=2,2000
  600 V(J)=-(((A(J,1)*V(J-1))+(A(J,3)*U(J+1)))/A(J,2))
      V(2001)=(B-(A(2001,1)*V(2000)))/A(2001,2)
      DAM =(U(1)-V(1))
      J=1
  670 IF(J-2001)680,680,690
  680 DIF=U(J)-V(J)
      IF(DAM-DIF)671,672,672
  671 DAM=DIF
      J=J+1
      GO TO 670
  672 J=J+1
      GO TO 670
  690 IF(DAM-.00001)803,800,800
  800 DO 802 J=1,2001
  802 U(J)=V(J)
      K=K+1
      IF(K-50)660,660,803
C     CALCULATE STRESS AMPLITUDE
  803 S(1)=0.
      DO 900 J=2,200
      J1=((J*10)-9)
  900 S(J)=E(J1)*((V(J1+1)-V(J1-1))/(2.*H))
      S(201)=E(2001)*((V(2001)-V(2000))/H)
      PRINT 420,K,DAM
      PRINT 410
      PRINT 901
      DO 902 J=1,201,5
      J1=((J*10)-9)
  902 PRINT 256,(J1,X(J1),S(J),V(J1))
  300 PRINT 410
      STOP
      END
         SCOPE
*LOAD
*RUN,2,3000
```

SAMPLE INPUT DATA OF FREQUENCIES

+.050E+005 +.075E+0 5 +.100E+005 +.125E+005 +.150E+005 +.175E+005 +.200E+005

SAMPLE INPUT DATA OF TEMPERATURE

+75.0	+76.0	+77.0	+78.0	+79.5	+81.5	+86.0	+95.0
+107.0	+120.0	+137.0	+164.0	+213.0	+293.0	+404.0	+570.0
+820.0	+1100.0	+1200.0	+1200.0				